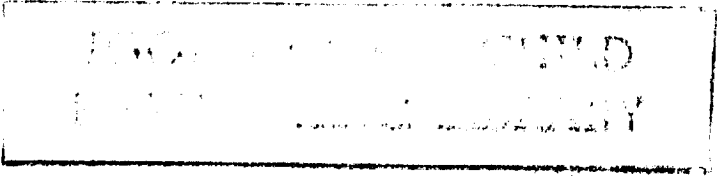# NATIONAL ADVISORY COMMITTEE
FOR AERONAUTICS

TECHNICAL NOTE 3179

MAY 10 1954

A THEORETICAL INVESTIGATION OF THE HEATING-UP PERIOD
OF INJECTED FUEL DROPLETS VAPORIZING IN AIR

By M. M. El Wakil, O. A. Uyehara, and P. S. Myers

University of Wisconsin

NACA

Washington

May 1954

NACA TN 3179

reach the combustion zone while still in the —

In most cases, during the unsteady state, more of the heat arriving at the surface of the liquid droplet goes to sensible heat than goes to latent heat of vaporization. This is especially true for low-volatility

mass transfer decreases with time, although the droplet is being heated up. The time required by a certain size droplet to reach its wet-bulb temperature is less for higher volatility fuels at the same ambient and initial conditions.

It should be realized that the calculated curves depend upon the use of heat and mass transfer correlations that are extended far beyond the conditions under which they were obtained. Thus, extensive use of the values shown on the calculated curves should not be made until either the curves or the extrapolations of the heat and mass transfer correlations have been checked experimentally.

In addition to the theoretical work, in order to verify the results of the calculations, which showed the unsteady state to be of importance, apparatus was set up to obtain experimental temperature-time histories of comparatively large droplets vaporizing in air streams at constant velocities and atmospheric pressure. This apparatus is described and a few experimental curves are included. These curves show the relative distribution of the time interval between the unsteady and steady states when different air temperatures and different fuels are used.

INTRODUCTION

Knowledge of the phases through which a heterogeneous mixture of air and fuel passes before ignition takes place is essential for the rational design of jet-engine combustion chambers. For discussion purposes, the time elapsed before ignition is often divided into physical and chemical components, although the relative magnitudes of these two components are not known. Since the physical component inevitably precedes and perhaps in part overlaps the chemical component, knowledge of the magnitude of and the factors affecting the physical component is of obvious importance in any study of the time interval before ignition.

Fuel injected through a nozzle into a combustion chamber is believed to pass through the following stages: The fuel leaves the nozzle orifices as a ligament or sheet. This ligament or sheet then breaks down into different size droplets. Appreciable heat transfer from the air present in the combustion chamber to the fuel occurs only after the ligament has broken up into droplets. This is due to the appreciable increase of surface area of the fuel that is exposed to the air. As heat transfer takes place, the droplets heat up (or possibly cool down depending upon ambient air conditions and initial fuel temperature) and at the same time lose part of their mass by vaporization and diffusion into the air, with both

relative to the air by aerodynamic drag forces. After a certain time
has elapsed, each droplet attains an asymptotic or equilibrium tempera-
ture equal to the wet-bulb temperature corresponding to the conditions
present at that moment.

The larger droplets are slower in attaining equilibrium conditions;
but, although they have essentially the same initial speed as the smaller
droplets, they are slowed down relative to the air at a lesser rate, and
they move along with the air ahead of the smaller ones that were injected
at the same instant. The smaller drops, however, give away their mass
and completely vaporize faster and travel a shorter distance through the
combustion chamber than the larger droplets.

A cloud of vapor due to the smaller droplets is thus rapidly formed
and moves along with the air. The mass of vapor given away by the
incoming larger droplets is added to this vapor cloud. Somewhere in the
combustion chamber a combustible mixture of air and fuel vapor is formed
and is ready for ignition at that point. In the absence of outside
ignition, this mixture must be heated by the air until it reaches its self-
ignition temperature if combustion is to take place. By definition, the
physical portion of the ignition delay extends until a combustible mixture
is formed and heated to the ignition temperature. Since some chemical
reaction may take place at temperatures lower than the ignition tempera-
ture, the chemical portion of the ignition delay period probably overlaps
the physical portion. The vaporization process is thus an essential part
of the ignition delay period.

Although the fuel droplets reach their equilibrium or wet-bulb tem-
peratures asymptotically with time, the vaporization process can roughly
be separated into the unsteady state and the steady or equilibrium state.
Numerous investigations have been conducted covering the latter stage
(refs. 1 and 2), but only a few attempts have been made to study the
unsteady state (ref. 3). It was the intent of this investigation to
determine theoretically temperature-time histories of droplets of dif-
ferent size and fuel composition under different ambient air conditions
in an attempt to determine whether the unsteady-state period is of
importance in the history of the fuel droplets previous to ignition.

This report, then, presents a detailed study of the unsteady-state
portion of the total vaporization time of single fuel droplets injected
into air. Calculations were performed for numerous combinations of the
following conditions:

Fuels . . . . n-octane, benzene, n-pentane
Initial radii, μ 10, 50, 100
Initial droplet temperatures, $^\circ$F 50, 200
Initial droplet velocities, fps 100, 400
Air pressures, atm 0.5, 1, 5
Air temperatures, $^\circ$F 100, 500, 1,000

The three fuels have standard atmospheric boiling temperatures of $96.9°$, $176.2°$, and $258.2°$ F, respectively. The calculations covered all combinations of the above conditions except when the initial droplet temperatures were higher than the boiling points of the fuels at the corresponding air pressures.

The properties of the three fuels under investigation and for air were obtained from various references as shown in table I.

This work was conducted at the University of Wisconsin under the sponsorship and with the financial assistance of the National Advisory Committee for Aeronautics.

SYMBOLS

A_c	cross-sectional area of liquid droplet, sq in.
A_o	surface area of liquid droplet, sq in.
B_o	thickness of air-vapor film surrounding droplet, in.
C_D	coefficient of drag for spheres, unitless
C_{p_a}	specific heat of air at constant pressure, $Btu/(lb)(°F)$
C_{p_f}	specific heat of fuel vapor at constant pressure, $Btu/(lb)(°F)$
C_{p_L}	specific heat of liquid fuel, $Btu/(lb)(°F)$
C_{p_m}	average specific heat of air-vapor mixture in film at constant pressure, $Btu/(lb)(°F)$
D_v	diffusion coefficient of air-vapor system, sq in./sec
d	penetration or distance traveled relative to air, in.
F	drag force, lb
g_a	weight fraction of air in film, unitless
g_f	weight fraction of fuel vapor in film, unitless
h	coefficient of heat transfer in film in absence of mass transfer, based on surface area of liquid droplet A_o, $Btu/(sq\ in.)(sec)(°F)$

h_L coefficient of heat transfer to liquid, $Btu/(sq\ in.)(sec)(^\circ F)$

K_1, K_2, K_3, . . .   constants

k_a thermal conductivity of air, $Btu/(in.)(sec)(^\circ F)$

k_f thermal conductivity of fuel vapor, $Btu/(in.)(sec)(^\circ F)$

k_g coefficient of mass transfer in film, $1/sec$

k_L thermal conductivity of liquid fuel, $Btu/(in.)(sec)(^\circ F)$

k_m average thermal conductivity of air-vapor mixture in film, $Btu/(in.)(sec)(^\circ F)$

M ratio of instantaneous mass to original mass of droplet, percent

M_a molecular weight of air, $lb/mole$

M_f molecular weight of fuel vapor, $lb/mole$

M_m apparent molecular weight of air-vapor mixture, $lb/mole$

m mass of liquid droplet, lb

N_{Nu} Nusselt number for heat transfer, unitless

N_{Nu}' Nusselt number for mass transfer, unitless

N_{Pr} Prandtl number, $C_{p_m}\mu_m/k_m$, unitless

N_{Re} Reynolds number, $2r_o U\rho_m/\mu_m$, unitless

N_{Sc} Schmidt number $\mu_m/\rho_m D_v$, unitless

P_T total pressure, $lb/sq\ in.$ abs

p_a average partial pressure of air in film, $P_T - \dfrac{p_{f_L}}{2}$, $lb/sq\ in.$ abs

p_{aB} partial pressure of air at outer edge of film, $lb/sq\ in.$ abs

p_{aL} partial pressure of air at liquid droplet surface, lb/sq in. abs

p_f average partial pressure of fuel vapor in film, lb/sq in. abs

p_{fB} partial pressure of fuel vapor at outer edge of film, considered to be zero, lb/sq in. abs

p_{fL} partial pressure of fuel vapor at liquid droplet surface, equal to vapor pressure of fuel at droplet temperature T_L, lb/sq in. abs

Q total heat transfer from air to droplet, Btu/sec

Q_L sensible heat received by droplet, Btu/sec

Q_s heat carried away from droplet by diffusing vapor in form of superheat, Btu/sec

Q_v heat received at droplet surface, Btu/sec

Q_λ heat of vaporization, Btu/sec

R universal gas constant, in-lb/(mole)(°F)

r radius at any point in film, in.

r_a molal rate of diffusion of air in equimolal diffusion, moles/(sec)(sq in.)

r_f molal rate of diffusion of fuel vapor in equimolal diffusion, based on surface area of liquid droplet A_o, moles/(sec)(sq in.)

r_o radius of liquid droplet, in.

T temperature in film at radius r, °R

T_{as} asymptotic or wet-bulb temperature of droplet, °R

T_B temperature of air outside film, °R

T_L temperature of liquid droplet, °R

T_m logarithmic mean temperature in film, °R

U   droplet velocity relative to air, in./sec

w   mass of fuel vapor diffused out, lb/sec

x   proportionality factor

y   fraction of film thickness at radius r, $\dfrac{r - r_o}{B_o}$, unitless

z   factor, wC_{p_f}/hA_o, unitless

α correction factor of mass transfer due to semipermeability
              of film, unitless

θ time, sec

λ latent heat of vaporization of fuel, Btu/lb

μ_a viscosity of air, lb/(in.)(sec)

μ_f viscosity of fuel vapor, lb/(in.)(sec)

μ_m average viscosity of air-vapor mixture in film, lb/(in.)(sec)

ρ_a density of air, lb/cu in.

ρ_L density of liquid droplet, lb/cu in.

ρ_m average density of air-vapor mixture in film, lb/cu in.

ANALYSIS

    In the following theoretical study of the vaporization of single
droplets, two assumptions were made. The first assumption was that an
endless supply of air surrounded the droplet at all times. This means
that there is no interaction between different droplets in the same air
stream, or that only a single droplet was considered present. The
partial pressure due to the fuel vapor at the outer edge of the air-
vapor surrounding the droplet was thus considered to be zero at all
times. The second assumption was that the air pressure and temperature
remained unchanged throughout the vaporization process. It is known

that during injection in a continuous-flow air stream the air temperature
decreases because of heat transfer and that in the absence of friction
its pressure should increase because of the slowing down of the stream;
the second assumption is consistent, however, with the assumption of a
single droplet in a large volume of air.

Figure 1 shows a spherically symmetrical droplet surrounded by a
film containing an air - fuel-vapor mixture. At any one instant, the
mixture strength varies from a maximum at the droplet surface to a mini-
mum at the outer edge of the film. The shape of the temperature gradient
curve depends on the relative temperatures of the fuel droplet and air
and the mass of vapor being diffused out at that instant. Under the
ambient conditions considered in this study, eliminating the case where
the droplet was introduced with a vapor pressure higher than the total
pressure, the vaporization process can take place in three different
cases:

(1) When the initial temperature of the droplet is lower than the
air temperature and lower than its own wet-bulb temperature, in which
case the droplet heats up continuously during the unsteady-state portion
of the vaporization time. This case comprises the larger part of the
calculated conditions contained in this report.

(2) When the initial temperature of the droplet is lower than the
air temperature but higher than its own wet-bulb temperature at the
ambient air conditions. In this case the droplet cools down continu-
ously while vaporizing and the sensible heat lost by the liquid supplies
part of the heat of vaporization of the diffusing vapor. Heat is always
transferred from the air to the droplet, however.

(3) When the initial temperature of the droplet is higher than both
the air temperature and its own wet-bulb temperature. In this case the
droplet cools down continuously until it reaches its wet-bulb temperature
which is lower than the air temperature. During that time when the droplet
temperature is higher than the air temperature, there is a net heat trans-
fer from the droplet to the air and thus heat and mass transfer take place
in the same direction. When the droplet temperature has dropped below
the air temperature, the process is the same as that in case (2).

It is convenient to divide the analysis into three parts - the heat
transfer, the mass transfer, and the velocity change.

Heat Transfer

Referring to figure 1, and assuming that the droplet is vaporizing
under the conditions of case (1), the total or net heat transfer Q from
the air to the film surrounding the droplet, prior to ignition, goes three

ways: (1) To heat up the liquid droplet, Q_L; (2) to vaporize the liquid, Q_λ; and (3) to be carried or peeled back with the diffusing vapor in the form of superheat, Q_S. The heat that arrives at the droplet surface is denoted by Q_v and equals the sum of Q_L and Q_λ.

It should be noted that in developing the relationship used Q does not include radiant heat transfer.

If at any instant during vaporization a point in the air-vapor film at a radius r from the center of the droplet and at temperature T is considered:

$$Q_v = Q_L + Q_\lambda$$

$$= Q - Q_S \tag{1}$$

$$Q_v = hA_o \frac{dT}{dy} - wC_{p_f}\left(T - T_L\right) \tag{2}$$

where w is the rate at which the vapor is diffusing out, y is the fraction of the film thickness at radius r_o, h is the coefficient of heat transfer through the film in the absence of mass transfer, C_{p_f} is the specific heat of the fuel vapor, T is the temperature of the mixture at the position y, and T_L is the temperature of the surface of the droplet.

Rearranging equation (2) gives:

$$dy = \frac{hA_o}{Q_v - wC_{p_f}T_L + wC_{p_f}T}\, dT$$

Integrating across the film between $y = 0$ to $y = 1.0$ where $T = T_L$ to $T = T_B$ and considering the specific heat of the fuel vapor C_{p_f} to be constant throughout the film:

$$1 = \frac{hA_o}{wC_{p_f}} \log_e \frac{Q_v + wC_{p_f}\left(T_B - T_L\right)}{Q_v}$$

or by rearranging and expressing as an exponential:

$$e^{wC_{p_f}/hA_o} = \frac{Q_V + wC_{p_f}\left(T_B - T_L\right)}{Q_V}$$

Defining z as wC_{p_f}/hA_o gives:

$$Q_V = \frac{wC_{p_f}\left(T_B - T_L\right)}{e^z - 1}$$

$$Q_V = hA_o\left(T_B - T_L\right)\frac{z}{e^z - 1} \tag{3}$$

$$Q_V = Q\left(\frac{z}{e^z - 1}\right) \tag{4}$$

Thus the factor $z/(e^z - 1)$ represents that fraction of the total heat transfer Q from the air that finally arrives at the surface of the liquid droplet and supplies the latent heat of vaporization for the vapor diffusing out as well as the sensible heat added to the liquid droplet itself. The factor $z/(e^z - 1)$ therefore represents a correction factor to the heat transfer coefficient h without mass transfer from the droplet.

Several investigators have presented correlations for the heat transfer coefficient h. However, as will appear later, it was necessary for these studies that a mass transfer coefficient also be available. The correlations used in this paper were taken from Ranz and Marshall's work (ref. 1). It was felt that the nature of the investigation conducted in their work was similar to the problems being studied in this paper, although the maximum air temperatures used in their work were not so high as the maximum air temperatures used in this investigation.

From their correlation the Nusselt number for heat transfer used is:

$$N_{Nu} = \frac{h(2r_o)}{k_m} = 2 + 0.6\left(N_{Pr}\right)^{1/3}\left(N_{Re}\right)^{1/2} \tag{5}$$

The factors in this equation were evaluated for the average film conditions. This required knowledge of the air and droplet temperatures as well as the partial pressures in the film (see appendixes A and B). The Ranz and Marshall correlations were obtained from experiments conducted at low temperatures and low vapor pressures. In their work, therefore, the correction factor $z/(e^z - 1)$ was unity and it is not clear whether their correlation includes this factor as a variable. Since the correlation was to be used under conditions where this factor was not unity, and since the correlation is similar in form to those obtained without mass transfer, it was decided to extrapolate the correlation by assuming that it did not include the correction factor. The correction factor therefore was computed and used in all of the calculations presented herein.

It can be seen from the above equations that a calculation of the heat transfer through the film at any instant during the vaporization process of the droplet would require the knowledge of the temperatures on both sides of the air-vapor film surrounding the droplet, of the velocity of the droplet relative to the air, and of its radius, which is dependent on the mass transferred up to that point and on the droplet temperature.

Mass Transfer

Neglecting thermal diffusion and assuming all diffusion to result from the driving force of a concentration or partial pressure gradient which exists in the direction of diffusion, the following equations are obtained for counterdiffusion systems (ref. 4):

$$\frac{dp_f}{dr} = -\frac{x}{RT}\left(r_f p_a - r_a p_f\right) \tag{6}$$

and

$$D_v = \frac{(RT)^2}{x P_T} \tag{7}$$

In this case equimolal rates of diffusion must take place if the total pressure is to be maintained, or:

$$r_f = -r_a \tag{8}$$

and

$$P_T = p_a + p_f \tag{9}$$

However, in most cases of a fuel droplet vaporizing in air essentially unidirectional diffusion takes place. Equimolal diffusion would be approached only if a droplet approached its critical temperature during the heating-up period. In the cases under consideration in this report essentially unidirectional diffusion exists; that is, there will be diffusion of the fuel vapor away from the droplet while the rate of diffusion of the air in the opposite direction, toward the droplet, is zero. In this case,

$$r_a = 0 \tag{10}$$

Combining equations (6), (7), and (10) and rearranging:

$$\frac{dp_f}{dr} = - \frac{RT}{D_v P_T} r_f p_a \tag{11}$$

Integrating between $r = r_o$ and $r = r_o + B_o$ where $p_a = p_{aL}$ and $p_a = p_{aB}$:

$$r_f = \frac{D_v P_T}{RTB_o} \log_e \frac{p_{aB}}{p_{aL}}$$

$$= \frac{D_v}{RTB_o} \left(p_{aB} - p_{aL}\right) \frac{P_T}{\dfrac{p_{aB} - p_{aL}}{\log_e \dfrac{p_{aB}}{p_{aL}}}} \tag{12}$$

This is the equation for the rate of diffusion of the fuel vapor in terms of the partial pressures of the air. Using equation (9) and assuming that the partial pressure of the fuel vapor at the outer edge of the film p_{fB} is zero, an assumption discussed earlier in the analysis, the rate of diffusion of the fuel vapor can be written in terms of partial pressures in the film as follows:

$$r_f = \frac{D_v}{RTB_o} \, p_{fL} \, \frac{P_T}{\dfrac{p_{fL}}{\log_e \dfrac{P_T}{P_T - p_{fL}}}} \tag{13}$$

$$r_f = \frac{D_v}{RTB_o} \, p_{fL} \, \alpha \tag{14}$$

where

$$\alpha = \frac{P_T}{\dfrac{p_{fL}}{\log_e \dfrac{P_T}{P_T - p_{fL}}}}$$

Equation (14) states that the unidirectional diffusion of the fuel vapor into the air equals the equimolal rate of diffusion, which is a function of the concentration, times the factor α which is greater than unity. This increase in rate represents a correction for the fact that the net rate of movement of the air is zero, while the diffusion velocities of the fuel vapor and the air relative to each other must be maintained.

Because of the difficulty in evaluating B_o and by analogy with heat transfer a semiempirical, semitheoretical relationship is set up for mass transfer. Thus it is customarily considered on a semiempirical basis that the mass of fuel vapor diffused out per unit time under the conditions of interest here is given by

$$w = A_o k_g p_{fL} \alpha \tag{15}$$

where k_g is the mass transfer coefficient for the film in the case of equimolal diffusion. Ranz and Marshall (ref. 1) present a correlation for k_g, but again it was necessary to extrapolate their correlation to conditions far removed from the experimental conditions under which it was obtained. In making this extrapolation the line of reasoning was as follows: The correlation was for the film. Therefore, when the density of the air and of the film were markedly different, the mean density of the film ρ_m should be used instead of ρ_a. Another choice to be made in the extrapolation was whether the Ranz and Marshall correlation is for k_g or for the product of k_g and α, since the data for

the Ranz and Marshall correlation were taken under conditions where α was essentially unity and therefore not a variable. The factor p_a is sometimes used as a correction factor instead of α (ref. 4). However, when it is so used, it is a logarithmic mean average, while in all of their calculations for their correlations Ranz and Marshall used an arithmetic mean average. The difference between the two averages is almost undetectable over the range of conditions covered in their experiments and thus it is not clear whether their correlation included α via the factor p_a. It is also not clear whether the use of the arithmetic mean rather than the logarithmic mean is an essential part of their correlation. For extrapolation purposes for these computations, it was decided to use p_a as an arithmetic average and to assume that α was not included in the correlation of Ranz and Marshall. Thus the final equation used was

$$N_{Nu}' = \frac{2r_o p_a k_g}{D_v \rho_m} = 2 + 0.6 \left(N_{Sc}\right)^{1/3} \left(N_{Re}\right)^{1/2} \tag{16}$$

The factors in the mass transfer equations were also computed for the average film conditions (see appendix B). The values of the diffusion coefficient D_v were arrived at by using the techniques recommended by Hirschfelder, Curtiss, and Bird (ref. 5). It can be seen again from the above equation that, to calculate the mass transfer at any instant, a knowledge of the heat transfer and of the radius and velocity of the droplet at that instant is essential.

Velocity Equation

The velocity of the droplet at any instant during the vaporization process is essential to the calculation of both the heat and mass transfer at that instant, since it enters into both correlations. The droplet is assumed to be injected with a certain initial velocity relative to the air. Aerodynamic drag forces will then either slow it down or speed it up so that its velocity approaches that of the air. The less the density of the air, that is, the lower its pressure and the higher its temperature, the less effective the drag forces and the greater and more rapid the penetration through the combustion chamber.

From aerodynamic theory the drag force exerted by a moving fluid upon an immersed body may be calculated from the equation

$$F = C_D A_c \rho_m \frac{U^2}{2} \tag{17}$$

where C_D is the coefficient of drag for the given body form and is a function of the Reynolds number; A_c, the cross-sectional area of the body; and ρ_m, the density of the fluid.

For a spherical droplet:

$$F = -m \frac{dU}{d\theta} = -C_D A_c \rho_m \frac{U^2}{2}$$

or

$$\frac{dU}{d\theta} = -\frac{3}{8} C_D \frac{\rho_m}{\rho_L} \frac{U^2}{r_o} \tag{18}$$

Here C_D is taken as the drag coefficient for spheres (ref. 6) at the Reynolds number for which the calculation is performed. It has been pointed out by Hughes and Gilliland (ref. 7) that the drag coefficients for solid spheres and for droplets are not equal. However, the conditions for which the corrections are shown do not correspond to the conditions for which the calculations were performed and therefore no correction was made. Furthermore, extrapolation of the data of Hughes and Gilliland would indicate that the correction should be close to unity for the conditions considered here. It is again evident that, to calculate the deceleration of the droplet at any instant, a knowledge of both the heat and mass transfers is essential.

Method of Calculation

The dependency of the heat transfer, mass transfer, and velocity equations upon each other and the complexity of the equations necessitated a stepwise integration process where the values required are evaluated for small increments of droplet temperature over a small period of time during which all properties of the droplet and fluid may be assumed to be constant. A sample calculation is shown in appendix A. The procedure followed was first to assume an increment of time $\Delta\theta$, a final velocity U_2, and a final radius r_{o2} for a certain increment of droplet temperature ΔT_L, the initial values of velocity U_1, radius r_{o1}, and temperature T_{L1} for that increment being already known from the previous step, or, if this were the first increment, being specified.

For that increment the mean values of the droplet temperature T_L, radius r_o, and velocity U are calculated. Knowing the pressure and temperature of the air, which are assumed to remain constant throughout the process, the various properties in the film are calculated (see appendix B).

Then $\Delta U/\Delta\theta$ is calculated from equation (18) and U_2 is evaluated:

$$U_2 = U_1 - \left(\frac{\Delta U}{\Delta\theta}\right)\Delta\theta \qquad (19)$$

This is repeated several times, correcting for C_D each time, until a value of U_2 is found that satisfies the velocity equation and the Reynolds number is fixed at the mean velocity of the increment U.

The next step would be to calculate the mass transfer coefficient k_g and the average mass transfer w in pounds per second for the increment from equations (15) and (16). This requires a knowledge of the partial pressure of the fuel. The total mass transfer for the increment is then found from $w\,\Delta\theta$ and the average droplet mass m would be

$$m = \frac{m_1 + m_2}{2} = \frac{m_1 + \left(m_1 - w\,\Delta\theta\right)}{2} \qquad (20)$$

In this equation m_1 would be specified or known from calculations of the previous step.

The heat transfer to the droplet surface Q_v is then calculated from equations (3) and (4) and the remaining calculations take place as follows:

$$Q_L = Q_v - w_\lambda$$

For all calculations shown here it was assumed that the thermal conductivity of the fuel was high and the droplet temperature was uniform. The validity of these assumptions is discussed in appendix C. Therefore,

$$\Delta\theta = \frac{mC_{p_L}\,\Delta T_L}{Q_L} \qquad (21)$$

$$r_{o2} = \left(\frac{3m_2}{4\pi\rho_{L2}}\right)^{1/3} \qquad (22)$$

4U

NACA TN 3179   17

The values of U_2, $\Delta\theta$, and r_{o2} calculated from equations (19),
(21), and (22) are compared with those assumed at the beginning of the
computations and are usually recalculated at least once more. The final
values for this increment then become the initial values of the next
increment and the computations are continued for small increments of
ΔT_L until Q_L is found to approach zero. At this point the temperature
asymptote is about to be reached. Here the computations were stopped,
since only the unsteady state was being studied. Since the asymptotic
temperature was not known for most conditions prior to each calcula-
tion, ΔT_L and the number of steps were difficult to determine. It was
found that between 12 and 16 steps usually gave sufficient accuracy.

A model 1, IBM Card-Programmed Electronic Calculator was used for
the computations. The special program to solve this problem uses the
floating-decimal general-purpose connections of the calculator. One
complete calculation for specified droplet conditions of initial radius,
temperature, and velocity and air conditions of pressure and temperature
takes approximately 2.0 hours on the CPC not counting the setup time,
computation of the properties at the successive droplet temperature incre-
ments, and card prepunching.

A typical vaporization history calculated by this method is shown
in figure 2 for a droplet of n-octane of 50-micron initial radius,
50° F initial temperature, and 100-fps initial velocity with respect to
air, vaporizing under air ambient conditions of 0.5-atmosphere pressure
and $1,000^\circ$ F temperature.

                                    Steady State

The droplet temperature approaches the wet-bulb temperature asymp-
totically during the vaporization process. At the wet-bulb or asymptotic
temperature

$$Q_V = Q_\lambda \tag{23}$$

Substituting values from equation (3) and changing T_L to T_{as} there
is obtained:

$$hA_o\left(T_B - T_{as}\right)\left(\frac{z}{e^z - 1}\right) = w\lambda \tag{24}$$

Substituting wC_{p_f}/hA_o for z and rearranging:

$$T_{as} = T_B - \frac{\lambda}{C_{p_f}} \left(e^z - 1 \right) \qquad (25)$$

This is a simple equation for the asymptotic or wet-bulb temperature as a function of the air temperature and the mass and heat transfers. A knowledge of the latter two values is essential for a solution of this equation. It can, however, be rewritten using only the properties of the liquid and film as follows: Combining equations (24) and (15) and rearranging give:

$$T_B - T_{as} = p_{fL} \lambda \frac{\alpha}{\dfrac{z}{e^z - 1}} \frac{k_g}{h}$$

Combining the above equation with equations (5) and (16) and rearranging:

$$T_{as} = T_B - \left(\frac{D_v \rho_m p_{fL} \lambda}{p_a k_m} \frac{\alpha}{\dfrac{z}{e^z - 1}} \frac{N_{Nu}{}'}{N_{Nu}} \right) \qquad (26)$$

Solution of equation (26) must necessarily be by trial and error, since the component properties are all functions of both T_{as} and T_B as well as of the air pressure and the fuel used. The factor $z/(e^z - 1)$ must be approximated since this factor is affected by the volatility of the fuel. It can be stated that for very low volatility fuels this factor can usually be taken as unity with little error. For high-volatility fuels at low air temperatures and high air pressures $z/(e^z - 1)$ can still be taken as unity with little error. For example, using n-pentane, this factor has a value of 0.957 at 100° F air temperature and 5-atmosphere air pressure while n-octane, a less volatile fuel, has a value of 0.998 for this factor at the same conditions. However, for high-volatility fuels at high air temperatures and low air pressures lower values have to be used. n-Pentane has a value of about 0.63 at 500° F and 1 atmosphere air conditions.

The mass transfer during the steady-state period of vaporization can be determined by combining equations (15) and (16) as follows:

$$w = \frac{2D_v \rho_m p_{fL} \alpha}{p_a} r_o \left[2 + 0.6 \left(N_{Sc} \right)^{1/3} \left(N_{Re} \right)^{1/2} \right]$$

Since the temperatures across the film have become essentially constant, the above equation can be rewritten as:

$$w = K_1 r_o \left[2 + K_2 \left(r_o U \right)^{1/2} \right] \tag{27}$$

where K_1 and K_2 are constants.

Equation (27) shows that for a particular fuel the rate of mass transfer during the steady state is a function of only the radius and velocity of the droplet at any instant, provided the air temperature and pressure remain unchanged.

Equation (26) for the steady state where the temperatures across the film are fixed, and therefore all the properties in it, can be rewritten as

$$T_{as} = T_B - K_3 \frac{2 + K_4 \left(r_o U \right)^{1/2}}{2 + K_5 \left(r_o U \right)^{1/2}} \tag{28}$$

where K_3, K_4, and K_5 are constants for any particular fuel and air conditions at the asymptotic or wet-bulb temperature T_{as}. Therefore, T_{as} depends upon the ratio of the Nusselt numbers for mass and heat transfer. It can be deduced, after examining the above equation, that the wet-bulb temperature is dependent on the droplet radius and velocity. At high droplet speeds or for relatively large droplet radii the factor 2 in both the Nusselt numbers becomes relatively negligible and the ratio of the Nusselt numbers and consequently the wet-bulb temperature become essentially constant. However, at lower values of droplet speed or droplet radius the wet-bulb temperature rises slightly until either the speeds or radii approach zero, where the Nusselt number ratio approaches unity and the wet-bulb temperature is again fixed.

This dependence proved to be small for most conditions of interest in this paper. Figure 3(a) shows ΔT_{as} as calculated for various velocities, where ΔT_{as} is defined as the deviation of the actual wet-bulb temperature from that calculated at large Reynolds numbers; figure 3(b) shows ΔT_{as} for various radii for n-pentane at 1-atmosphere air pressure and 100° F air temperature. It should be noted that no attempt was made to include a dependence of the vapor pressure of fuels on droplet size as the droplet radius became very small in calculating the information shown in figure 3(b). It is to be expected that the rise of vapor pressure as corrected for very small droplet radii would lower the values of the wet-bulb temperature again at small drop radii.

Further examination of equation (26) reveals that the wet-bulb temperature approaches the air temperature in case of low-volatility fuels. This is to be expected, since the mass transfer has to be high enough to carry away the entire heat transferred to the droplet. In the case of no mass transfer, the wet-bulb temperature equals the air temperature.

APPARATUS

After investigating theoretically the importance of the unsteady state during the vaporization period and conducting a number of calculations in the unsteady state, it was felt that experimental verification of its importance was desirable. Accordingly, experimental apparatus has been set up in an attempt to establish the importance of the unsteady state and a few experimental records have been obtained.

Figure 4 shows a schematic diagram of the apparatus constructed to determine the temperature-time histories of vaporizing droplets. Air is tapped from the house line at 100 lb/sq in. abs and passed through a porous-stone filter to remove water, oil, and other impurities. Its pressure is then controlled by a pressure regulator, after which it passes through a $2\frac{1}{2}$ -inch pipe where its pressure and temperature are measured by a precision Bourdon gage and a thermometer. The diameter of the pipe at this measuring section is made large enough so that the difference between total and static temperatures is negligible at the highest rate of flow to be used. The air is then passed through either the 3/32- or the 3/16-inch-diameter critical-flow orifice. The air is then heated with an electrical resistance heater, after which it passes through a calming section to a 14-inch-long section of 2-inch flexible tubing which terminates in a 1-inch I.S.A. standard flow nozzle. The exit section of the nozzle is covered with a 160-mesh screen. The screen assists in equalizing the velocity over the nozzle opening to a value calculated from the average volumetric velocity.

The liquid droplet is hung on the junction of the thermocouple about 1/2 inch above the exit section of the nozzle. A 0.010-inch iron-constantan thermocouple was used for the preliminary investigations reported herein. A clean and small thermocouple junction was found essential for a minimum of droplet distortion. It was found that droplets of 700- to 900-micron radius were the best size to be used with the above thermocouple wire size without distortion during the major portion of the heating-up and vaporization period.

An illuminating system was provided for viewing the droplet. A 300-watt General Electric $T8\frac{1}{2}$ projection lamp was used. A heat-absorbing

glass was placed in the path of the light to minimize the heating of the droplet by radiation from the lamp. An optical system having a maximum magnification of 86 was provided for measuring the diameter of the droplet. The optical system was calibrated by placing a wire of known diameter in place of the droplet.

The experimental procedure was as follows: The air was heated to the desired temperature with the exit nozzle swung away from the thermocouple.

The exit velocity of the air stream was adjusted by varying the inlet air pressure ahead of the critical flow orifice. Low air velocities were used to avoid blowing the droplet off the thermocouple junction.

The droplet was then formed and suspended on the thermocouple using a syringe and hypodermic needle. The initial droplet radius was then measured by the optical magnification system. The air nozzle at the end of the flexible tubing section was then suddenly swung under the droplet. The output of the thermocouple was measured and recorded by a 1-second full-scale model G Leeds & Northrup electronic self-balancing Speedomax potentiometer. The temperature of the droplet was measured by the calibrated thermocouple output, while the time scale was computed from the known speed of the recorder chart.

RESULTS AND DISCUSSION

The typical calculated vaporization-time histories shown in figures 2 and 5 through 8 contain the following information:

(1) Droplet temperature, T_L, $^\circ F$
(2) Droplet mass, percent of original, M, percent
(3) Radius, r_o, inches
(4) Velocity relative to the air, U, fps
(5) Penetration or distance traveled relative to the air, d, inches
(6) Instantaneous rate of mass transfer, w, pounds per second
(7) Instantaneous total heat transfer from the air to the film, Q, Btu/sec
(8) Instantaneous heat of vaporization, Q_λ, Btu/sec
(9) Instantaneous heat transfer to the liquid droplet, Q_L, Btu/sec

The fuel, initial droplet radius, initial droplet temperature, initial droplet speed relative to the air, air pressure, and air temperature are indicated in the title of each figure. The portion of the total heat transfer Q that is carried back with the diffusing vapor in the form of

superheat can be determined from the curves by taking the difference between Q and the sum of Q_L and Q_λ.

Figures 2 and 5 through 8 represent the results of only 7 out of the 252 cases for which calculations were performed. A complete set of graphs presenting the results of all the calculations is contained in the manuscript copy of this report. This copy is available for loan or reference in the Division of Research Information, National Advisory Committee for Aeronautics, Washington, D. C.

Examination of these typical graphs (figs. 2 and 5 to 8) yields the following conclusions:

For low-volatility fuels, for example, figure 2 for n-octane, speaking of the heat transferred to the surface of the liquid droplet, the amount of heat going to sensible heat far exceeds the amount of heat going to supply the latent heat of vaporization during most of the unsteady-state or heating-up period and especially right after injection. The higher the air temperature or the higher the air pressure, the greater the portion going to sensible heat. Only as the droplet approaches the steady state does the relation reverse itself, as required by the fact that Q_L becomes negligible and essentially equal to zero during the steady state. This effect is, of course, largely dependent on the initial injection temperature of the liquid fuel. At high initial liquid temperatures sensible heat can be lost by the droplet or a net heat transfer Q from the liquid to the air may even occur (e.g., fig. 5 for n-octane at 200° F initial liquid temperature and 100° F air temperature).

For high-volatility fuels, however (e.g., fig. 6(a) for n-pentane at 1-atmosphere air pressure and 500° F air temperature), the latent heat of vaporization exceeds the amount going to sensible heat. In some cases, especially at low air pressures (e.g., fig. 6(b) for n-pentane), the liquid undergoes a cooling down or loses sensible heat at 0.5-atmosphere air pressure regardless of the air temperature. In this case the net heat transfer from the air goes entirely into latent heat of vaporization. The balance of the heat required to supply the latent heat of vaporization is drawn from the droplet itself. Only at high air temperatures and high air pressures does the sensible-heat requirement of the droplet exceed that of the heat of vaporization, and only for a shorter portion of the unsteady state.

The rate of mass transfer usually increases with time as the droplet is heating up. The increase is much more pronounced at higher air temperatures and lower air pressures (e.g., fig. 2 for n-octane at 0.5-atmosphere air pressure and 1,000° F air temperature). At high air pressures and low air temperatures (e.g., figs. 7 and 8(a) for benzene and n-octane at 5-atmosphere air pressure and 100° F air temperature)

the rate of mass transfer undergoes a decrease, although the droplet is heating up. The reason for this is that in this case the denser air slows down the droplet very rapidly with a consequent rapid drop in the Reynolds number which offsets the favorable effect of the exponential increase in the vapor pressure of the liquid fuel with temperature on the rate of mass transfer w. At intermediate cases, a rise in w followed by a drop can be noticed (e.g., fig. 8(b) for n-octane at 1-atmosphere air pressure and 100° F air temperature). In the case of droplets cooling down during the unsteady state, the rate of mass transfer consistently decreases with time. In the steady state the rate of mass transfer becomes a function of only the radius and velocity of the droplet and thus undergoes a small but steady decrease in value (see eq. (27)).

For comparison purposes the three-dimensional graphs shown in figs. 9 through 12 are presented. These are temperature-time history curves for the three fuels at different fuel and ambient air conditions. In all these curves the initial temperature of the droplets was 50° F and the initial velocity relative to the air was 100 fps.

Figure 9(a) shows temperature-time histories of n-octane at an air temperature of 500° F, for various droplet sizes and air pressures. It can be seen that for the same air pressures but different radius droplets the asymptotic temperatures are equal and the three curves representing the three sizes at any one air pressure form a horizontal plane after all three droplets have reached their steady states. The ends of the horizontal planes shown by the broken lines have no particular meaning and were drawn for illustrative purposes only, since the 10-micron droplets would vaporize before reaching this point and the 100-micron droplets would last longer. Figure 9(b) shows similar temperature-time histories for n-octane except that the air pressure was kept constant at 1 atmosphere and the air temperature varied. Figure 9(c) shows temperature-time histories for n-octane where all the droplets had a 50-micron initial radius and both the air temperature and pressure were varied. In this case none of the nine temperature-time histories shown would have the same asymptotic temperature. The end lines joining the curves at the same air temperature represent, therefore, a variation of asymptotic temperatures with air pressures at three different air temperatures.

Figures 10(a) to 10(c) and 11(a) to 11(c) show the same histories described in figures 9(a) to 9(c) but for benzene and n-pentane, respectively.

Figure 12(a) shows temperature-time histories of the three fuels where the initial droplet radius was 50 microns, the air pressure was 1 atmosphere, and the air temperature was varied. Figure 12(b) shows the three fuel droplets having the same initial radius, with the air

temperature kept constant at 500° F and the air pressure varied. It
can be seen from these curves that the lower volatility fuels have
higher asymptotic temperatures and take a longer time to reach them for
the same operating and ambient conditions. By plotting the results of
the present calculations, it was found that, with all other conditions
constant, the time for droplets to reach the wet-bulb temperature varied
approximately as the initial radius to the 1.8 power.

In the combustion chambers the mass of the fuel droplets vaporized
and the penetrations of these droplets relative to the air are essential
in deciding the zone where combustion is likely to take place. Fig-
ures 13(a) through 13(i) show time histories of droplet penetration d,
relative to the air, and mass, percent of original, M during the
unsteady state for n-octane at nine different ambient air conditions.
Each of these figures contains the previous information for the three
initial droplet sizes and two initial droplet velocities. As the tem-
perature decreases but with the same air pressure, the droplets take
a longer time and penetrate farther before reaching their steady states;
as the air pressure increases but for the same air temperature, the
droplets take a longer time but penetrate less before reaching their
steady states.

Figure 14 presents a comparison of benzene and n-octane wet-bulb
temperatures calculated in this report with wet-bulb temperatures
experimentally obtained by Ingebo (ref. 2). Referring to the benzene
curves, it can be seen that the calculated wet-bulb temperatures are
always somewhat higher than the experimental wet-bulb temperatures.
This would indicate that the computed mass transfer was too low or the
computed heat transfer was too high or both. Referring to the n-octane
curves, it can be seen that there is a cross-over of the two curves.
Extrapolation of the data of Ingebo would indicate that the droplet
would boil, in contradiction to the diffusion theory. Whether this is
a deficiency in the theory or in the experimental data of Ingebo is not
clear.

A typical temperature-time history obtained in the experimental
investigations is shown in figure 15 for a droplet of n-octane of approxi-
mately 750-micron initial radius when exposed to air moving at a constant
velocity of about 16 fps. The portion 1-2 of this graph shows the output
of the thermocouple when initially in room air. At point 2 the droplet
was hung on the thermocouple. Portion 2-3-4 of the graph represents the
rapid response of the thermocouple to the cooler-than-room-air droplet
followed by a gradual cooling to the wet-bulb temperature corresponding
to room air at point 4. This period is of particular interest in that
it gives an indication of the speed of response of the thermocouple and
recording instrument.

At point 4 a stream of hot air was suddenly swung under the droplet.
The unsteady-state or heating-up portion of the curve can be seen from

point 4 to a point chosen arbitrarily at 5 where the droplet would be judged to have closely reached the wet-bulb temperature corresponding to the temperature of the air stream. The portion 5-6 of the graph is considered to be the steady-state vaporization period. The last part of this portion, near 6, is of questionable reliability, since observation showed that as the droplet nears complete vaporization it deviates from the spherical shape assumed in the calculations and, instead, takes a distorted shape depending on the exact shape of the thermocouple junction. It should also be noted that the purity of the fuels was only about 98 percent and that this portion of the curve may represent the vaporization of the high-boiling-point impurities in the mixture.

At point 6 a thin film of the liquid fuel still remains on the thermocouple element. This soon disappears and the thermocouple temperature rises to the air temperature as represented by point 7. At that point the thermocouple is completely dry and the temperature recorded at 7 is the air temperature during the entire plot. Since this takes only a short time, the air temperature is not likely to have varied during this period. This procedure has the advantage of using a single thermocouple to measure both the droplet and air temperatures.

Since the amount of liquid fuel remaining as a thin film on the thermocouple element at point 6 in the graph is minute compared with the total liquid contained in the initial droplet, the relative magnitudes of time of portions 4-5 and 5-6 of the graph can be assumed to represent the relative importance of the unsteady and steady states, respectively.

Figure 16 shows several time histories of droplets of n-octane all of approximately equal size as subjected to air of varying temperature. The portions of the curve corresponding to 2-3-4 in figure 15 have been omitted here. It can be seen from these curves that the unsteady-state portion of the vaporization time assumes greater importance and becomes dominant at higher air temperatures.

Figure 17 shows time histories of liquids of varying volatility vaporizing under the same conditions of pressure, temperature, and velocity.

Since in the calculated curves presented in this report the velocity of the droplet was made to decrease relative to the air because of aerodynamic drag forces, while the experimental curves were measured at essentially constant air velocity past the droplets, caution must be exercised in comparing the experimental results thus obtained with the calculated curves. Figure 18 shows two calculated temperature, velocity, and rate of mass transfer (unsteady-state) histories of two droplets of n-octane of 50-micron initial radius and 100-fps initial velocity each. One was made to slow down, while the other remained at 100-fps velocity throughout the calculated period. Other conditions were kept equal.

It can be seen that the constant-velocity droplet spends less time in the unsteady-state period but has a higher rate of mass transfer during that period with consequently shorter total vaporization time. The net result would be that the unsteady state is relatively longer for the droplet that is moving at a constant speed.

The following deductions can now be made.

(1) For the same fuel the unsteady state becomes relatively larger in magnitude with respect to the total vaporization time the higher the air temperature.

(2) For the same air temperatures the unsteady state is relatively larger in magnitude with respect to the total vaporization time the higher the volatility of the fuel.

(3) High-volatility fuels have lower wet-bulb temperatures for the same air conditions.

(4) At relatively low air temperatures extremely low volatility fuels have wet-bulb temperatures close to the air temperatures and spend only a very small portion of their vaporization time in the unsteady state. At high air temperatures, however, the difference between the air and wet-bulb temperatures increases.

(5) For any one fuel the wet-bulb temperature is higher the higher the air pressure or temperature.

The penetration - mass-vaporized relationships of different size droplets are of particular interest in jet-engine combustion-chamber design. When the fuel is injected continuously into a stream of moving air, it leaves the injector nozzle first as a ligament or sheet after which this ligament or sheet breaks down to different size droplets originally moving at the same speed. If the velocity of these droplets is higher than the air velocity, these droplets start slowing down relative to the air, with the smaller droplets slowing down faster, and penetrate a lesser distance while losing their mass faster and earlier along their travel path. The mass of vapor given away by each droplet is carried along with the air through the combustion chamber. To this vapor is continuously added the vapor given away by the larger droplets that have been formed later in time but that reached that point because of their more rapid and greater penetration. The total amount of fuel vapor present at a certain cross section of the combustion chamber therefore consists of the total vapor given away by all the drops before reaching that cross section. In order to have a short combustion chamber, a combustible air-vapor mixture should be formed a short distance after injection. This would necessitate that the largest number of the

drop sizes fall in the smaller radius range so that the weight distribution of different droplet sizes in the spray would not be weighted too highly in favor of the droplets of large radius range, since these large droplets have a much greater penetration before they contribute much vapor toward forming a combustible mixture.

To illustrate the possible use of the curves of droplet mass versus time for combustion-chamber design purposes, and to emphasize the importance of the unsteady portion of the time history of the droplets, the following example was worked out with certain arbitrary but reasonable assumptions made as to the combustion-chamber operating conditions. These assumptions were:

(1) No effect of one evaporating droplet upon the other. This is in obvious contradiction to the facts, but since this effect is unknown it was necessary to neglect it.

(2) A constant air velocity of 50 fps.

(3) An air pressure of 1 atmosphere and a temperature of 500° F. The 500° F air temperature is admittedly high with respect to the air temperature coming from the compressor, but calculations were available for this temperature and recirculation, which was neglected, would undoubtedly increase the air temperature.

(4) The fuel used was n-octane.

(5) A drop-size weight distribution of 25 percent for the 10-micron group, 65 percent for the 50-micron group, and 10 percent for the 100-micron group.

(6) An initial fuel velocity relative to the air of 100 fps.

The previously performed calculations were extended through the steady state until the droplets nearly disappeared. Such a calculation showing temperature, mass, and penetration relative to the air versus time for the 50-micron droplet is shown in figure 19. The masses vaporized from each size droplet were then calculated and plotted versus distance traveled by each droplet relative to the combustion chamber using the assumed airspeed of 50 fps, as shown in figure 20.

Using the arbitrarily chosen droplet size distribution, the percentage of the total fuel vaporized from each droplet size group up to any distance after droplet formation was then plotted in figure 21. The total vapor present, which is the sum of the three curves, is also shown in figure 21. Assuming a fuel-air mixture strength in the primary combustion zone to be in the neighborhood of 0.08, and a possible inflammability ratio of 0.03 of the vapor-air ratio, a total vaporization in the

neighborhood of 35 percent would be adequate for initiating combustion under these assumptions. According to the calculations presented in figure 21, this would take place 8 inches after the droplets have been formed.

It is to be noted that these calculations are approximate at best. Turbulence, backflow, and heat transfer by radiation have not been taken into account. However, they serve to show the possible use of the calculated curves for estimation purposes. A knowledge of droplet size distribution seems also to be fundamental in any such vaporization calculations.

An important observation shown by the above calculations is that the 50- and 100-micron droplets reach the combustion zone while still in the heating-up or unsteady-state portion of vaporization, a fact that further emphasizes the importance of the unsteady state in any combustion studies. It is the opinion of the authors that the unsteady state is of primary importance in forming a combustible mixture and that experimental studies which could be used either to verify or to correct the extrapolation of the heat and mass transfer correlations used should be conducted. Until these extrapolations are confirmed, the absolute accuracy of the curves can be questioned, although it is not believed that any of the conclusions reached would be altered. After these relationships have been confirmed or corrected, it would then seem necessary to determine the effect of one droplet upon another. This information together with drop size distribution should then permit a rational and reasonable determination of the time required to form a combustible mixture in a heterogeneous mixture of fuel droplets and air.

University of Wisconsin,
    Madison, Wisc., March 12, 1953.

APPENDIX A

SAMPLE OF CALCULATIONS

The unsteady-state portion of the vaporization time of a droplet of benzene was calculated for the following data:

Droplet initial radius r_{o1} = 50 microns = 1.9685×10^{-3} in.

Droplet initial temperature T_{L1} = 50° F = 510° R

Droplet initial velocity relative to the air U_1 = 400 fps = 4,800 in./sec

Air pressure P_T = 1 atm = 14.696 lb/sq in. abs

Air temperature T_B = $1,000^{\circ}$ F = $1,460^{\circ}$ R

A stepwise method was used in integrating the equations as follows: The temperature of the droplet was assumed to undergo a small increase ΔT_L over a small period of time $\Delta \theta$, during which the properties of the liquid fuel, fuel vapor, and air could be considered to be constant. The heat and mass transfer during this period were then calculated together with the velocity change, from which the time required for the temperature increase together with the radius and velocity at the end of the increment were calculated. However, these three values had to be assumed prior to the calculation and compared with the calculated values.

For a droplet-temperature increase of 5° F it was assumed that:

$$\Delta \theta = 2.7 \times 10^{-5} \text{ sec}$$

$$U_2 = 4,725 \text{ in./sec}$$

$$r_{o2} = 1.970 \times 10^{-3} \text{ in.}$$

For this increment:

$$T_L = \text{average temperature of droplet} = \frac{510 + 515}{2} = 512.5^{\circ} \text{ R}$$

The various properties in the film and for the droplet were then calculated and read as follows:

$$p_{fL} = 0.970 \text{ lb/sq in. abs}$$

$$\rho_m = 2.678 \times 10^{-5} \text{ lb/cu in.}$$

$$\mu_m = 1.475 \times 10^{-6} \text{ lb/(in.)(sec)}$$

$$k_m = 5.591 \times 10^{-7} \text{ Btu/(in.)(sec)(°F)}$$

$$c_{p_m} = 0.2609 \text{ Btu/(lb)(°F)}$$

$$D_v = 3.60 \times 10^{-2} \text{ sq in./sec}$$

$$\lambda = 189.0 \text{ Btu/lb}$$

$$c_{p_f} = 0.422 \text{ Btu/(lb)(°F)}$$

$$\rho_{L1} = 3.154 \times 10^{-2} \text{ lb/cu in.}$$

$$\rho_{L2} = 3.150 \times 10^{-2} \text{ lb/cu in.}$$

$$c_{p_L} = 0.4080 \text{ Btu/(lb)(°F)}$$

r_o = Average radius of the droplet for the increment

$$= \frac{r_{o1} + r_{o2}}{2}$$

$$= \left(\frac{1.9685 + 1.970}{2} \right) \times 10^{-3}$$

$$= 1.9693 \times 10^{-3} \text{ in.}$$

$$U = \text{Average velocity of the droplet}$$

$$= \frac{U_1 + U_2}{2}$$

$$= \frac{4,800 + 4,725}{2}$$

$$= 4,762.5 \text{ in./sec}$$

$$N_{Re} = \text{Reynolds number}$$

$$= \frac{2r_o U \rho_m}{\mu_m}$$

$$= 340.568$$

$$C_D \left(\text{at } N_{Re} \right) = 0.6633$$

Applying equation (18):

$$\frac{\Delta U}{\Delta \theta} = - \frac{3}{8} C_D \frac{\rho_m}{\rho_{L1}} \frac{U^2}{r_o} = 2.4326 \text{ in./sec}^2$$

and

$$U = 65.681 \text{ in./sec}$$

Therefore

$$U_2 = 4,800 - 65.681 = 4,734.319 \text{ in./sec}$$

as compared with the assumed value of 4,725 in./sec. This process was then repeated, selecting the correct coefficient of drag each time until a value for U_2 was arrived at that satisfied the velocity equation. Therefore

$$U_2 = 4,730.79 \text{ in./sec}$$

$$N_{Re} = 340.775$$

and

$$N_{Sc} = \frac{\mu_m}{\rho_m D_v} = 1.5299$$

Therefore

$$k_g = \frac{D_v \rho_m}{2 p_a r_o} \left[2 + 0.6 \left(N_{Sc} \right)^{1/3} \left(N_{Re} \right)^{1/2} \right]$$

$$= 2.5427 \times 10^{-4} \text{ sec}^{-1}$$

$$\alpha = \frac{\dfrac{p_T}{p_{fL}}}{\log_e \dfrac{p_T}{p_T - p_{fL}}} = 1.030$$

Therefore

$$w = k_g \alpha p_{fL} 4 \pi r_o^2 = 1.2381 \times 10^{-8} \text{ lb/sec}$$

$$N_{Pr} = \frac{C_{p_m} \mu_m}{k_m} = 0.6883$$

Therefore

$$h = \frac{k_m}{2 r_o} \left[2 + 0.6 \left(N_{Pr} \right)^{1/3} \left(N_{Re} \right)^{1/2} \right]$$

$$= 1.6721 \times 10^{-3} \text{ Btu/(sec)(sq in.)(°F)}$$

$$Q = h A_o \left(T_B - T_L \right) = 7.7213 \times 10^{-5} \text{ Btu/sec}$$

$$\frac{z}{e^z - 1} = 0.9683$$

Therefore

$$Q_v = Q \frac{z}{e^z - 1} = 7.4764 \times 10^{-5} \text{ Btu/sec}$$

$$Q_s = Q - Q_v = 2.4488 \times 10^{-6} \text{ Btu/sec}$$

$$Q_\lambda = w\lambda = 2.34006 \times 10^{-6} \text{ Btu/sec}$$

and

$$Q_L = Q_v - Q_\lambda = 7.2424 \times 10^{-5} \text{ Btu/sec}$$

$$m_1 = \text{Mass of droplet at beginning of increment}$$

$$= 4/3\pi r_{o1}^3 \rho_L \text{ (at } 510^\circ \text{ R)}$$

$$= 1.00936 \times 10^{-9} \text{ lb}$$

$$m_2 = \text{Mass of droplet at end of increment}$$

$$= m_1 - w \Delta\theta$$

$$= 1.00901 \times 10^{-9} \text{ lb}$$

$$m = \frac{m_1 + m_2}{2} = 1.009186 \times 10^{-9} \text{ lb}$$

Therefore

$$\Delta\theta = \frac{m C_{p_L} \Delta T_L}{Q_L} = 2.8426 \times 10^{-5} \text{ sec}$$

(as compared with the estimated value of 2.7×10^{-5} second).

$$r_{o2} = \left(\frac{3m_2}{4\pi \rho_{L2}}\right)^{1/3} = 1.97017 \times 10^{-3} \text{ in.}$$

(as compared with the estimated value of 1.970×10^{-3} inch).

The calculations for this first increment were then repeated taking the calculated values of time, velocity, and radius as new assumptions to obtain more accurate results. The final values of U_2, r_{o2}, and m_2, calculated for the first increment, then became the original values of the next increment and the same stepwise method was used for the second increment. The calculations were stopped when Q_L approached zero, indicating that the asymptotic or wet-bulb temperature has been approached.

APPENDIX B

CALCULATIONS OF PROPERTIES IN FILM

The computations described in the analysis require the use of the thermal conductivity, viscosity, density, and specific heat of the air-vapor mixture in the film surrounding the droplet. The concentrations of fuel vapor and air are not constant across the film, with the mixture being the richest in the vicinity of the droplet and leaner away from it. To a good approximation the molal ratio of fuel vapor to air equals the ratio of the partial pressure due to the fuel vapor to the partial pressure due to the air in the film. Thus the largest fuel-vapor - air ratio occurs at the surface of the droplet and is essentially equal to the ratio of the vapor pressure at the droplet temperature to the partial pressure due to the air, or p_{fL}/p_{aL}. This ratio becomes zero at the outer edge of the film, provided there is no interaction between droplets.

It has been shown for plane surfaces (ref. 8) that in the case of a fully permeable film, where mass transfer takes place in both directions and equimolal diffusion exists, the partial pressure gradients would be linear throughout the film. The temperature in the film which in most of the cases varies from a maximum of T_B, the air temperature at the outer edge of the film, to T_L, the droplet temperature at the inner edge, would follow a linear gradient only in the case of no mass transfer. In the case under consideration, that is, a semipermeable film with mass transfer in one direction only, where part of the incoming heat is picked up by the diffusing vapor, the linearity of both the partial pressure and temperature gradients in the film ceases to exist.

An exact evaluation of the properties in the film surrounding a spherical droplet would render the equations almost impossible to integrate, and furthermore the precision with which some of the properties are known probably does not justify the work required. Thus an averaging technique in the film was employed. The properties then have been calculated at the logarithmic average temperature in the film T_m and for a fuel-vapor - air mixture of constant concentration equal to one-half the concentration at the droplet surface. The following equations were used:

$$T_m = \frac{T_B - T_L}{\log_e \dfrac{T_B}{T_L}} \tag{29}$$

$$k_m = \left(1 - \frac{p_{fL}}{2p_T}\right)k_a + \frac{p_{fL}}{2P_T}\,k_f \tag{30}$$

$$\mu_m = \left(1 - \frac{p_{fL}}{2P_T}\right)\mu_a + \frac{p_{fL}}{2P_T}\,\mu_f \tag{31}$$

$$\rho_m = \frac{P_T M_m}{12RT_m}$$

$$= \frac{P_T}{12RT_m}\left[\left(1 - \frac{p_{fL}}{2P_T}\right)M_a + \frac{p_{fL}}{2P_T}\,M_f\right] \tag{32}$$

$$c_{p_m} = g_a c_{p_a} + g_f c_{p_f}$$

$$= \frac{\left(1 - \frac{p_{fL}}{2P_T}\right)M_a}{M_m}\,c_{p_a} + \frac{\frac{p_{fL}}{2P_T}\,M_f}{M_m}\,c_{p_f} \tag{33}$$

In these relations the pure properties of the fuel vapor and air have been taken at the logarithmic mean temperature in the film.

Figure 22 shows the properties in the film versus droplet temperature as calculated for n-octane and air.

APPENDIX C

JUSTIFICATION FOR ASSUMPTION OF HIGH FUEL CONDUCTIVITY

AND UNIFORM DROPLET TEMPERATURE

As can be deduced from equation (21), the calculations performed
in this project assumed a large thermal conductivity through the liquid
droplet and a resulting uniform temperature throughout the droplet at
all times. An estimation of the validity of the above assumptions can
be made from the charts prepared by Gurney and Lurie (ref. 9; discussion
given in ref. 10) for determining the relationship between temperature
and time at various points in spheres and other shapes. To adapt this
method to the cases of interest here, the resistance ratio $k_L/h_L r_o$ was
used, where k_L is the thermal conductivity of the liquid fuel evaluated
at the temperature of the droplet; h_L, a coefficient of heat transfer to
the liquid droplet based on the portion of heat transferred to the droplet
that appears as sensible heat $\left(Q_L\right)$; and r_o, the radius of the droplet.
The use of this parameter together with the charts permits an estimation
of the possible difference between the temperature at the surface of the
droplet and the temperature at its center, respectively. The Gurney-
Lurie charts specify that the temperatures at the midpoint and at the
surface would differ considerably when the resistance ratio is small and
only slightly when it is large. Referring specifically to the Gurney-
Lurie charts for spheres, if the resistance ratio is 6 or more, the tem-
perature difference is negligibly small; while, if the resistance ratio
is 1 or 2, the temperature difference is appreciable and should be taken
into account. However, the Gurney-Lurie charts were based on the assump-
tions of constancy in the temperature surrounding the surface of the body,
the resistance ratio, and the thermal diffusivity in the body under con-
sideration; and it should be realized that, under the conditions of an
evaporating droplet, the charts should be used for estimation purposes
only.

Values for the resistance ratio are plotted in figure 23 for n-octane,
benzene, and n-pentane versus heating-up time together with the droplet
temperatures calculated by the methods previously described in this report
for an air pressure of 1 atmosphere and an air temperature of 500° F.
Figures 24(a) and 24(b) show the resistance ratio plotted for benzene at
a constant air pressure of 1 atmosphere and a constant air temperature
of 500° F, respectively.

The data of figures 23 and 24 indicate that the assumption of high
thermal conductivity in the liquid droplet is unquestionably good for

high-volatility fuels, is of reasonable validity for medium-volatility
fuels, and should be further investigated for the low-volatility fuels.
If internal circulation (ref. 7) exists in t': droplets under the con-
ditions of interest here, it could effectively increase the conductivity
of the liquid.

REFERENCES

1. Ranz, W. E., and Marshall, W. R.: Evaporation From Drops. Part I. Chem. Eng. Prog., vol. 48, no. 3, Mar. 1952, pp. 141-146; part II, no. 4, Apr. 1952, pp. 173-180.

2. Ingebo, Robert D.: Vaporization Rates and Heat-Transfer Coefficients for Pure Liquid Drops. NACA TN 2368, 1951.

3. Wentzel, W.: Zum Zündvorgang im Dieselmotor. Forsch. Geb. Ing.-Wes., Bd. 6, Nr. 3, May-June 1935, pp. 105-115. (Available in English translation as NACA TM 797.)

4. Hougen, Olaf A., and Watson, Kenneth M.: Chemical Process Principles. Part III - Kinetics and Catalysis. John Wiley & Sons, Inc., 1947.

5. Hirschfelder, J. O., Curtiss, C. F., and Bird, R. B.: Molecular Theory of Gases and Liquids. John Wiley & Sons, Inc., 1954.

6. Rouse, H.: Elementary Mechanics of Fluids. John Wiley & Sons, Inc., 1947.

7. Hughes, R. R., and Gilliland, E. R.: The Mechanics of Drops. Chem. Eng. Prog., vol. 48, no. 10, Oct. 1952, pp. 497-504.

8. Ackermann, G.: Wärmeübergang und molekulare Stoffübertragung im gleichen Feld bei grossen Temperatur- und Partialdruckdifferenzen. Forschungsheft 382, Forsch. Geb. Ing.-Wes., 1937.

9. Gurney, H. P., and Lurie, J.: Charts for Estimating Temperature Distributions in Heating or Cooling Solid Shapes. Ind. and Eng. Chem., vol. 15, no. 11, Nov. 1923, pp. 1170-1172.

10. McAdams, William H.: Heat Transmission. Second ed., McGraw-Hill Book Co., Inc., 1942.

11. Maxwell, J. B.: Data Book on Hydrocarbons. D. Van Nostrand Co., Inc., 1950.

12. National Research Council (Edward W. Washburn, ed.): International Critical Tables. Vols. I-VII. McGraw-Hill Book Co., Inc., 1926-1930.

13. Timmermans, J.: Physico-Chemical Constants of Pure Organic Compounds. Elsevier Pub. Co., 1950.

14. Anon.: Selected Values of Properties of Hydrocarbons. Res.
    Proj. 44, A.P.I. and Nat. Bur. Standards, July 1949.

15. Smith, J. F. Downie: The Thermal Conductivity of Liquid. Trans.
    A.S.M.E., vol. 58, no. 8, Nov. 1936, pp. 719-725.

TABLE I

REFERENCES FROM WHICH PROPERTIES WERE OBTAINED

FOR FUELS AND FOR AIR

Property	Reference			
	n-Octane	Benzene	n-Pentane	Air
ρ_L	11 and 12	11	13	--
k_f	11	12	11 and 12	1
μ_f	11	12	11	1
λ	11	12	11	--
p_{fL}	11	11	11	--
c_{p_f}	14	14	14	11
c_{p_L}	13 and 14	13	13 and 14	--
k_L	15	15	15	--
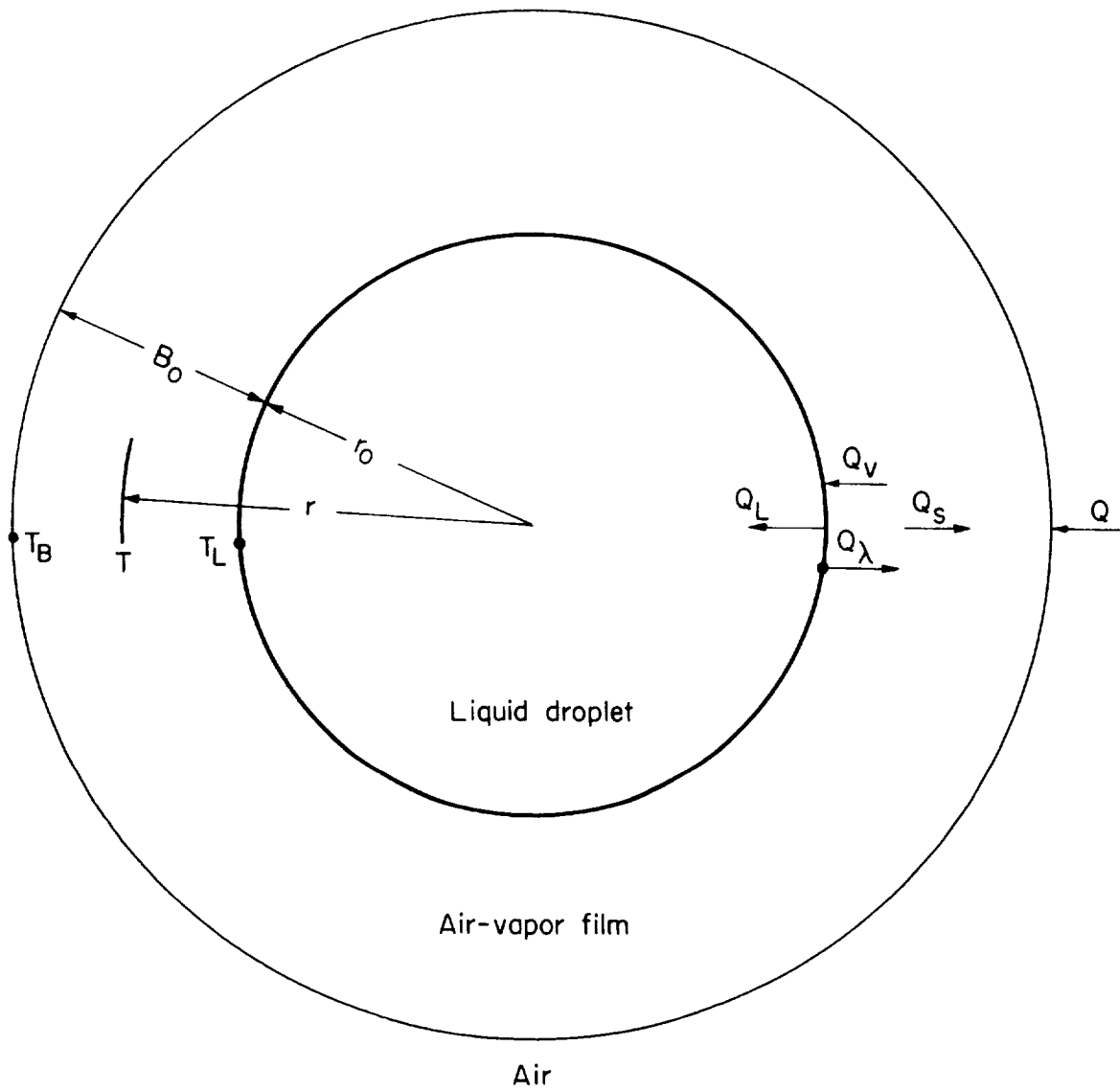
Figure 1.- Heat transfer to droplet.
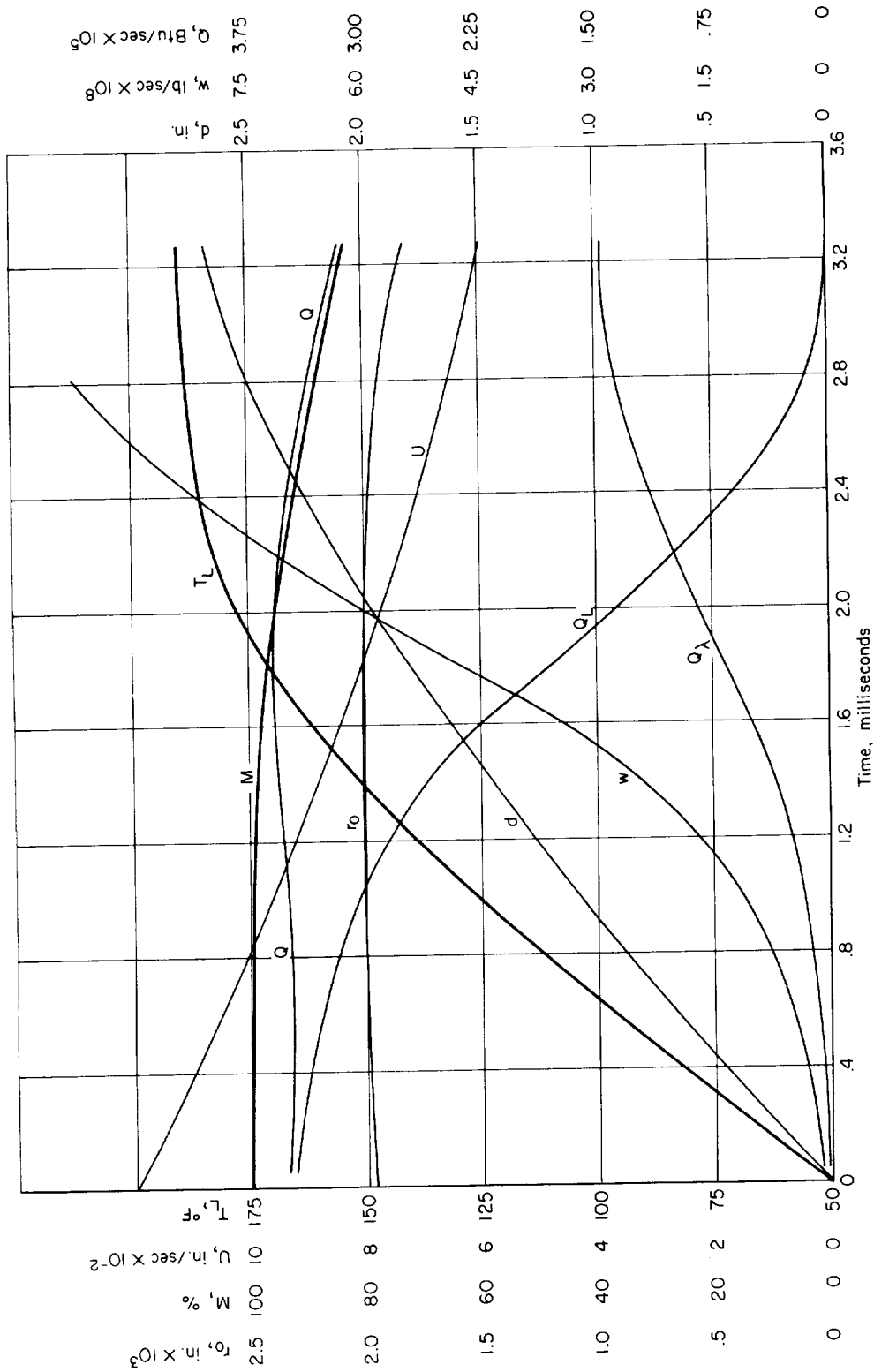
Figure 2.- Typical vaporization-time history for droplet of n-octane with initial radius of 50 microns. $T_l = 50°$ F; $U_l = 100$ fps; $P_T = 0.5$ atmosphere; $T_B = 1,000°$ F.
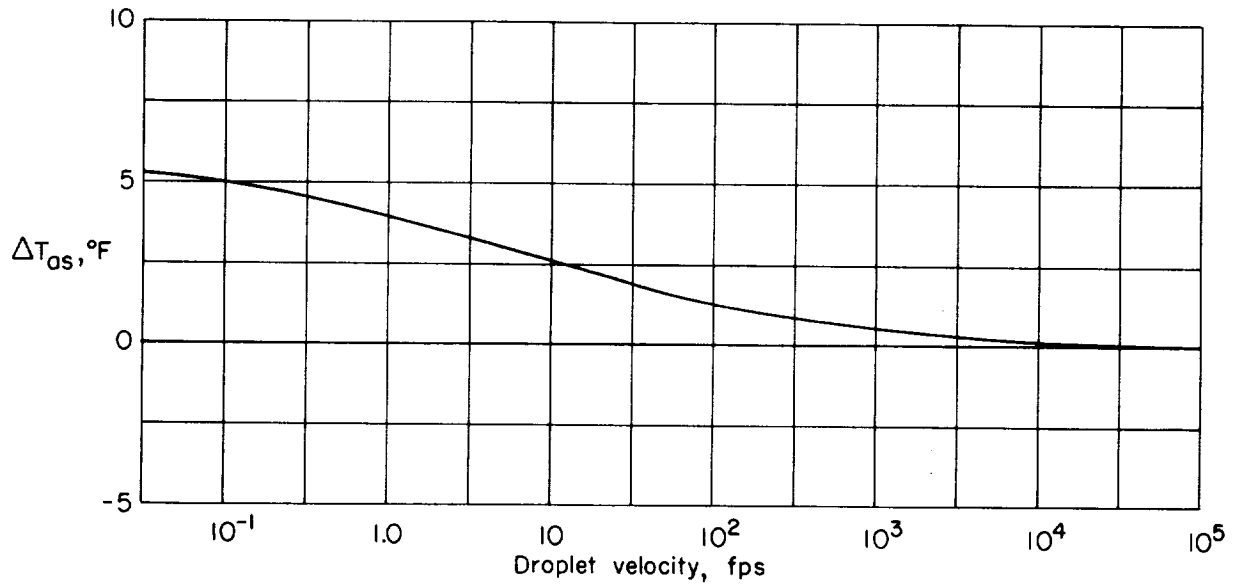
(a) Effect of droplet velocity. $r_0 = 10$ microns.
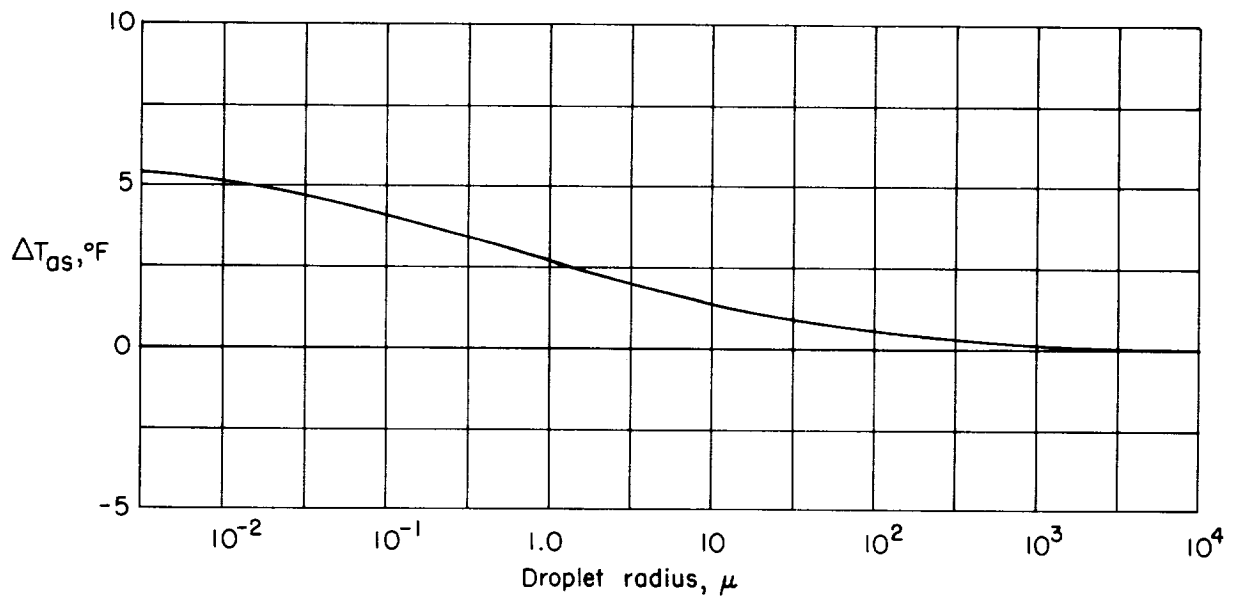
(b) Effect of droplet radius. Velocity, 100 fps.

Figure 3.- Effect of droplet velocity and radius on T_{as}. Fuel, n-pentane; $P_T = 1$ atmosphere; $T_B = 100^\circ$ F.
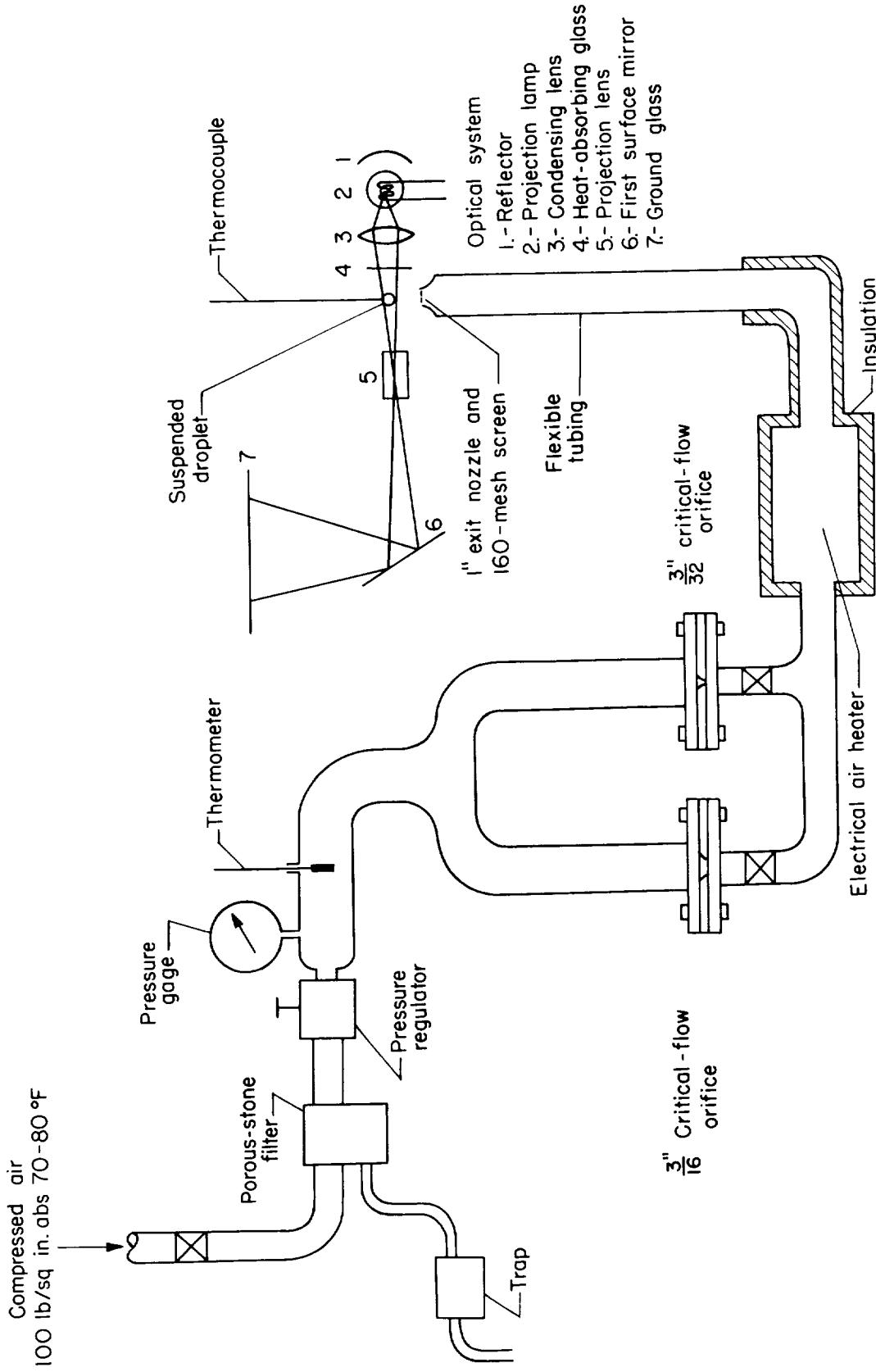
Figure 4.- Schematic diagram of vaporization equipment.
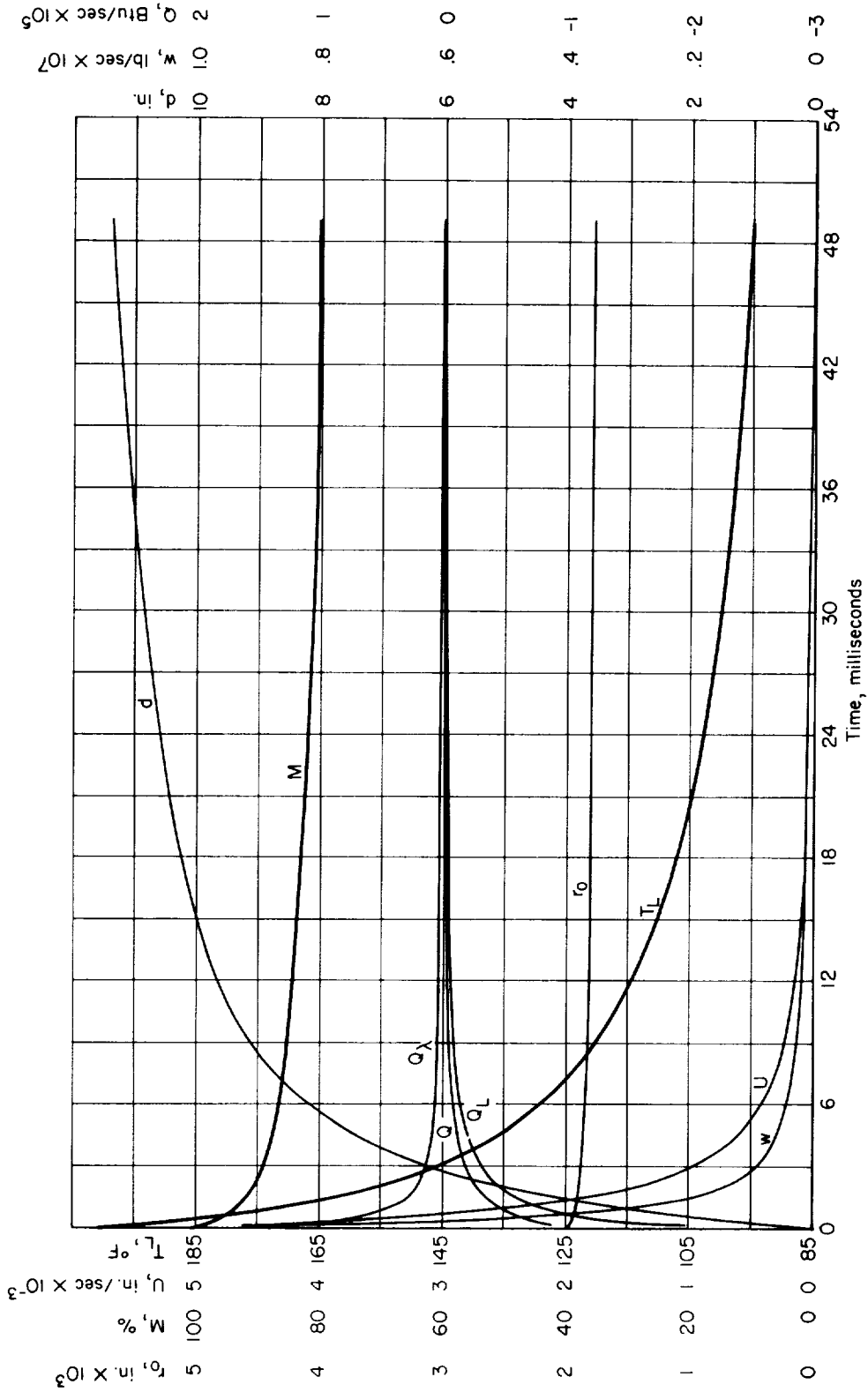
Figure 5.- Vaporization-time history for droplet of n-octane with initial radius of 50 microns. $T_1 = 2000°$ F; $U_1 = 400$ fps; $P_T = 1$ atmosphere; $T_B = 100°$ F.
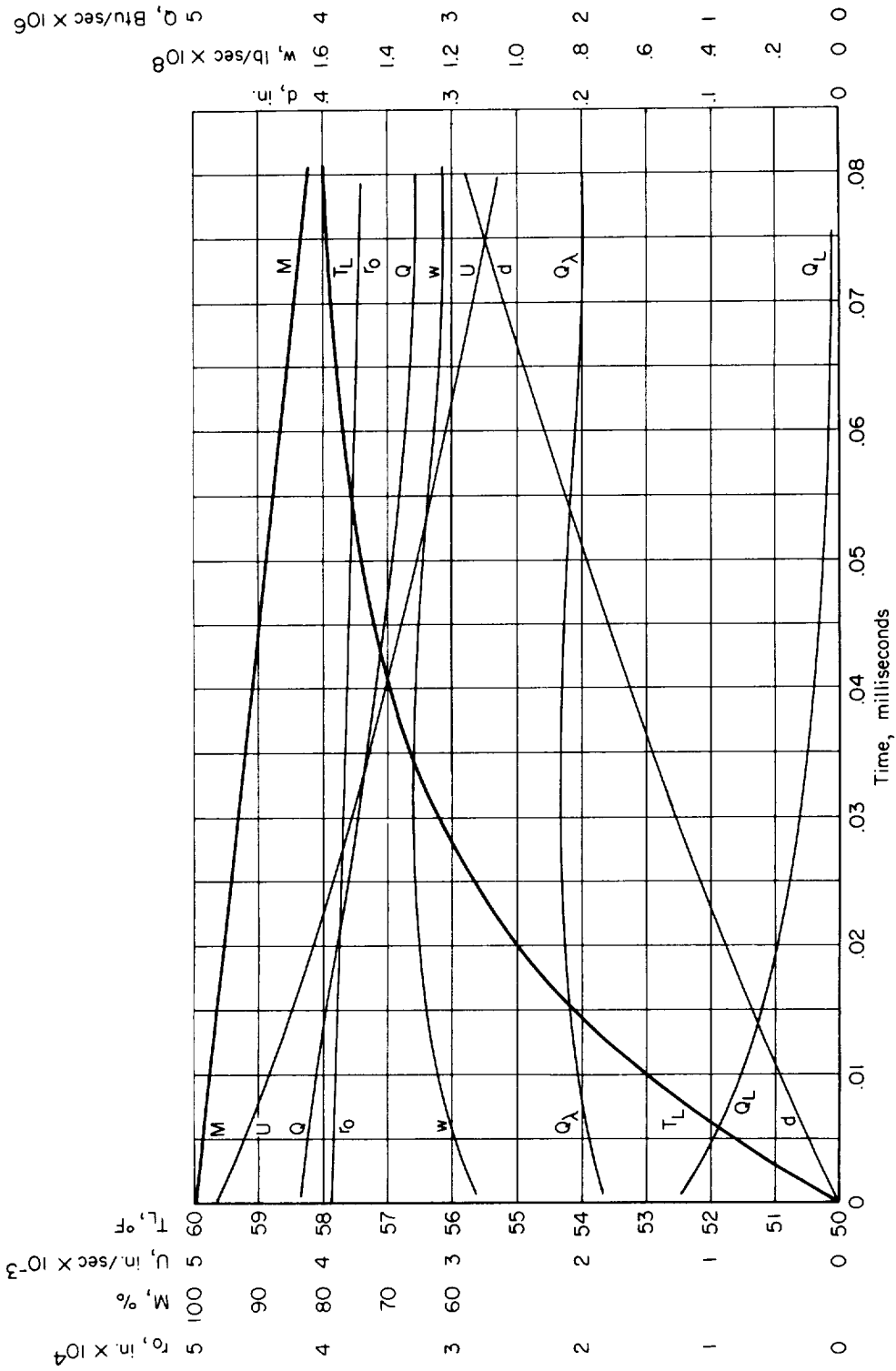
(a) Initial radius, 10 microns; $P_T = 1$ atmosphere. $T_1 = 50^\circ$ F;
$U_1 = 400$ fps; $T_B = 500^\circ$ F.

Figure 6.- Vaporization-time history for droplet of n-pentane.
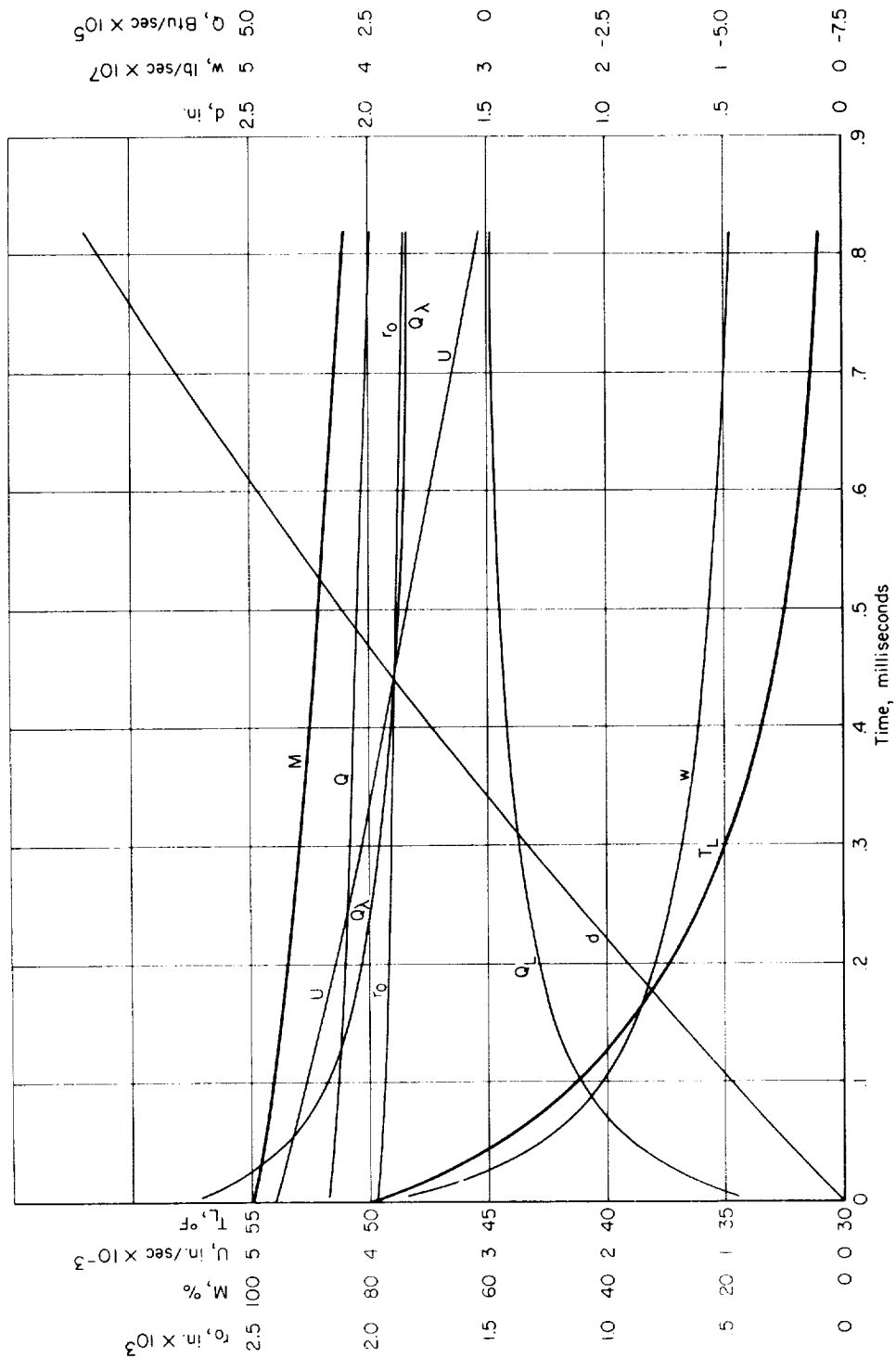
(b) Initial radius, 50 microns; $P_T = 0.5$ atmosphere.

Figure 6.- Concluded.
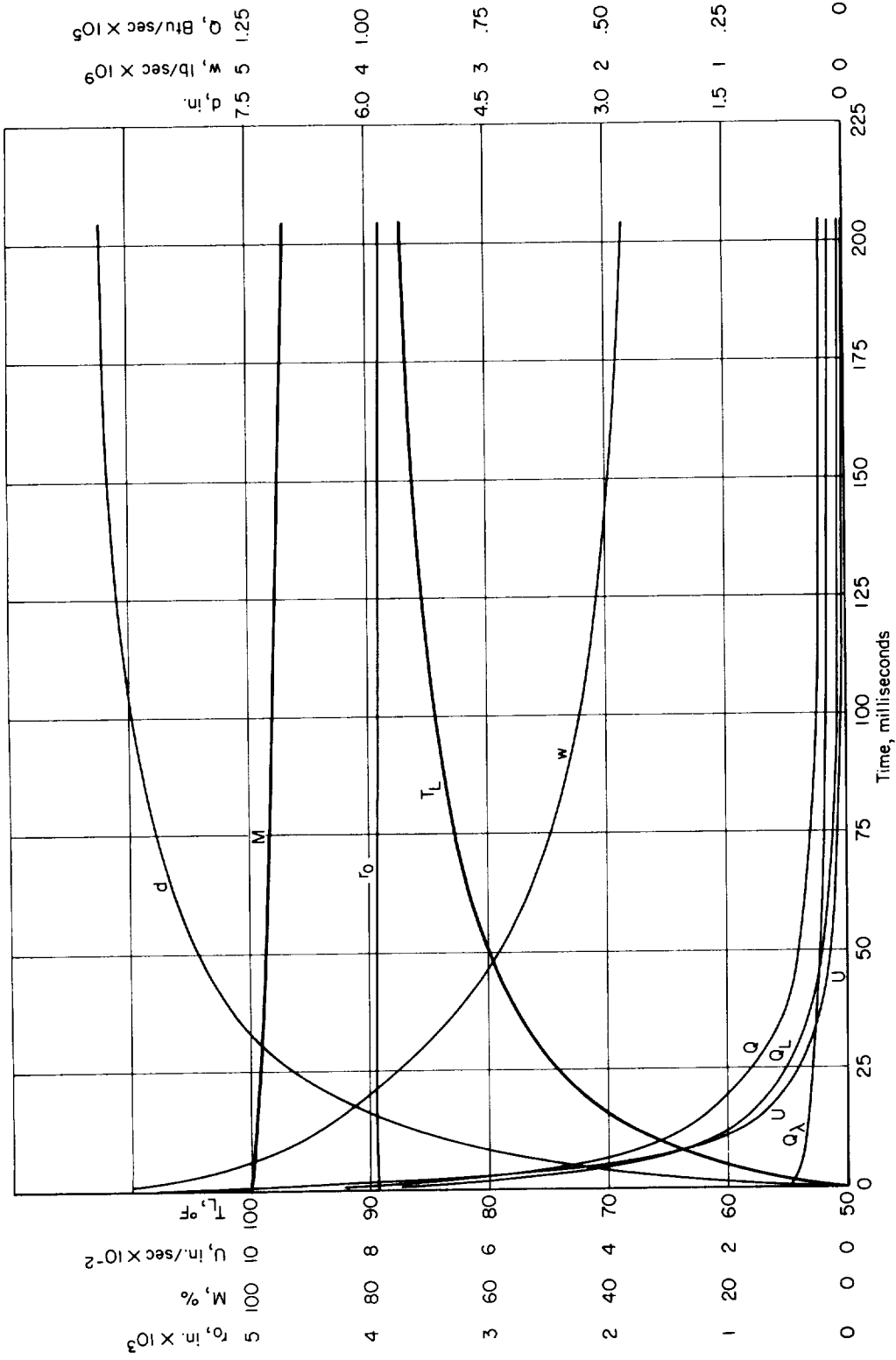
Figure 7.- Vaporization-time history for droplet of benzene with initial radius of 100 microns. $T_l = 50^\circ$ F; $U_l = 100$ fps; $P_T = 5$ atmospheres; $T_B = 100^\circ$ F.
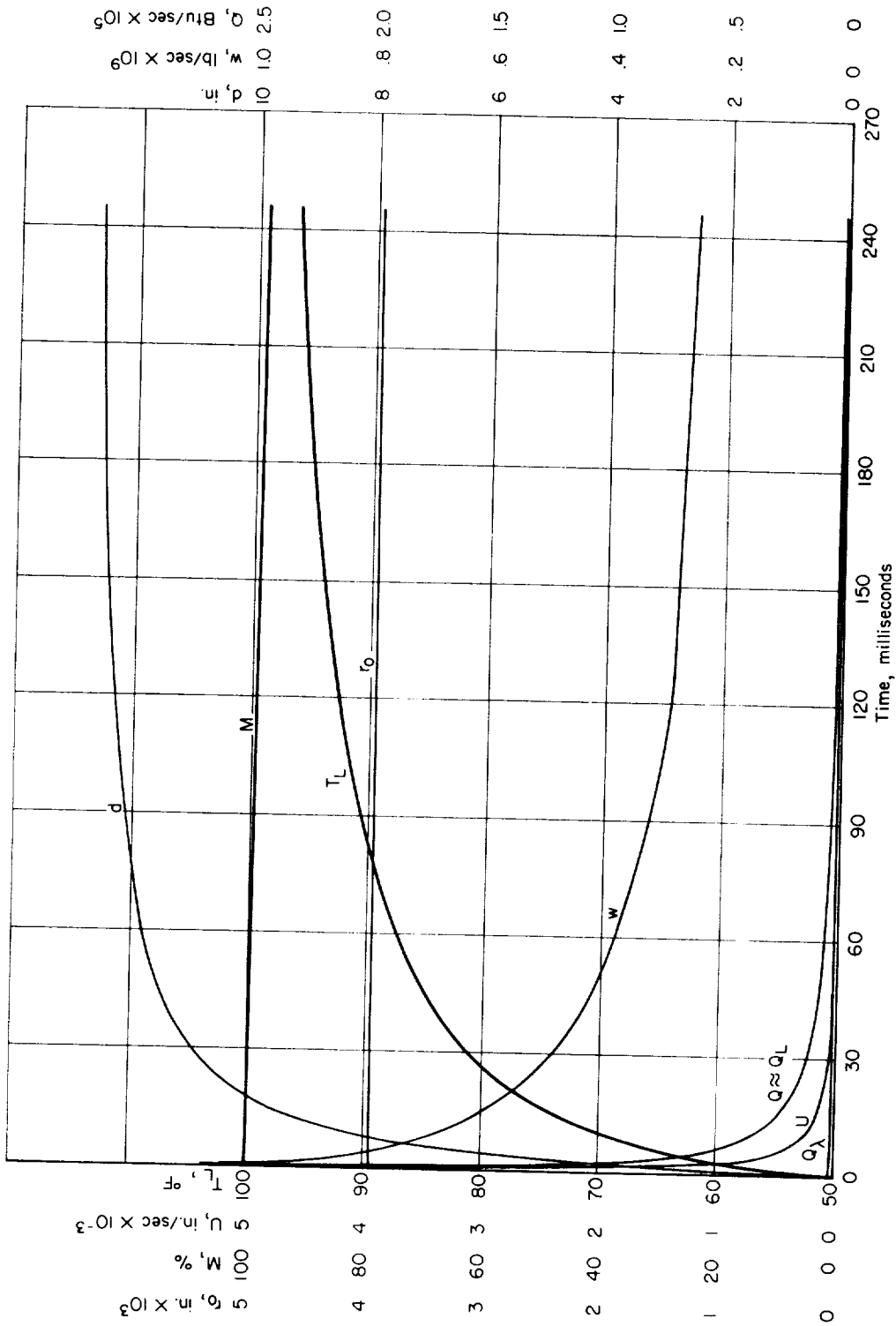
(a) $U_l = 400$ fps; $P_T = 5$ atmospheres.

Figure 8.- Vaporization-time history for droplet of n-octane with initial radius of 100 microns. $T_l = 50°$ F; $T_B = 100°$ F.
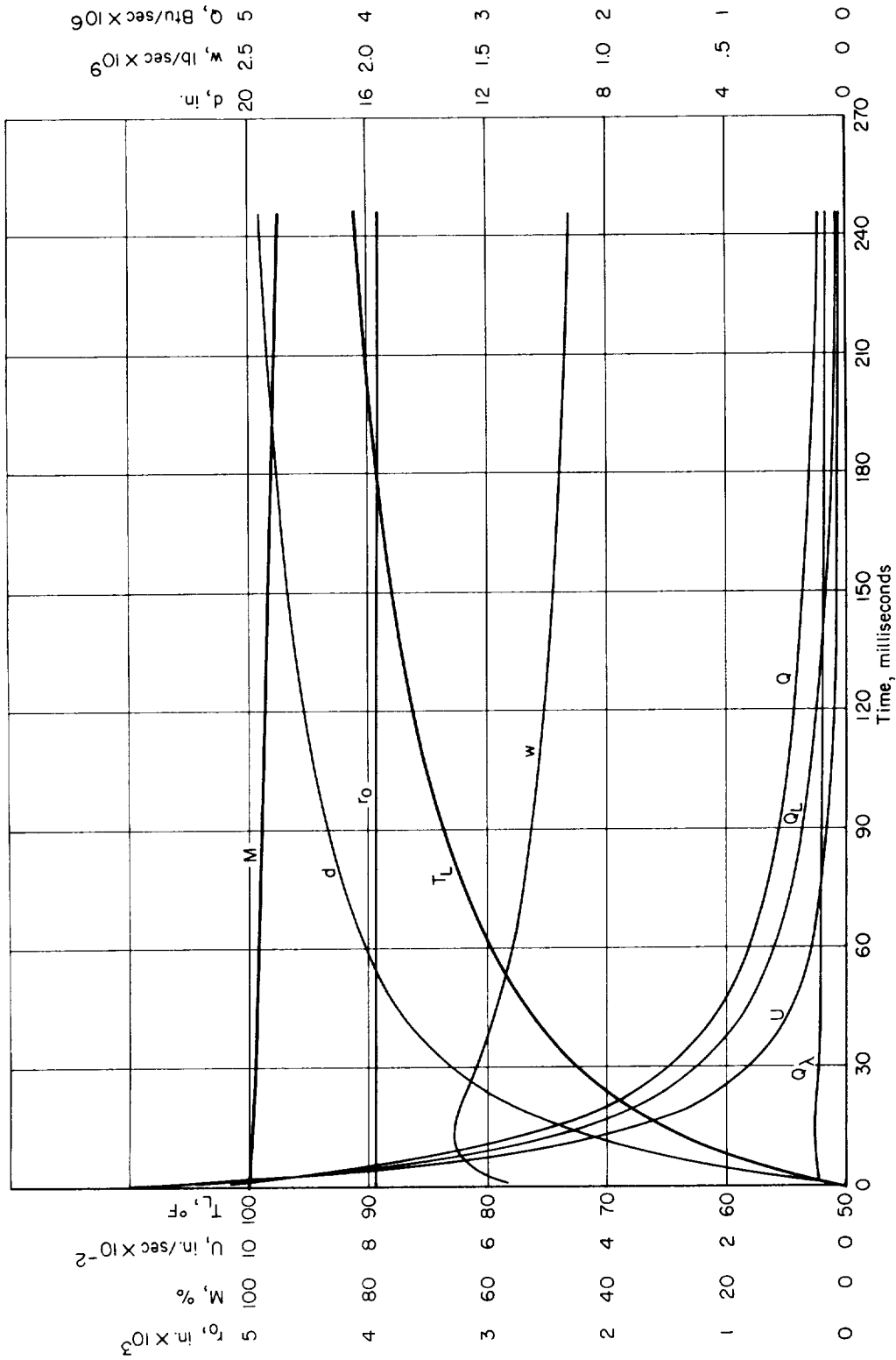
(b) $U_1 = 100$ fps; $P_{T1} = 1$ atmosphere.

Figure 8.- Concluded.
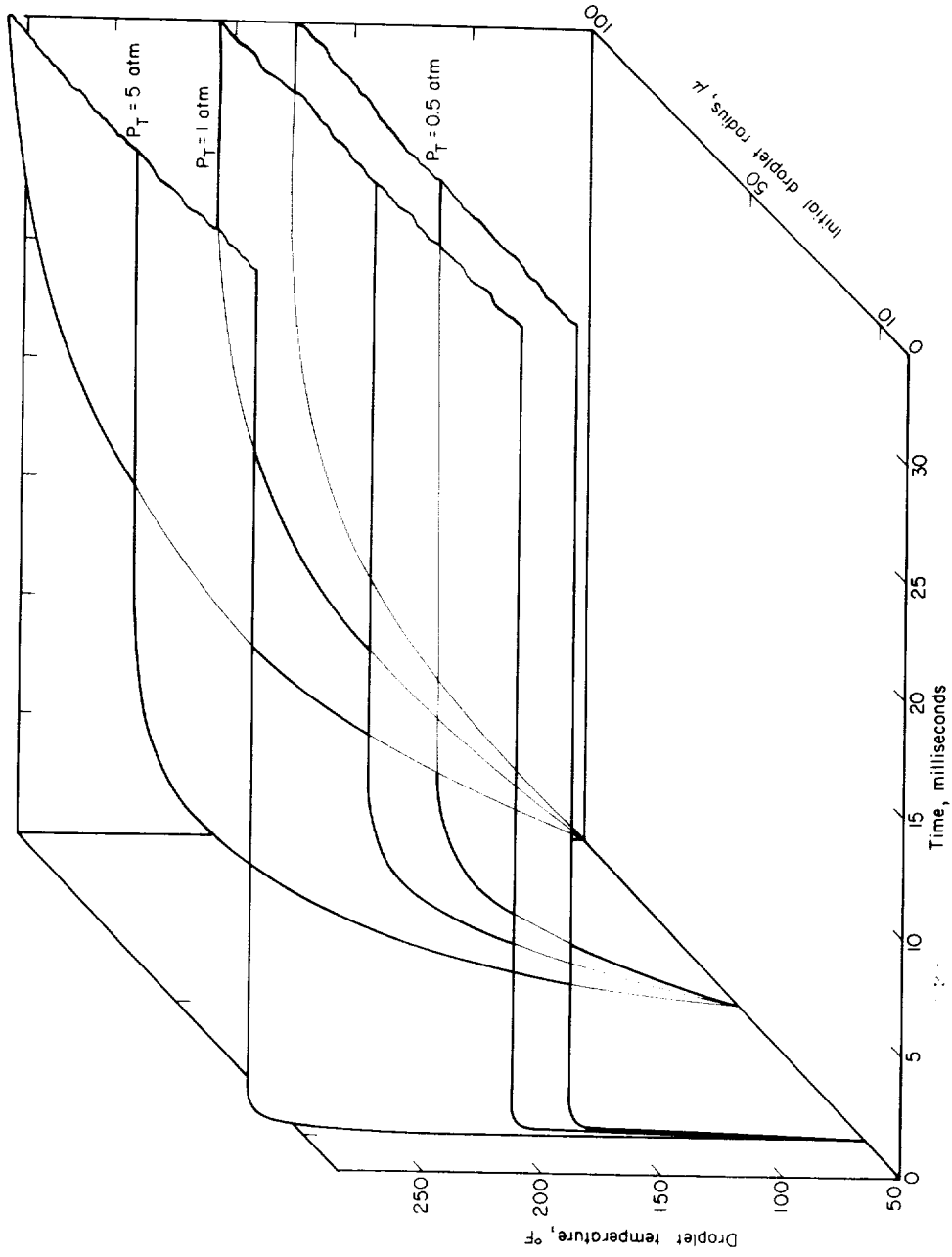
(a) At constant air temperature T_B of 500° F.

Figure 9.- Temperature-time histories of n-octane. T_l = 50° F; U_l = 100 fps.
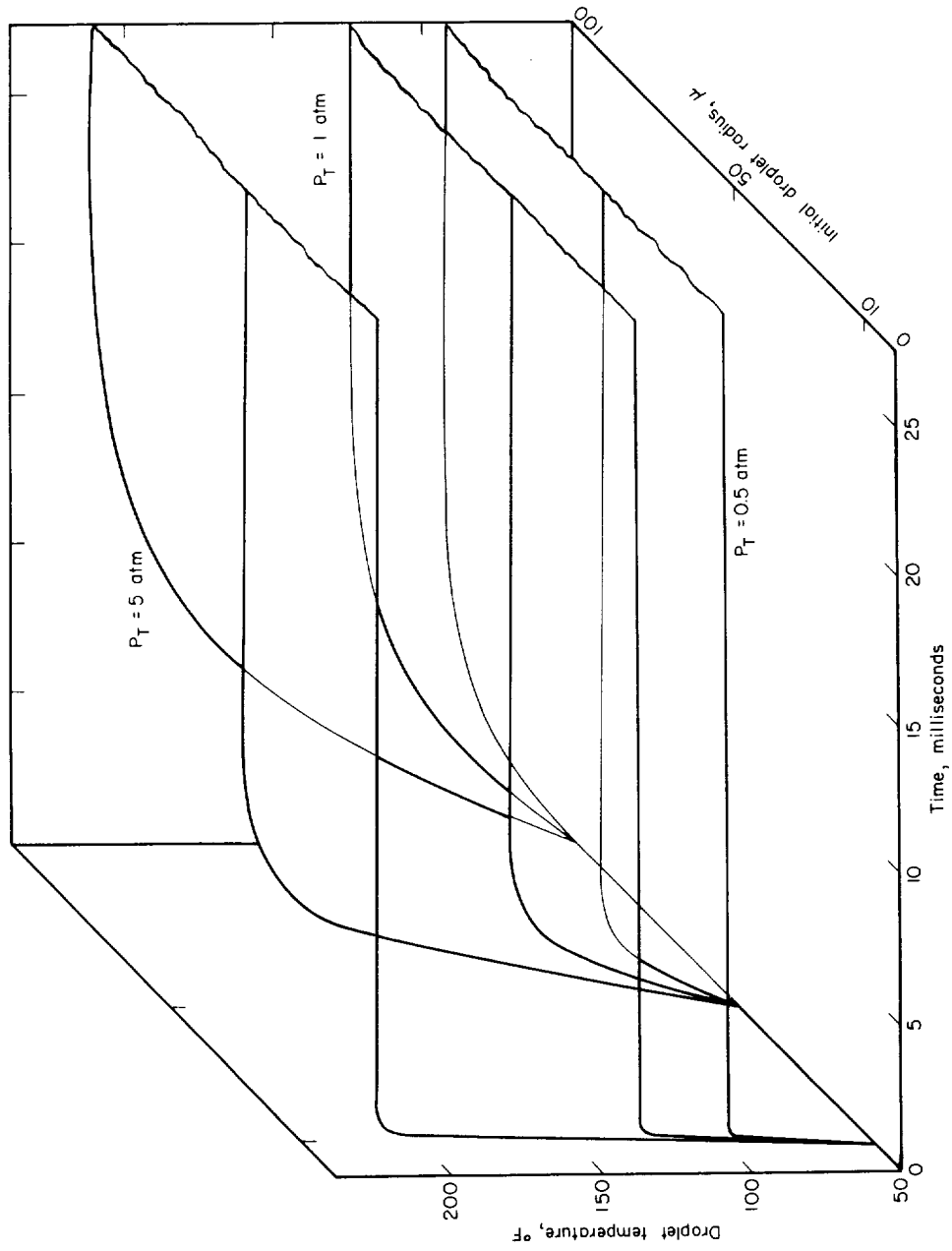
(a) At constant air temperature T_B of 500° F.

Figure 10.- Temperature-time histories of benzene. $T_1 = 50°$ F; $U_1 = 100$ fps.
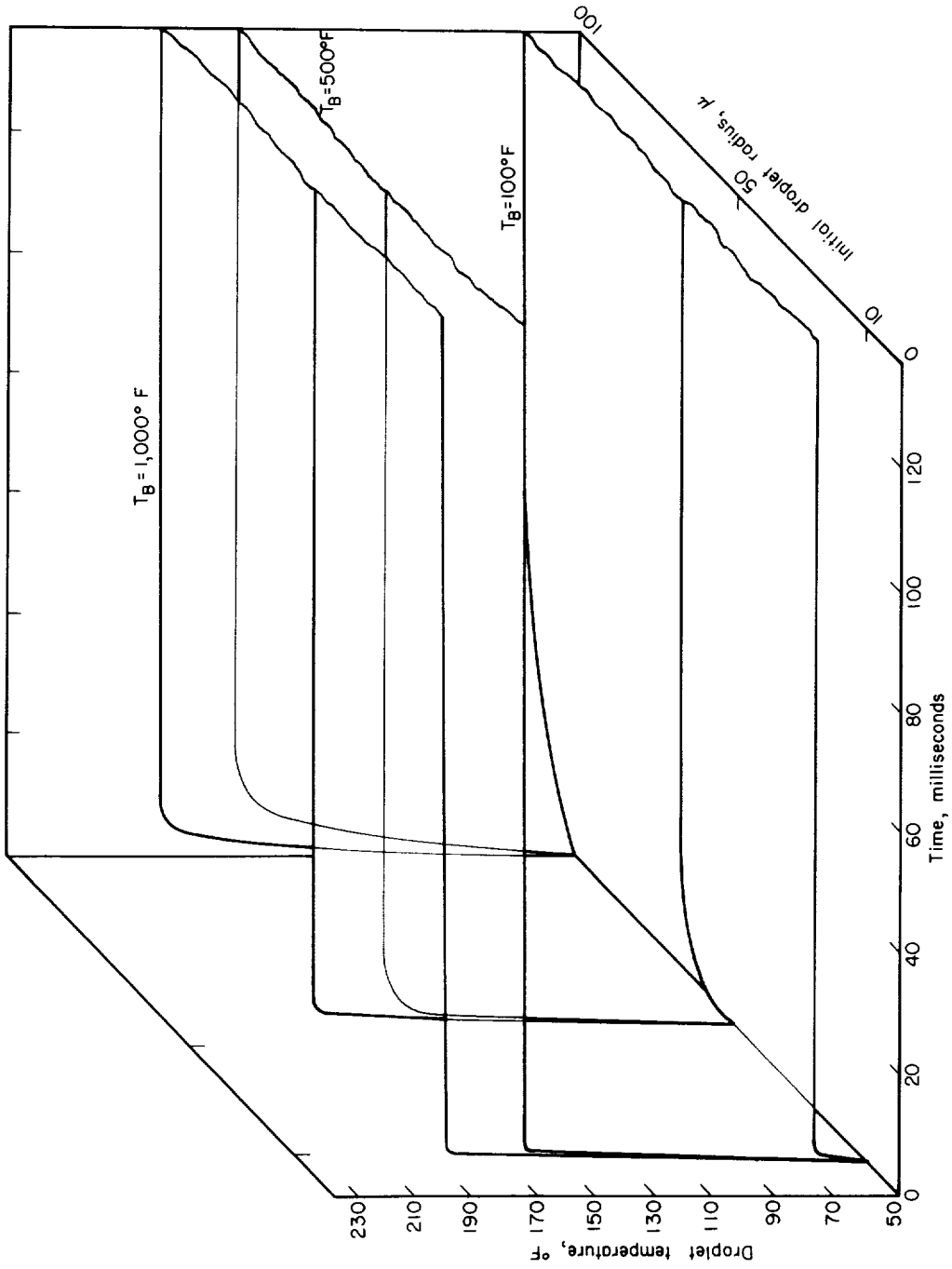
(b) At constant air pressure P_T of 1 atmosphere.

Figure 10.- Continued.
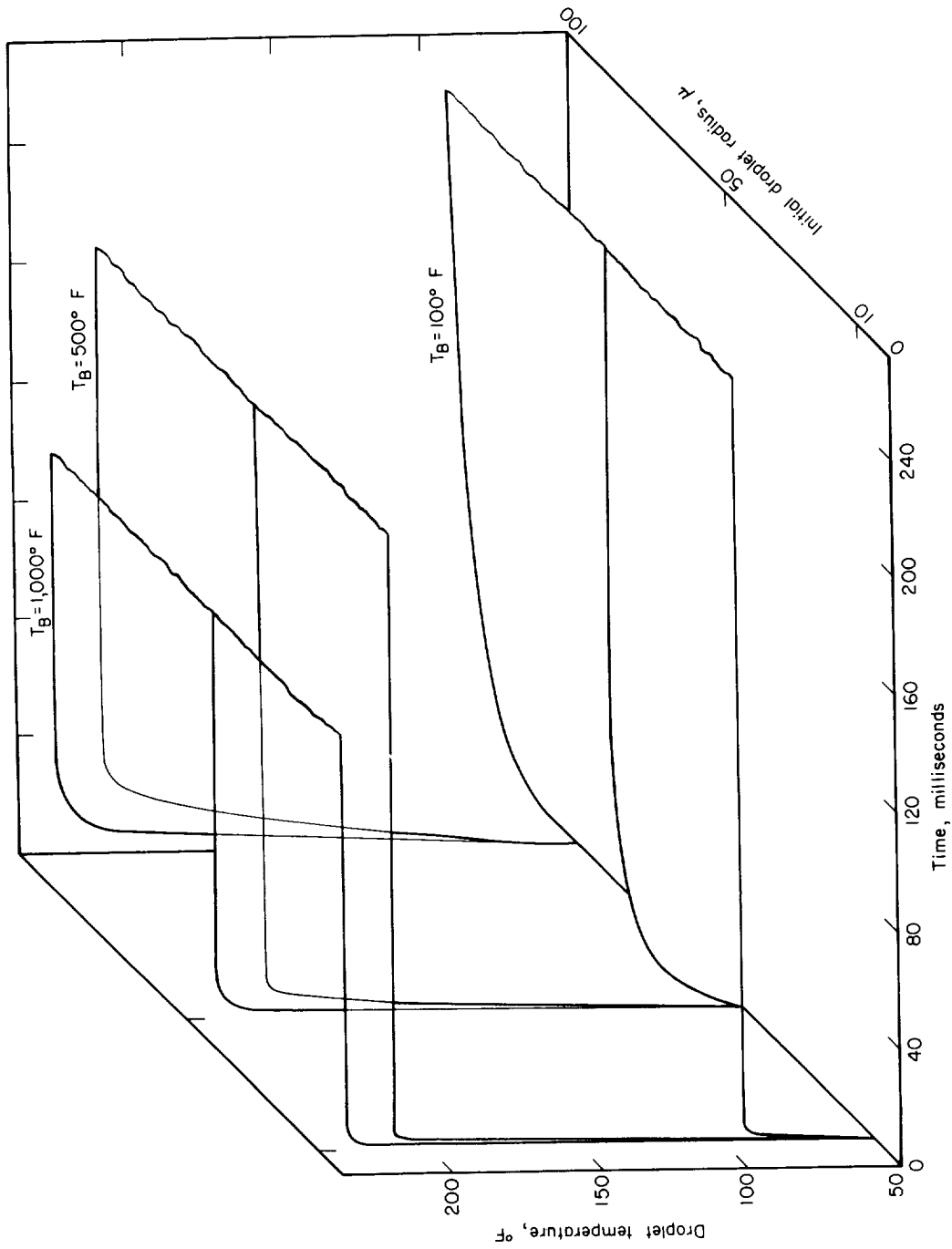
(b) At constant air pressure P_T of 1 atmosphere.

Figure 9.- Continued.
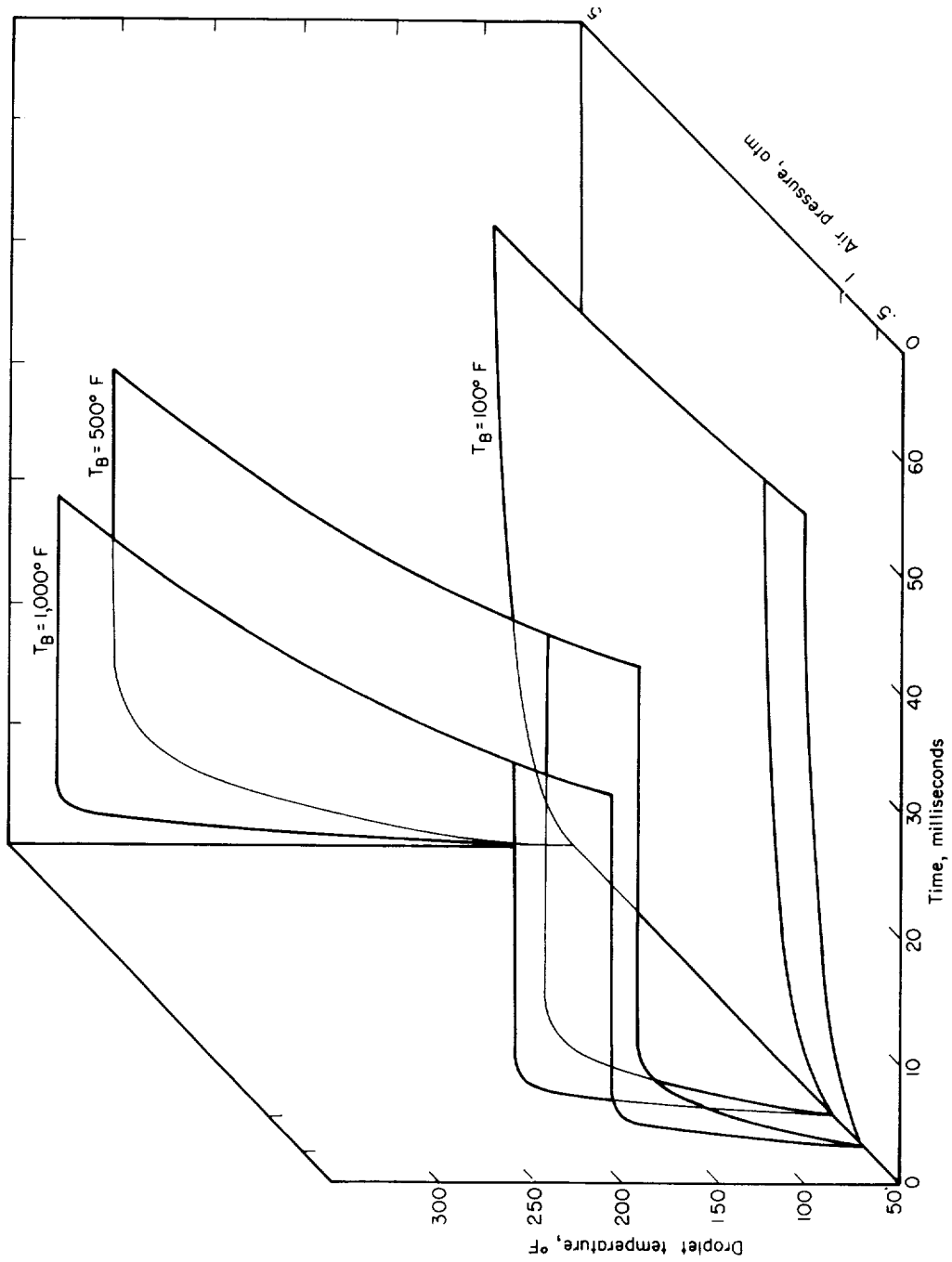
(c) With constant initial radius r_{ol} of 50 microns.

Figure 9.- Concluded.
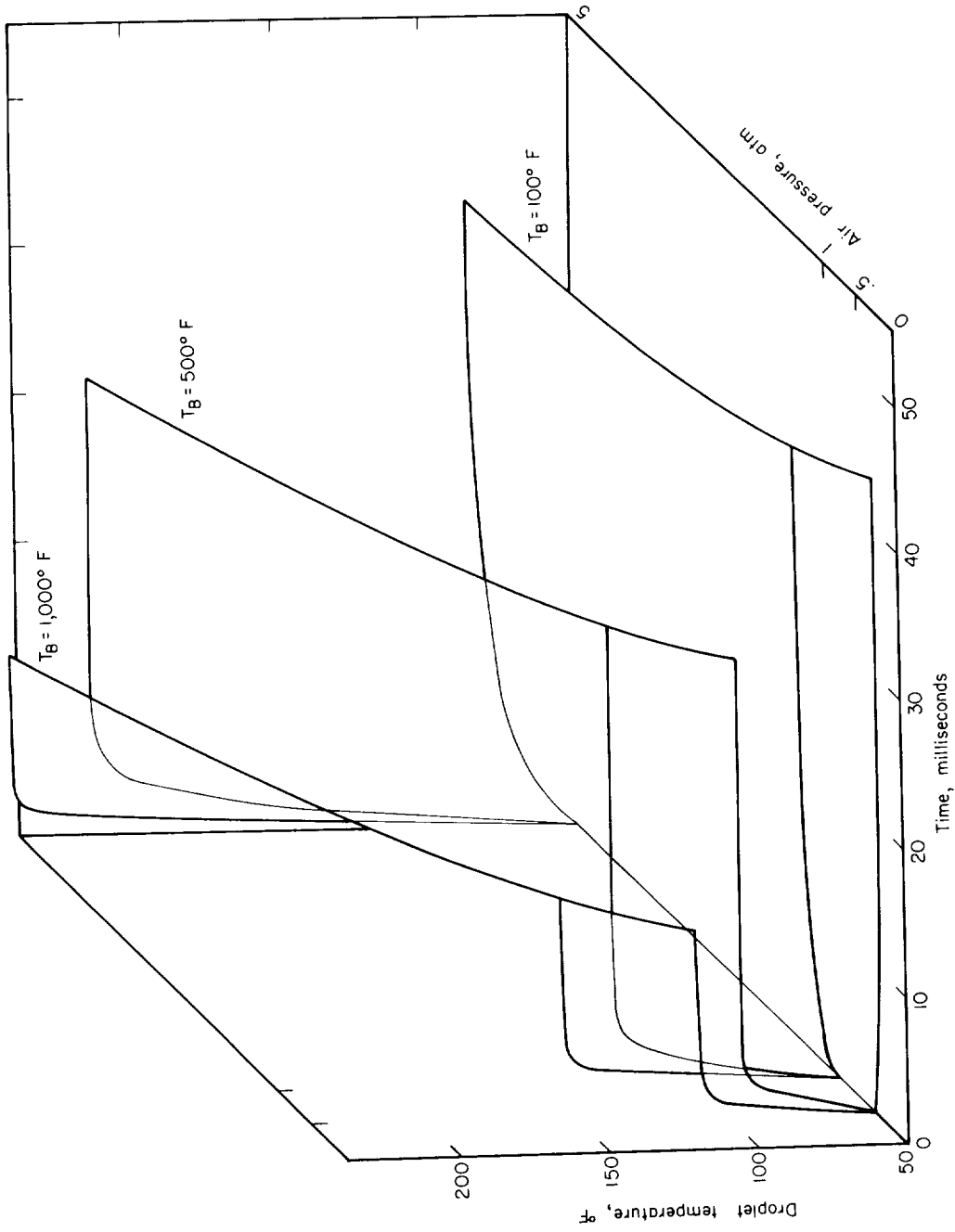
(c) With constant initial radius r_{o1} of 50 microns.

Figure 10.- Concluded.
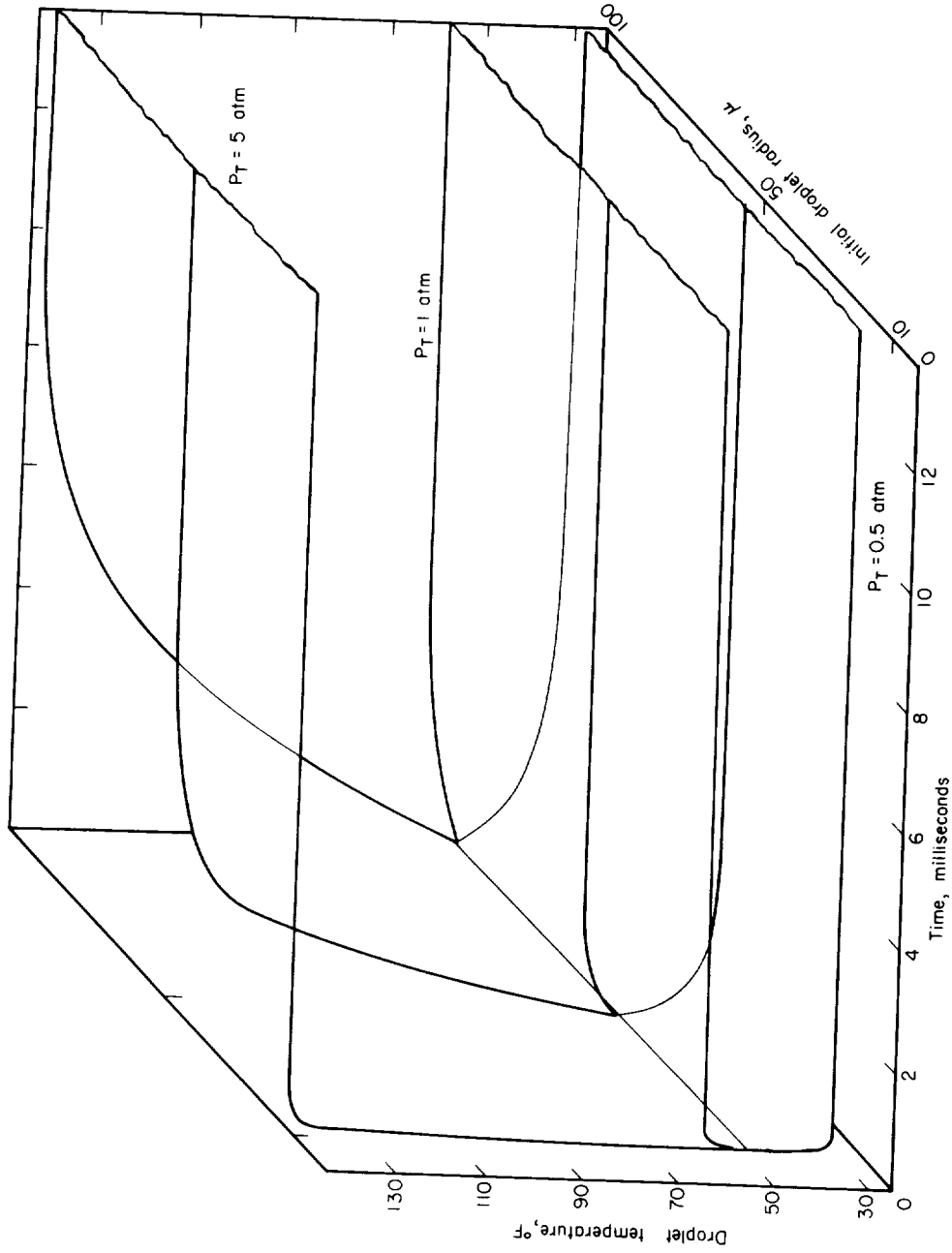
(a) At constant air temperature T_B of 500^0 F.

Figure 11.- Temperature-time histories of n-pentane. $T_1 = 50^0$ F; $U_1 = 100$ fps.
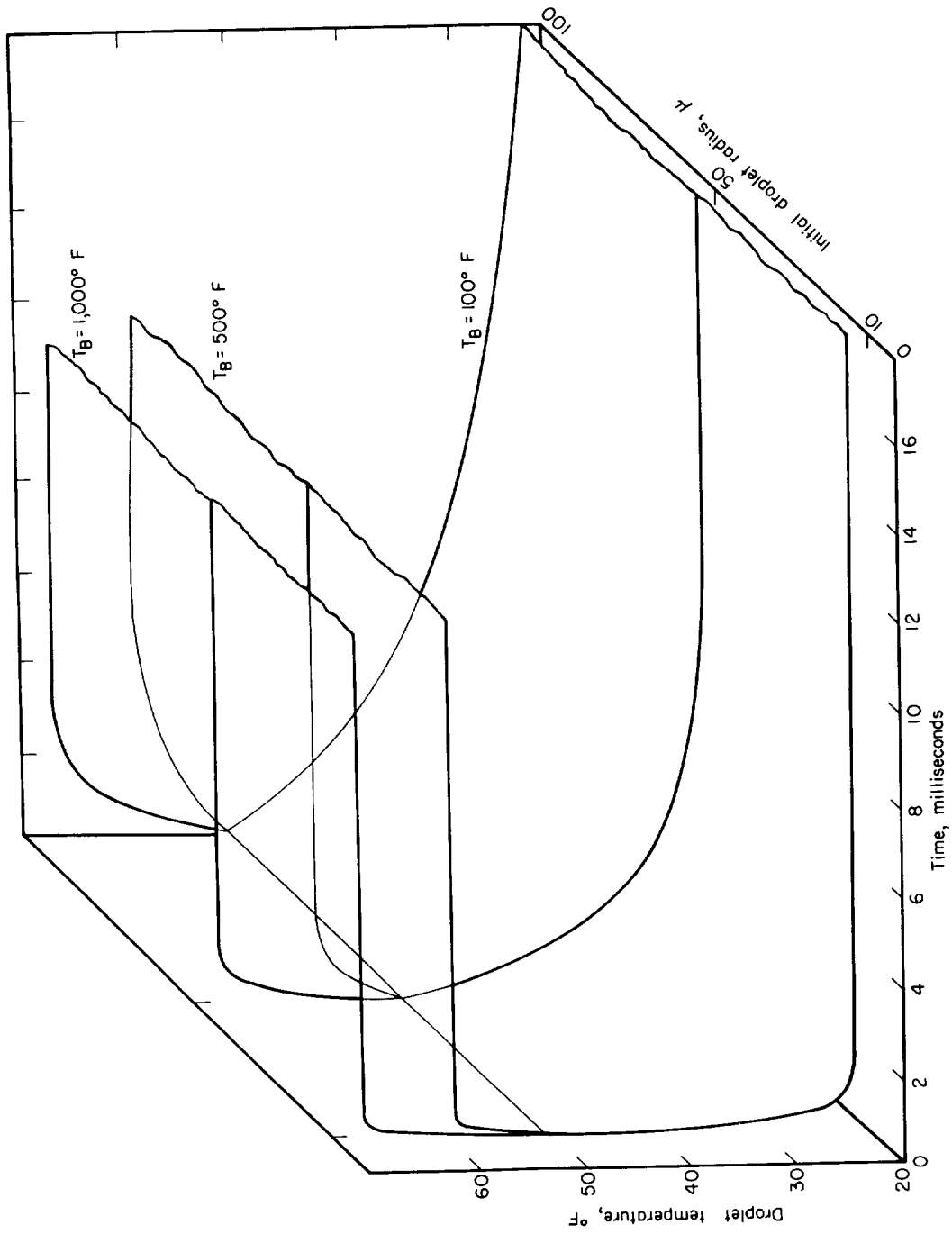
(b) At constant air pressure P_T of 1 atmosphere.

Figure 11.- Continued.
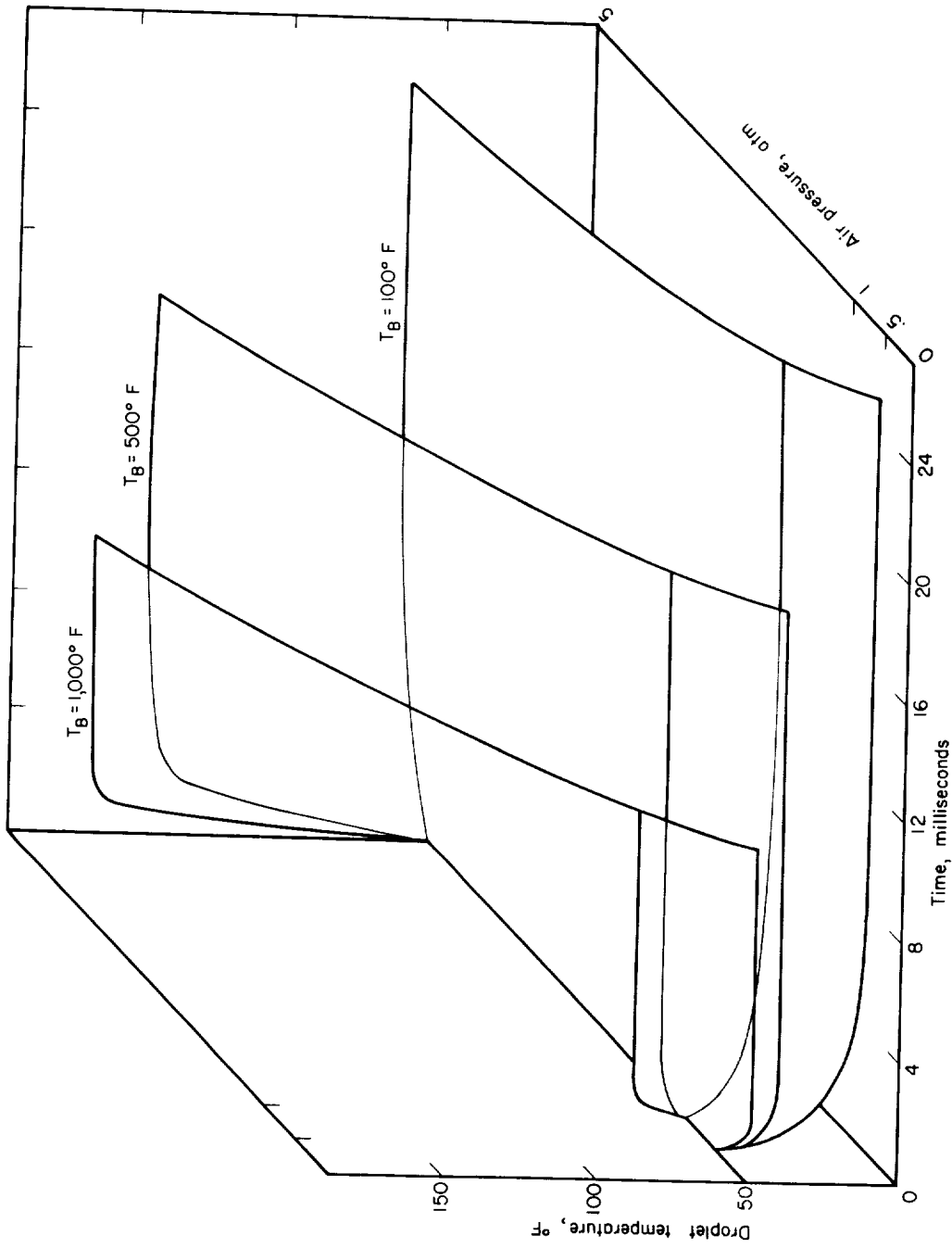
(c) With constant initial radius r_{0l} of 50 microns.

Figure 11.- Concluded.
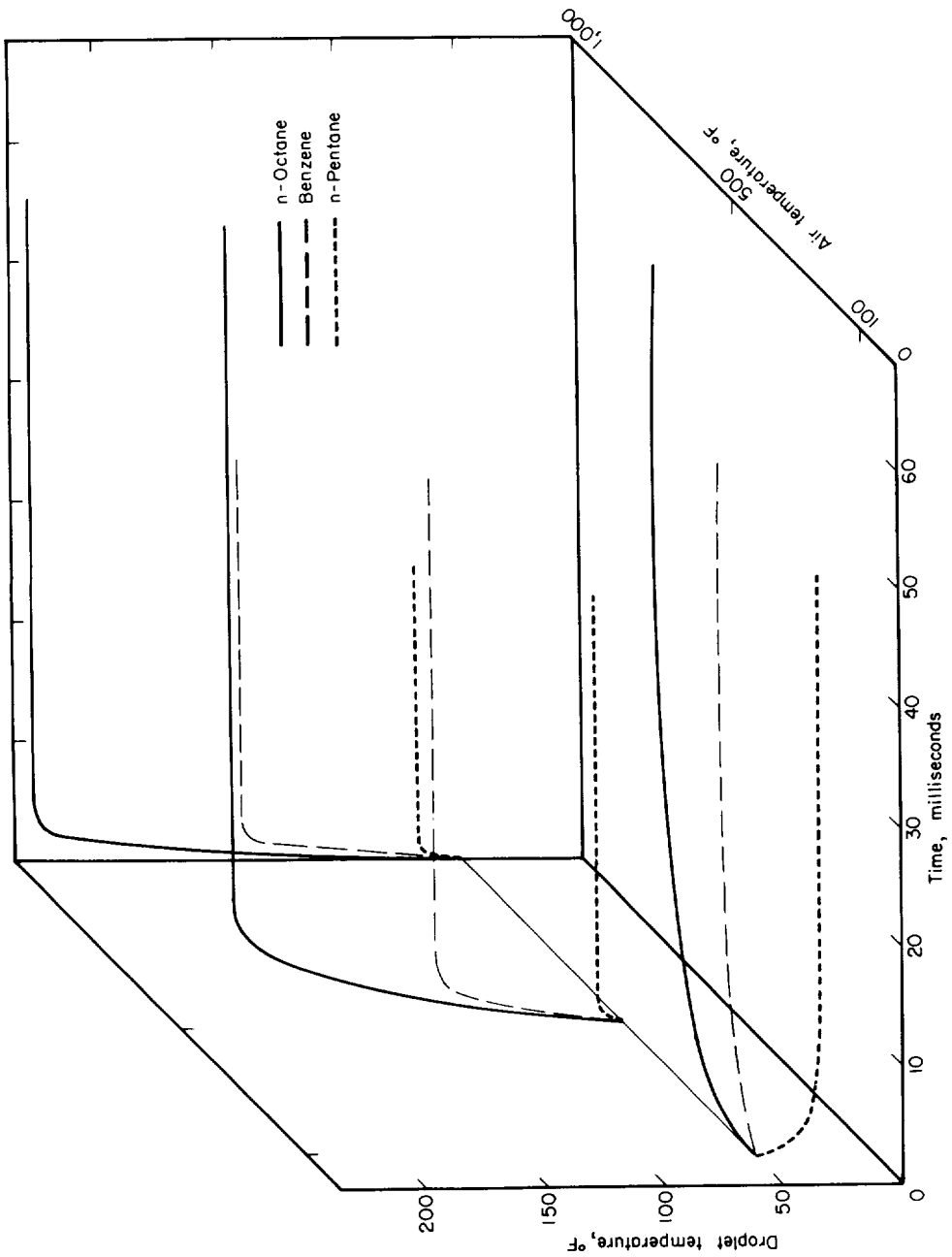
(a) At constant air pressure P_T of 1 atmosphere.

Figure 12.— Temperature-time histories of three fuels. $T_1 = 50^\circ$ F; $U_1 = 100$ fps; $r_{ol} = 50$ microns.
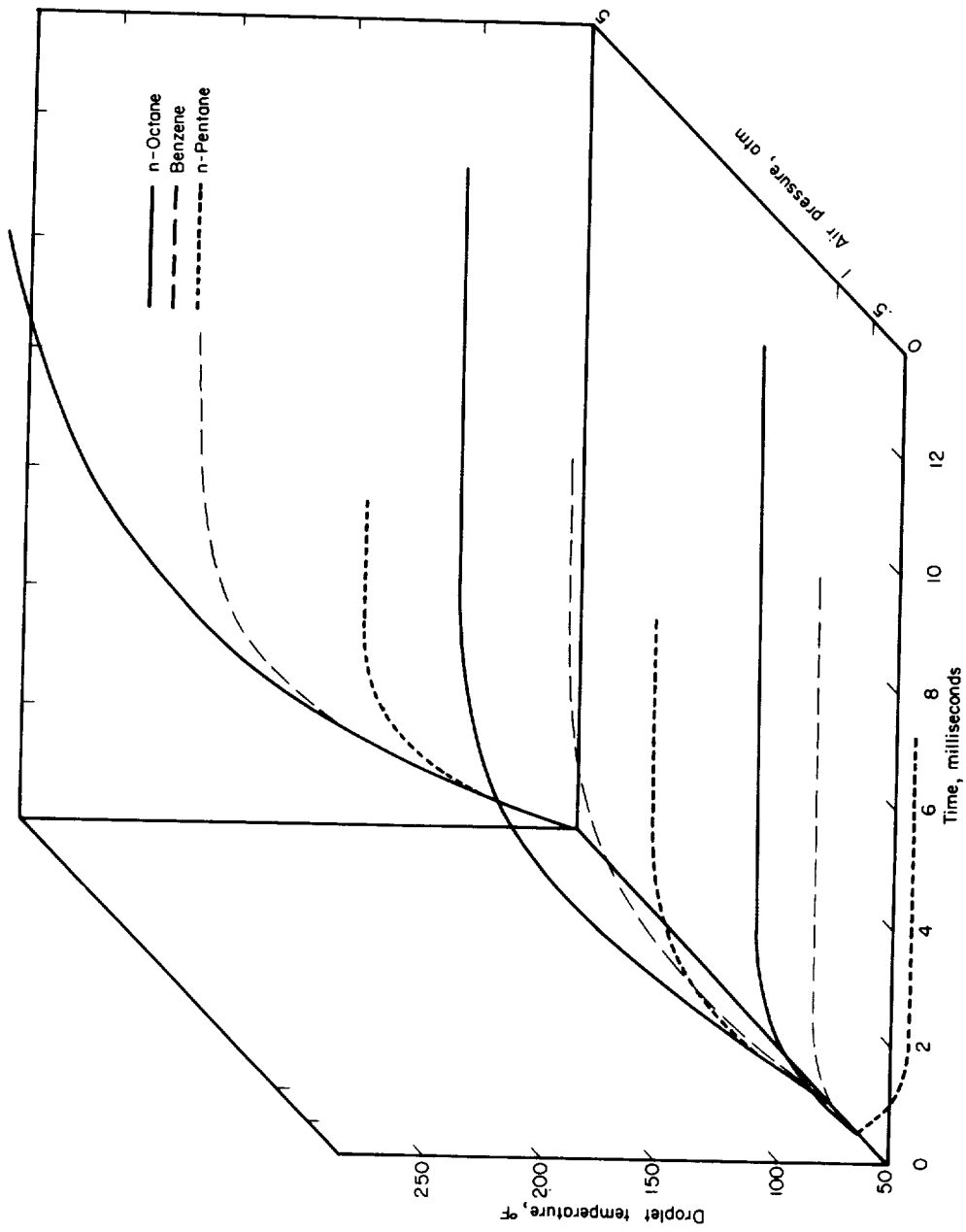
(b) At constant air temperature T_B of 500° F.

Figure 12.- Concluded.
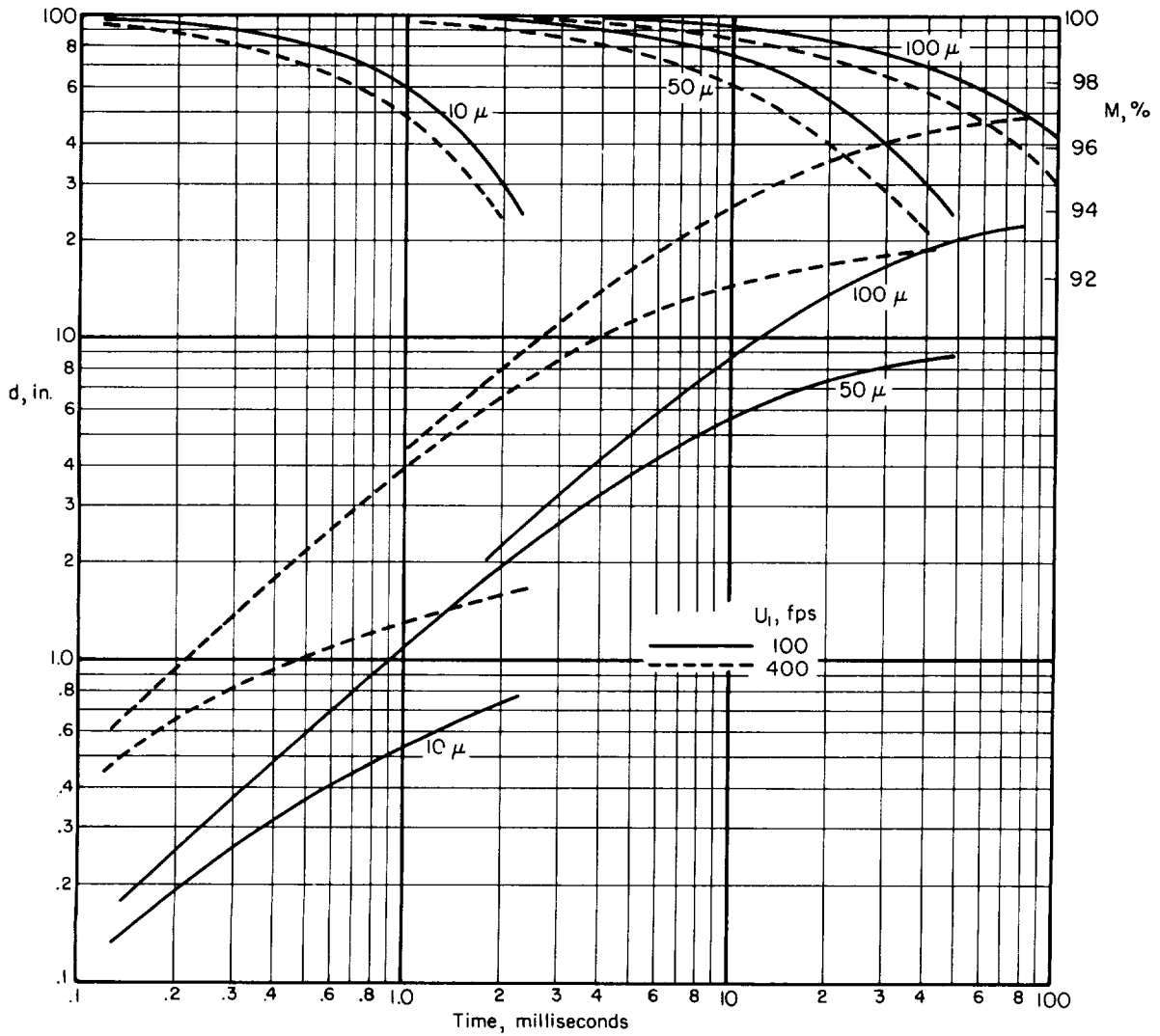
(a) P_T = 0.5 atmosphere; T_B = 100° F.

Figure 13.- Penetration-time and mass-time histories during unsteady
state for n-octane at nine different ambient air conditions.
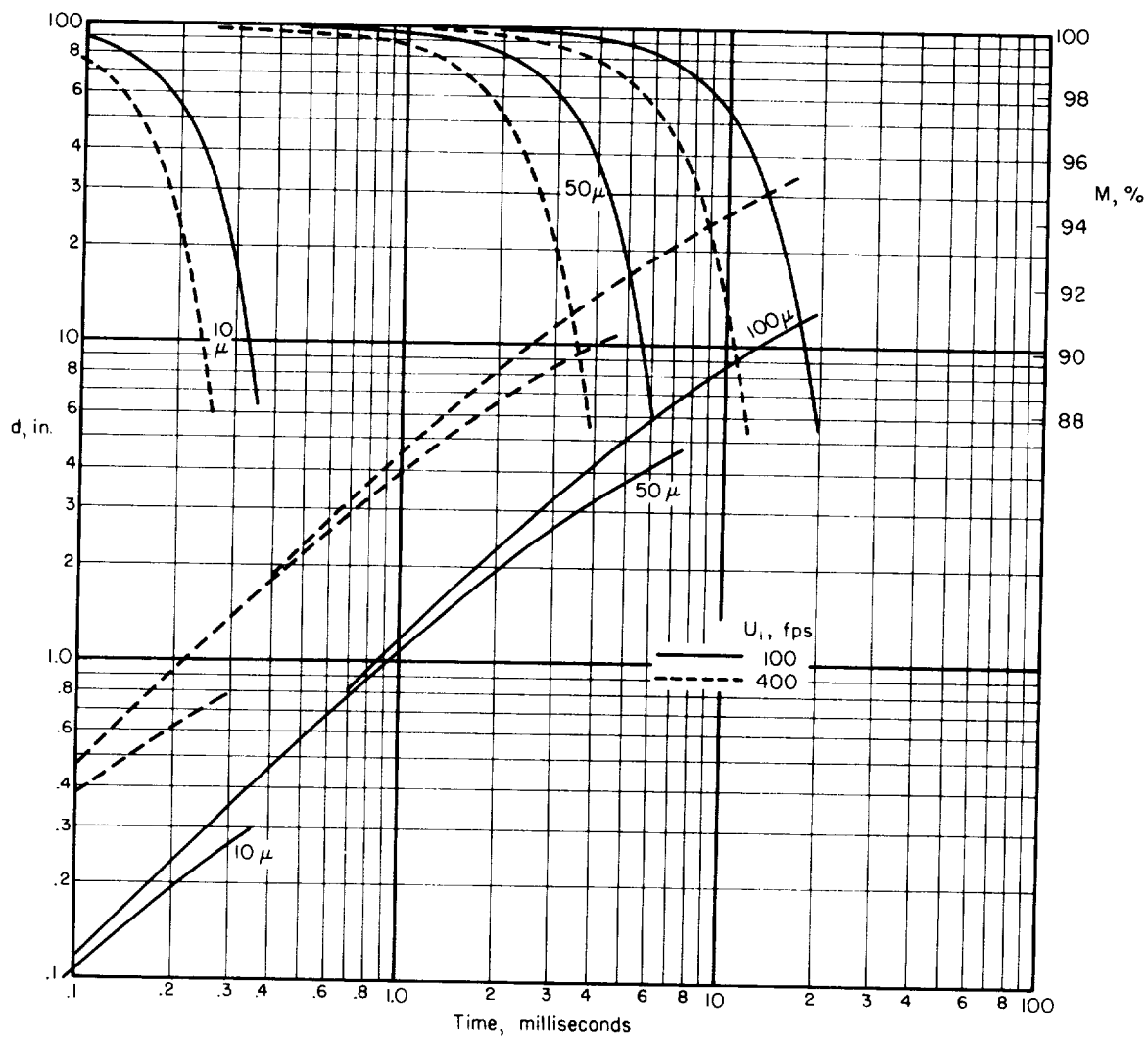
(b) $P_T = 0.5$ atmosphere; $T_B = 500^0$ F.

Figure 13.- Continued.

(c) $P_T = 0.5$ atmosphere; $T_B = 1,000^{\circ}$ F.

Figure 13.- Continued.
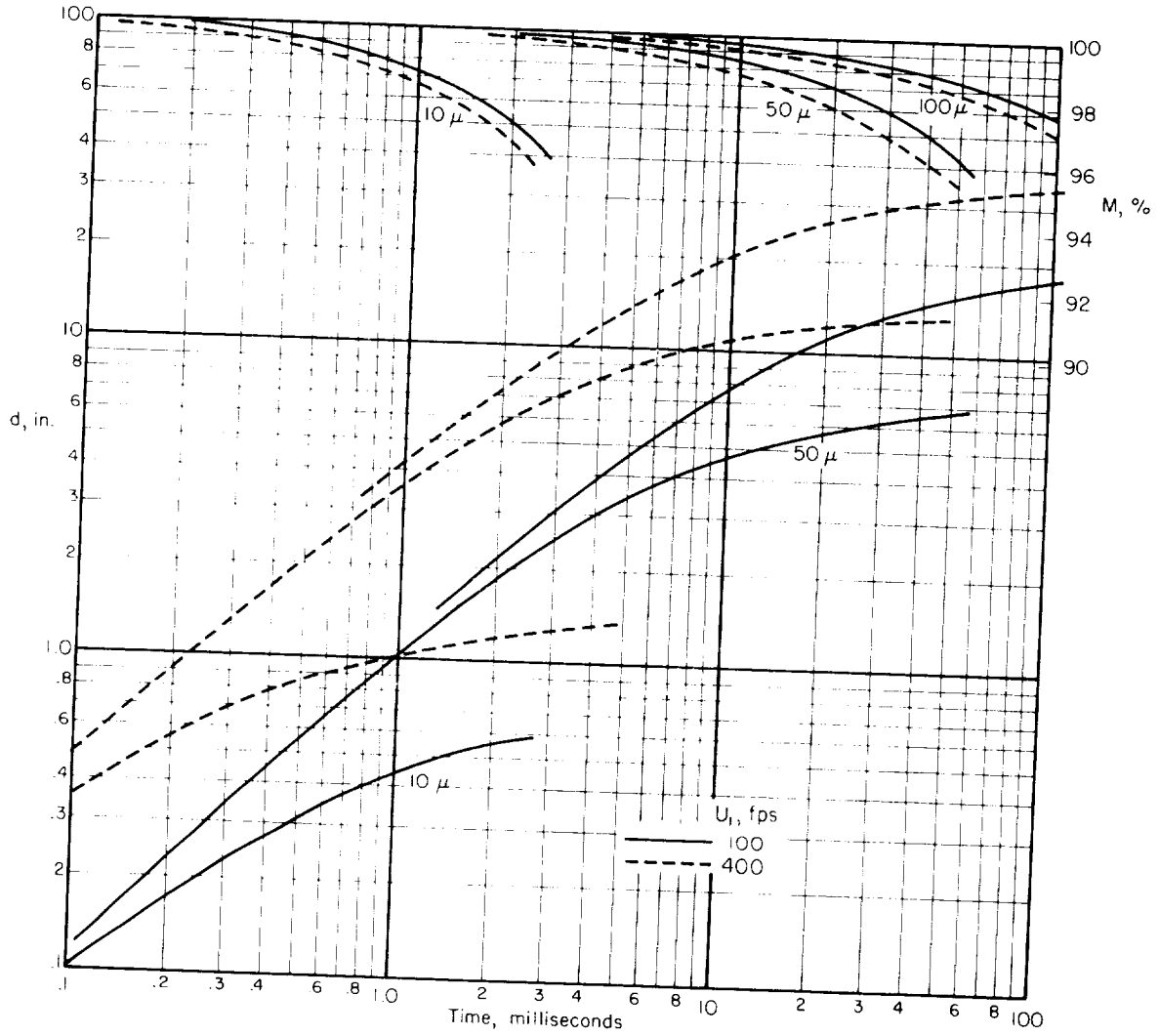
(d) $P_T = 1$ atmosphere; $T_B = 100^\circ$ F.

Figure 13.- Continued.
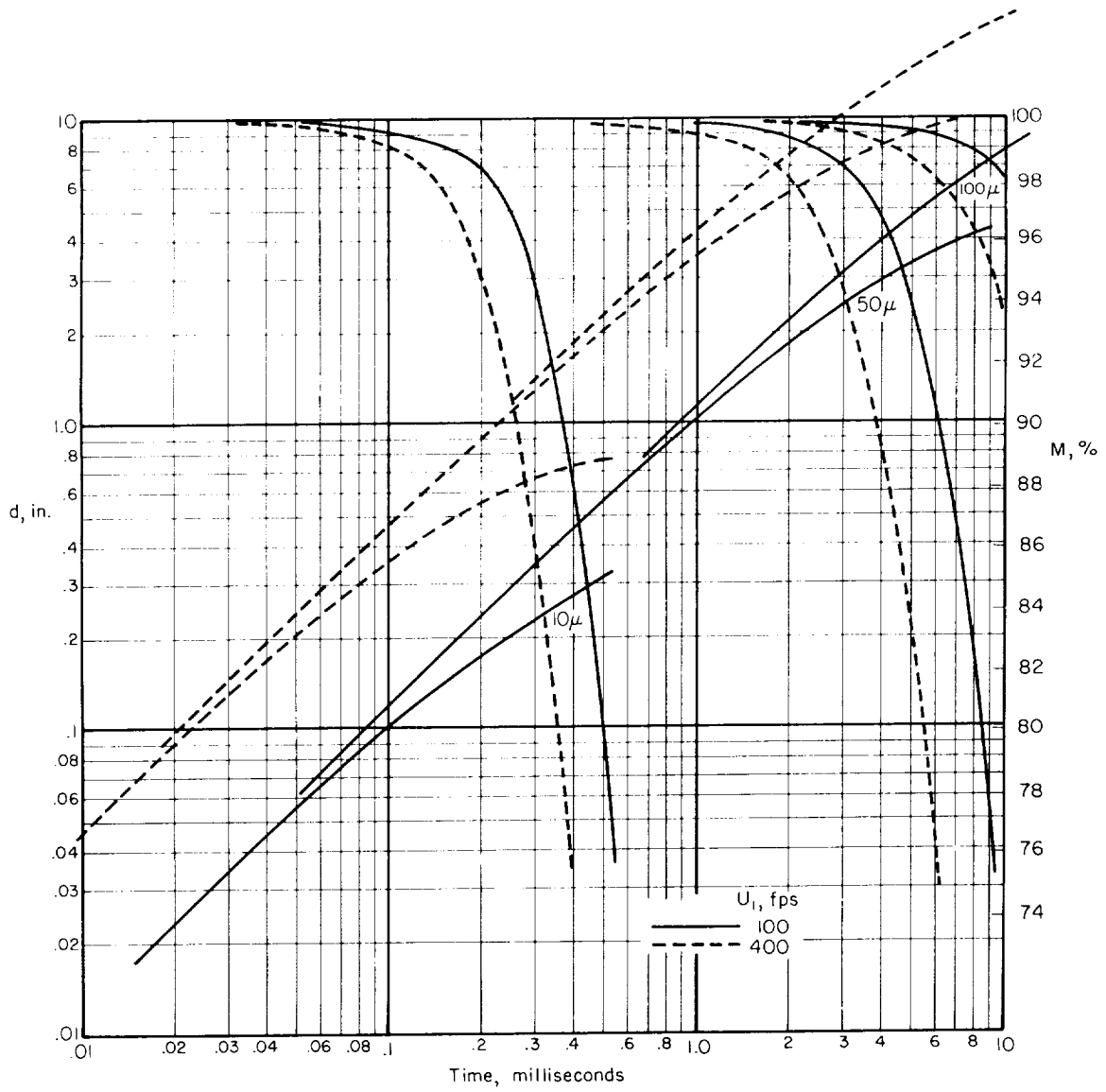
(e) $P_T = 1$ atmosphere; $T_B = 500^\circ$ F.

Figure 13.- Continued.
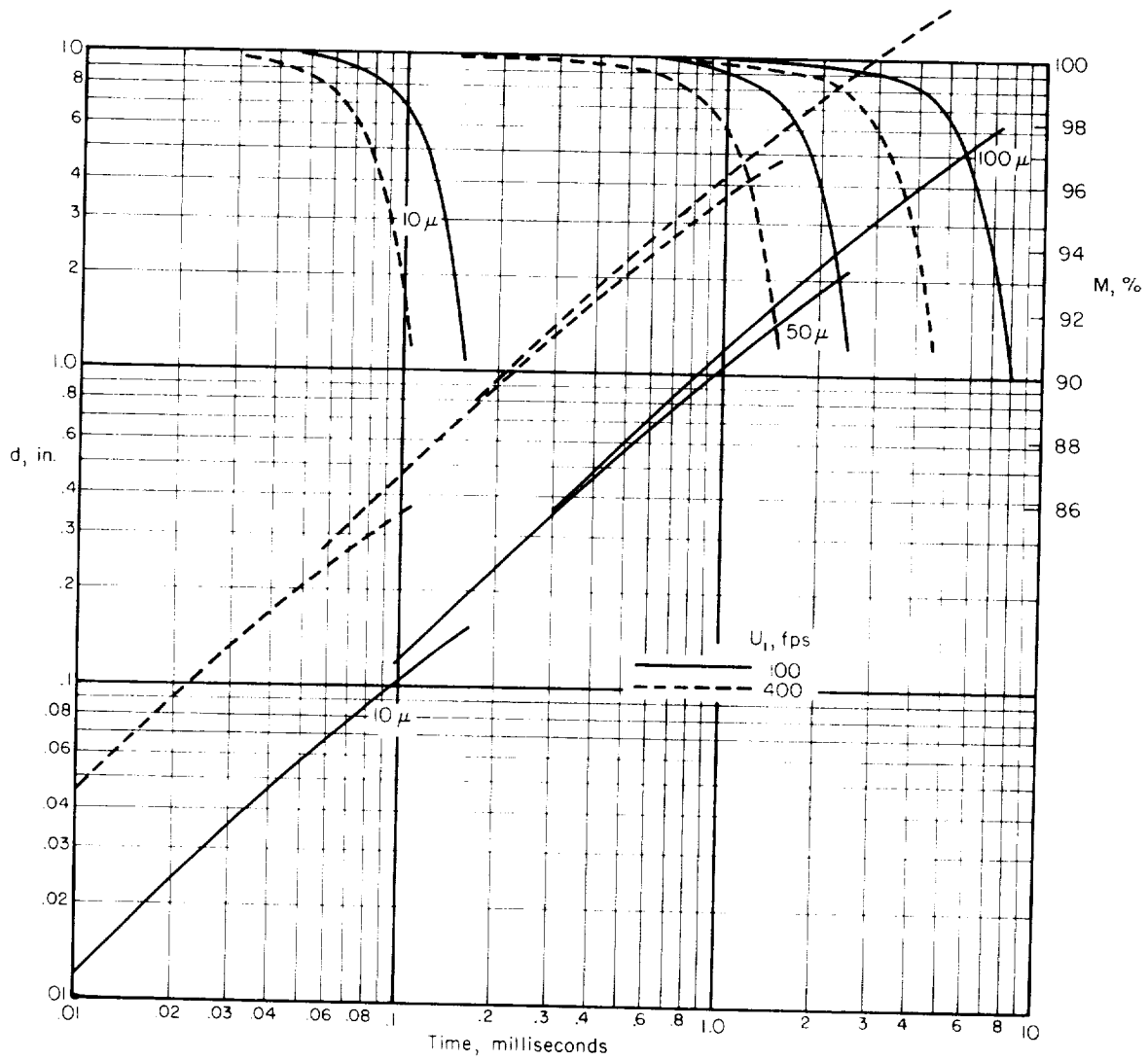
(f) $P_T = 1$ atmosphere; $T_B = 1,000^\circ$ F.

Figure 13.- Continued.
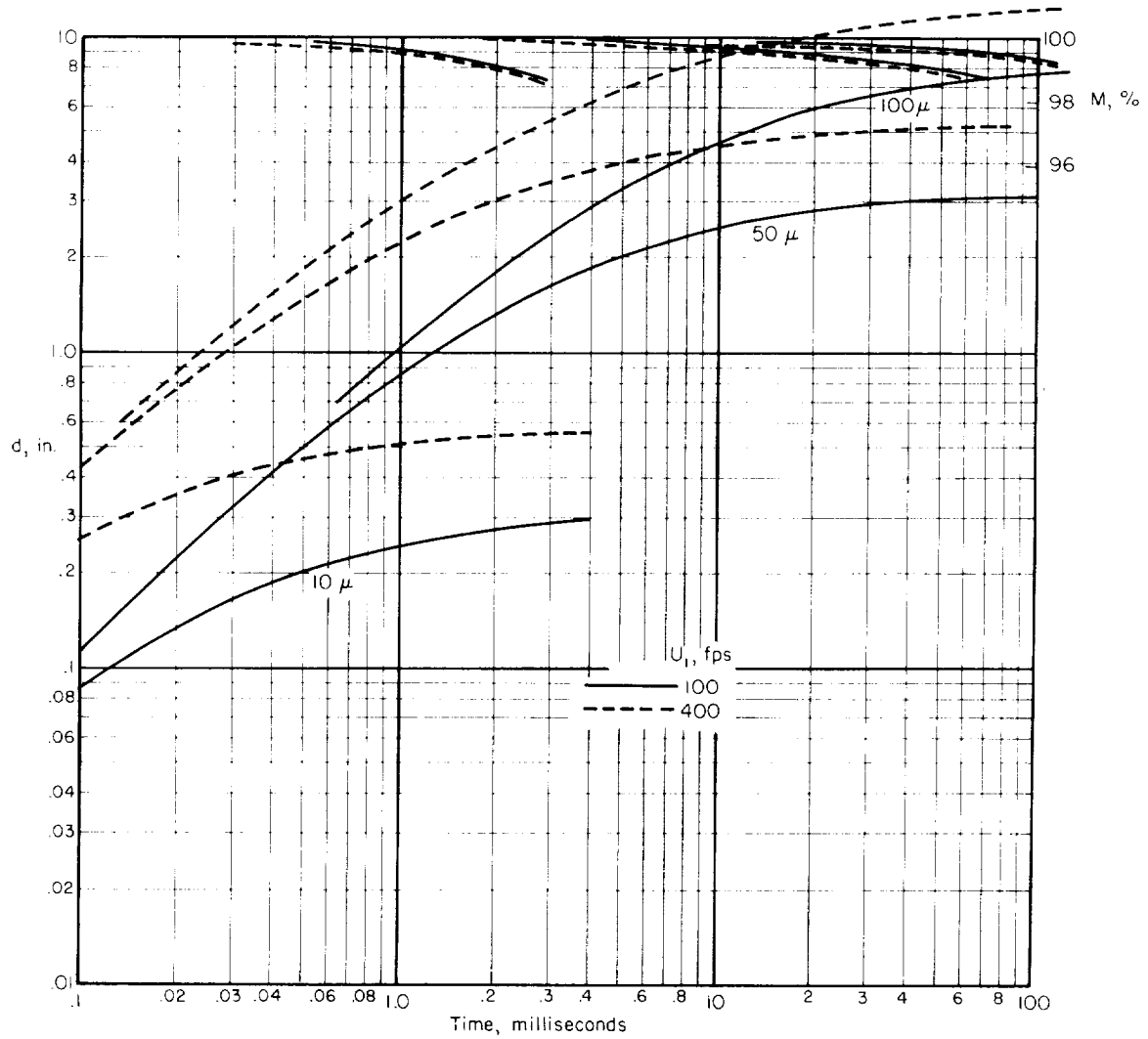
(g) P_T = 5 atmospheres; T_B = 100° F.

Figure 13.- Continued.
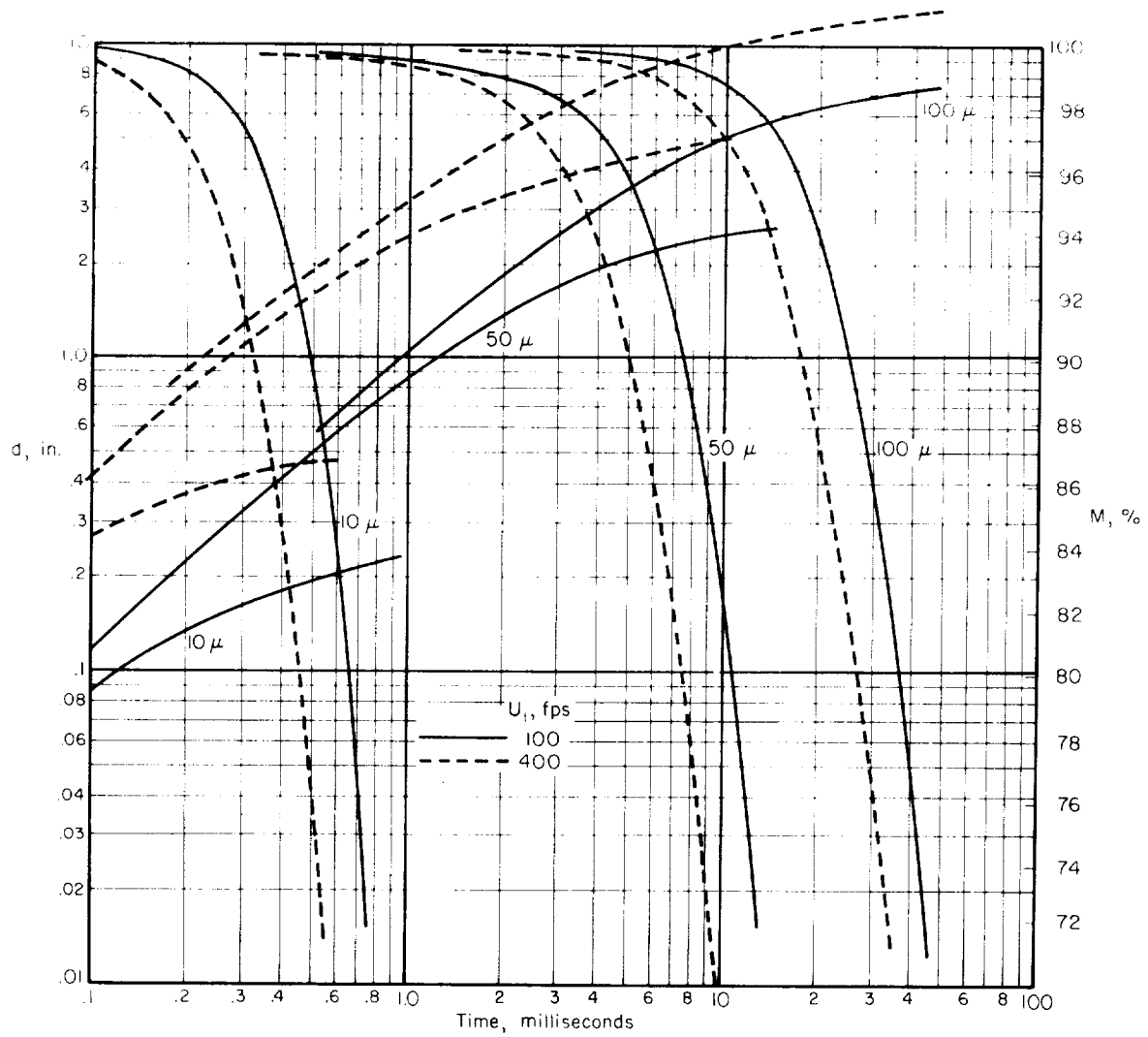
(h) $P_T = 5$ atmospheres; $T_B = 500°$ F.

Figure 13.- Continued.
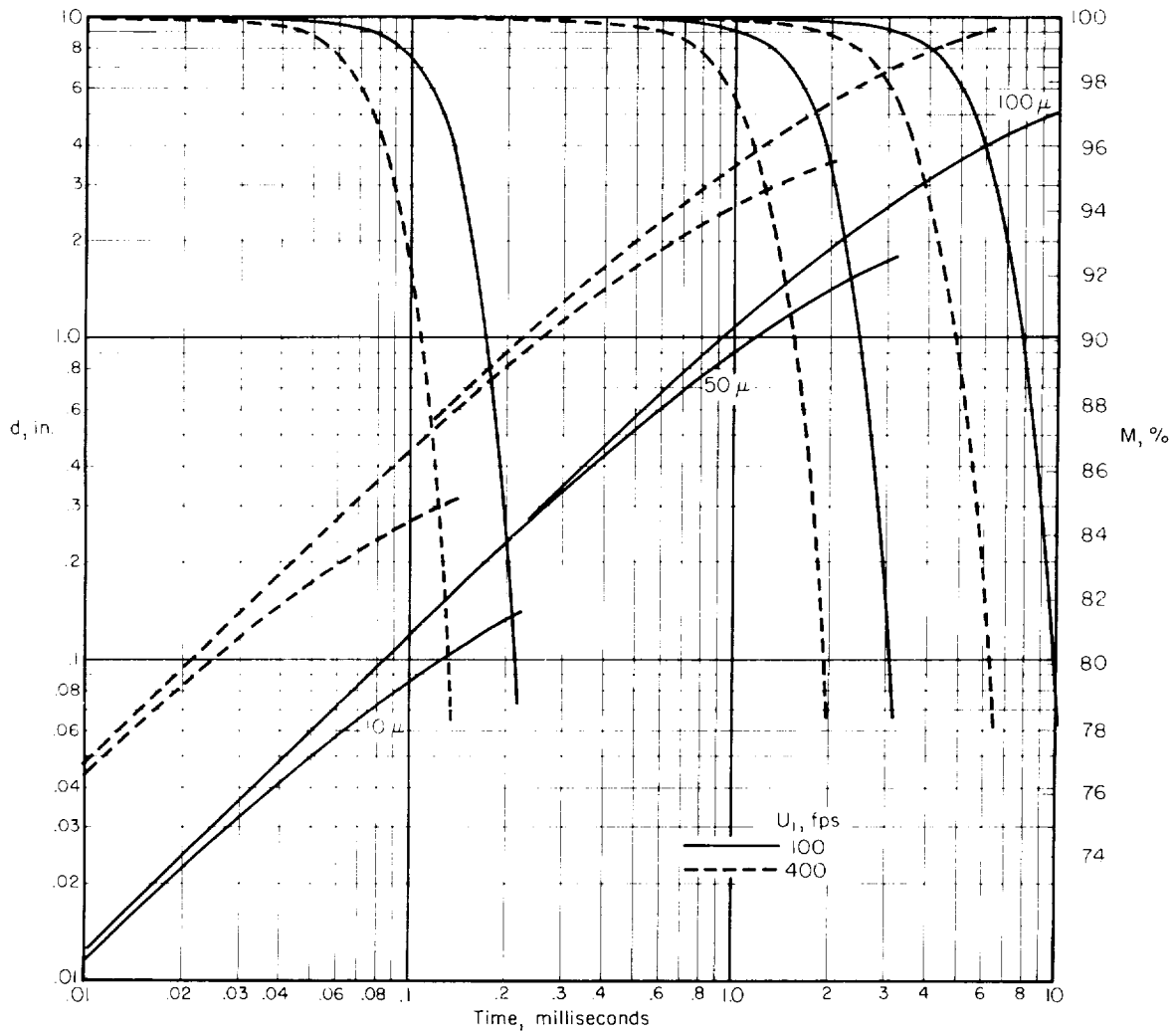
(i) P_T = 5 atmospheres; T_B = 1,000° F.

Figure 13.- Concluded.
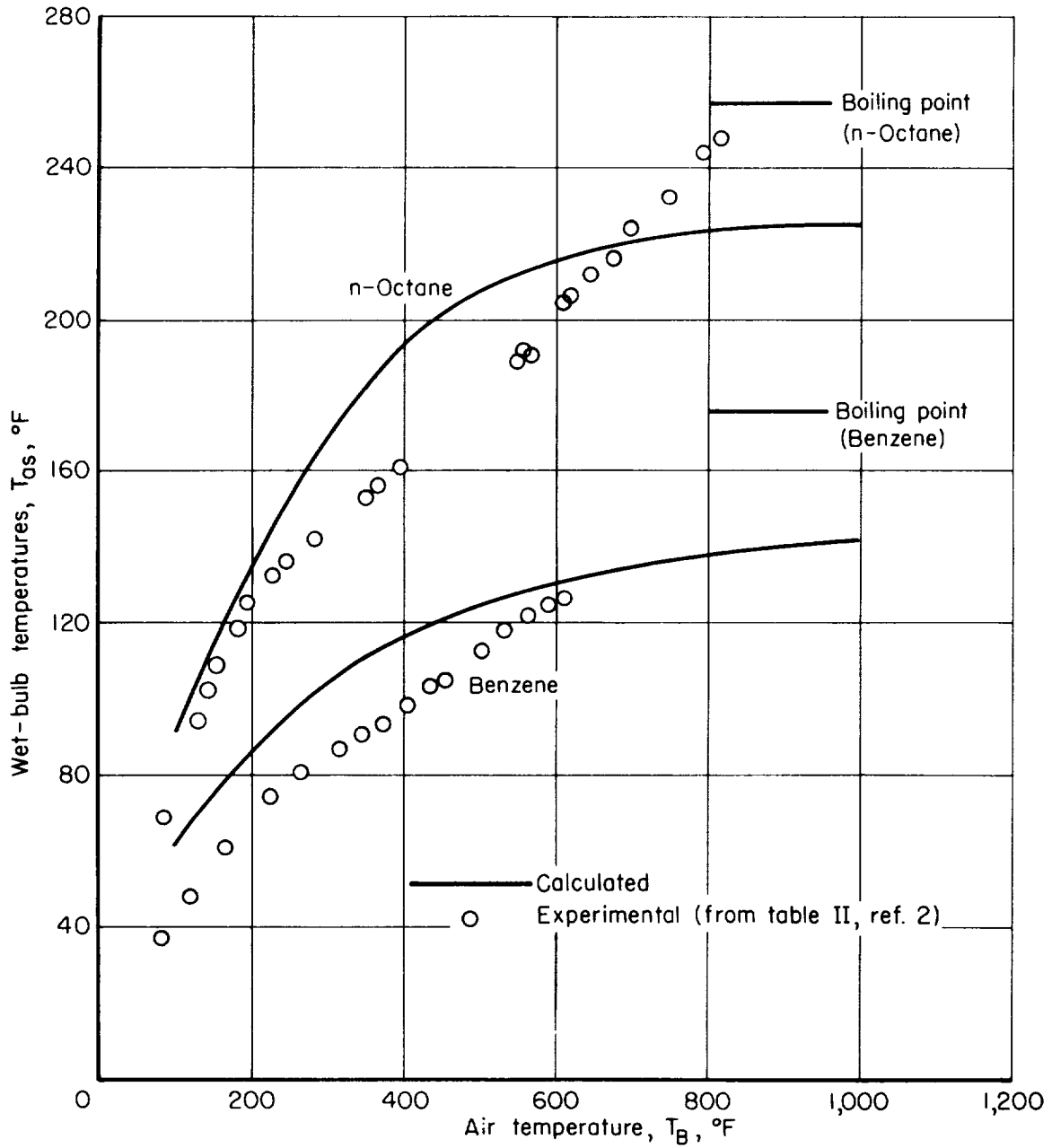
Figure 14.- Comparison of calculated and experimental wet-bulb temperatures at atmospheric pressure.
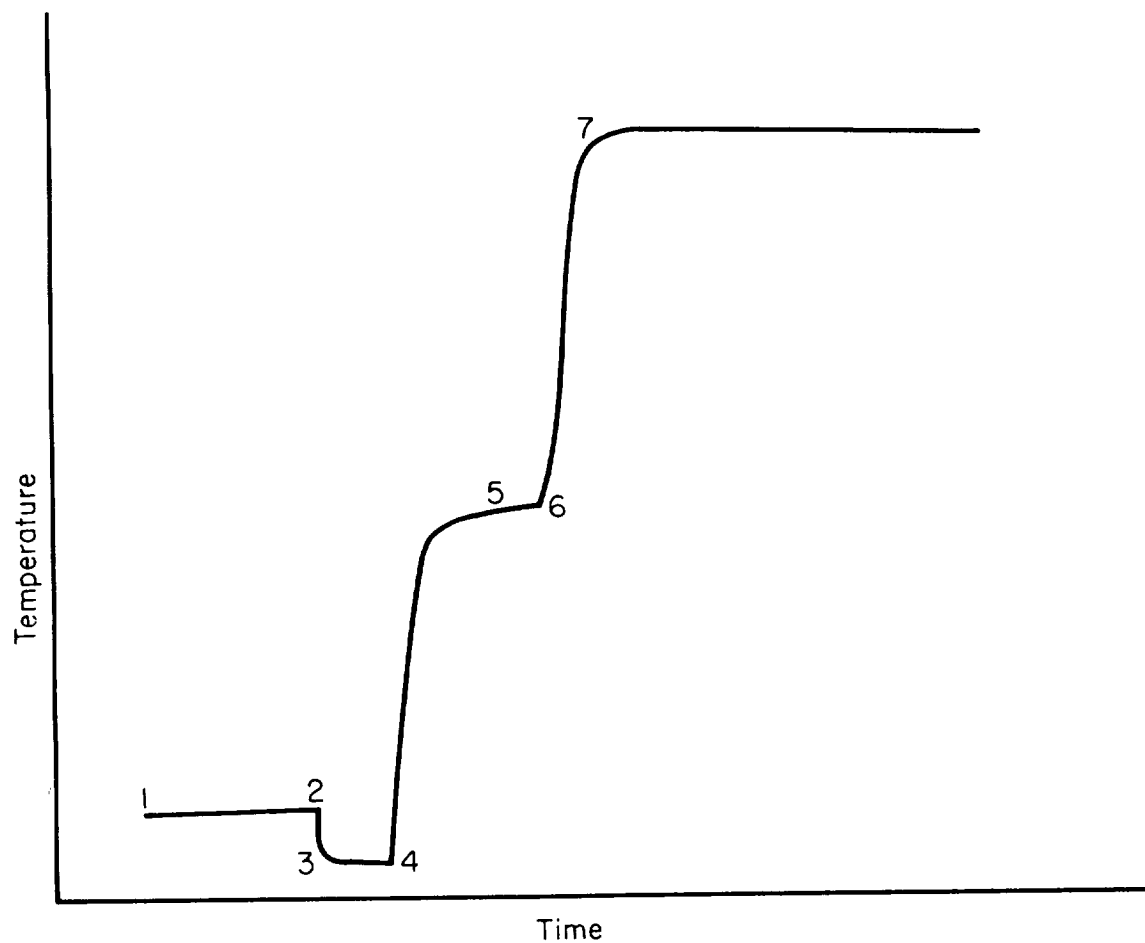
Figure 15.- Temperature-time history of a droplet of n-octane.

1 - 2 Room air temperature
      2 Droplet placed on thermocouple
2 - 3 Rapid self-cooling to approximately wet-bulb temperature
          at room air temperature
3 - 4 Gradual approach to wet-bulb temperature
      4 Hot air suddenly swung under droplet
4 - 5 Heating-up or unsteady-state period to wet-bulb temperature
          corresponding to hot air
5 - 6 Steady state at wet-bulb temperature
6 - 7 Heating up of thermocouple to air temperature
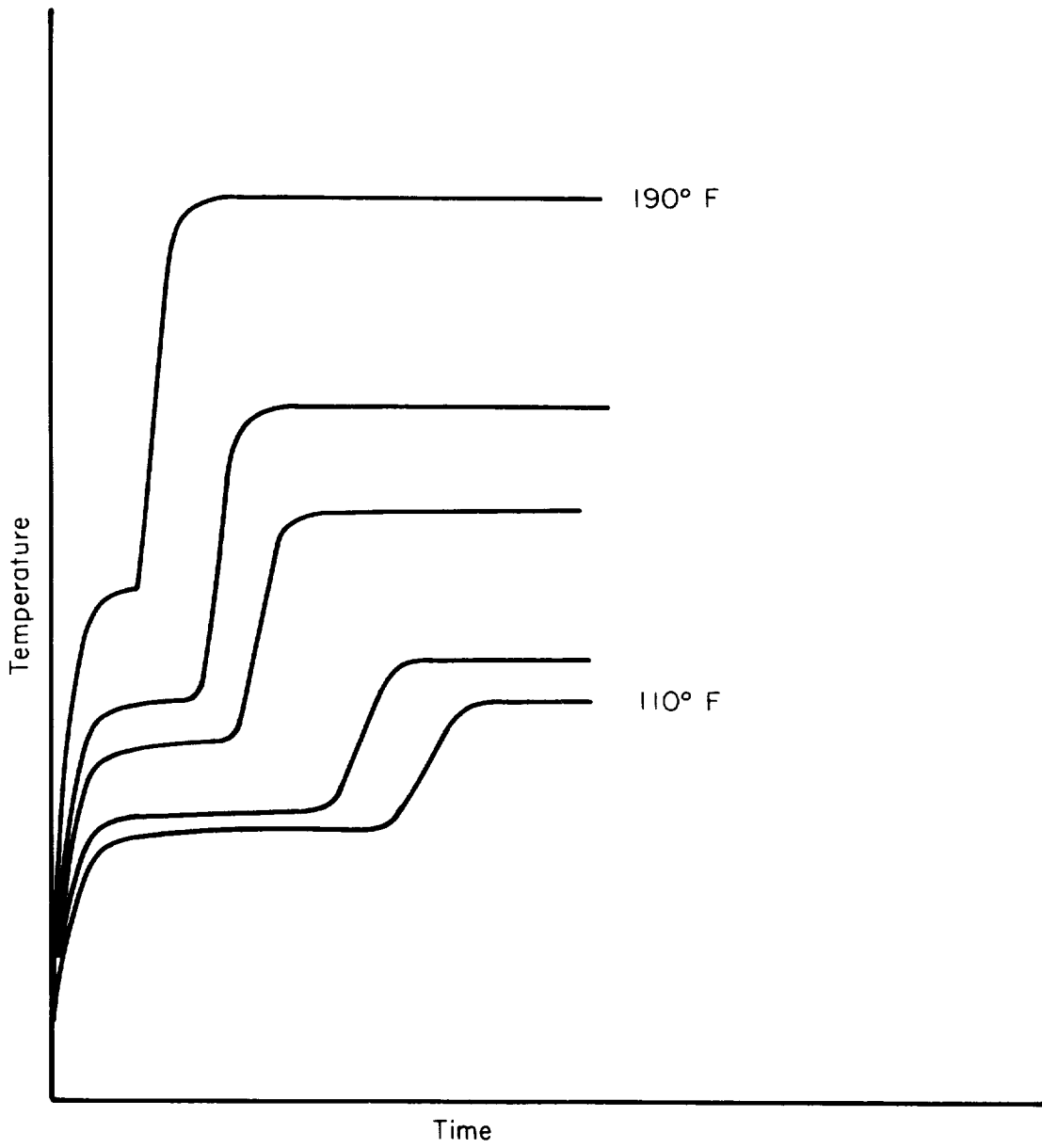
Figure 16.- Effect of air temperature on heating up of n-octane.
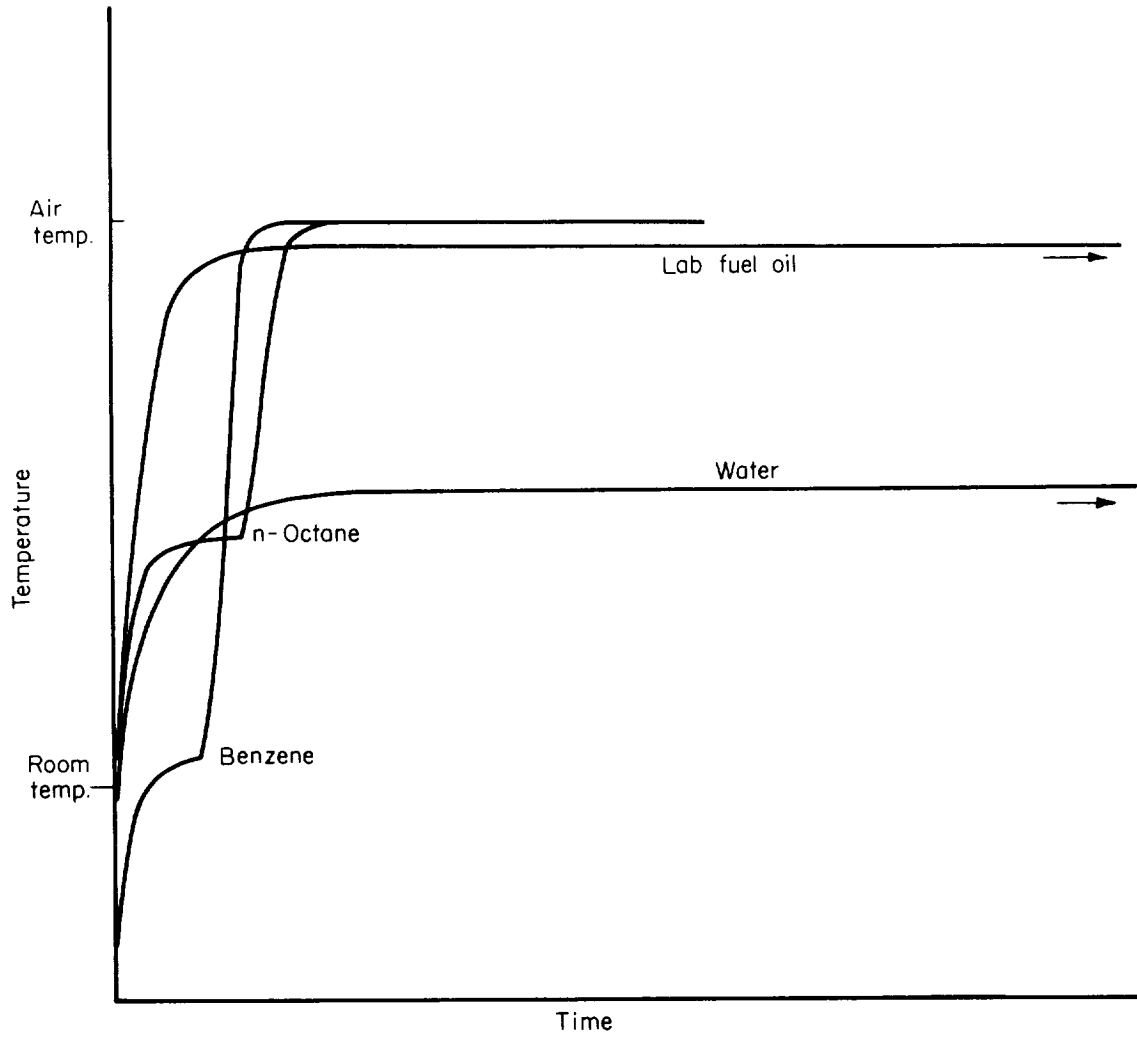
Figure 17.- Effect of fuel composition on heating-up time at constant
air temperature.
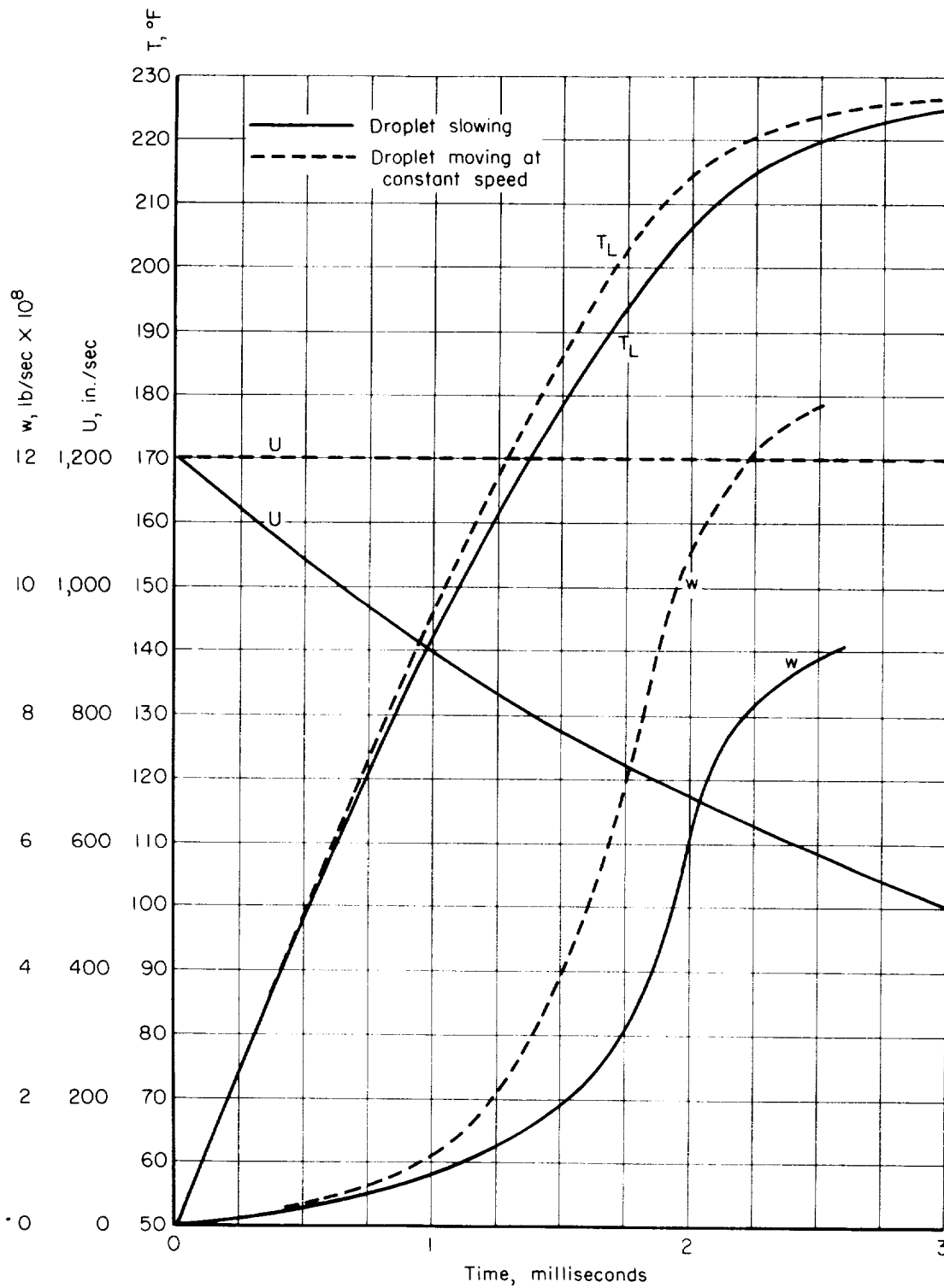
Figure 18.- Temperature, velocity, and rate of mass transfer histories of two droplets of n-octane of 50-micron initial radius. $T_1 = 50^\circ$ F; $U_1 = 100$ fps; $P_T = 1$ atmosphere; $T_B = 1,000^\circ$ F.
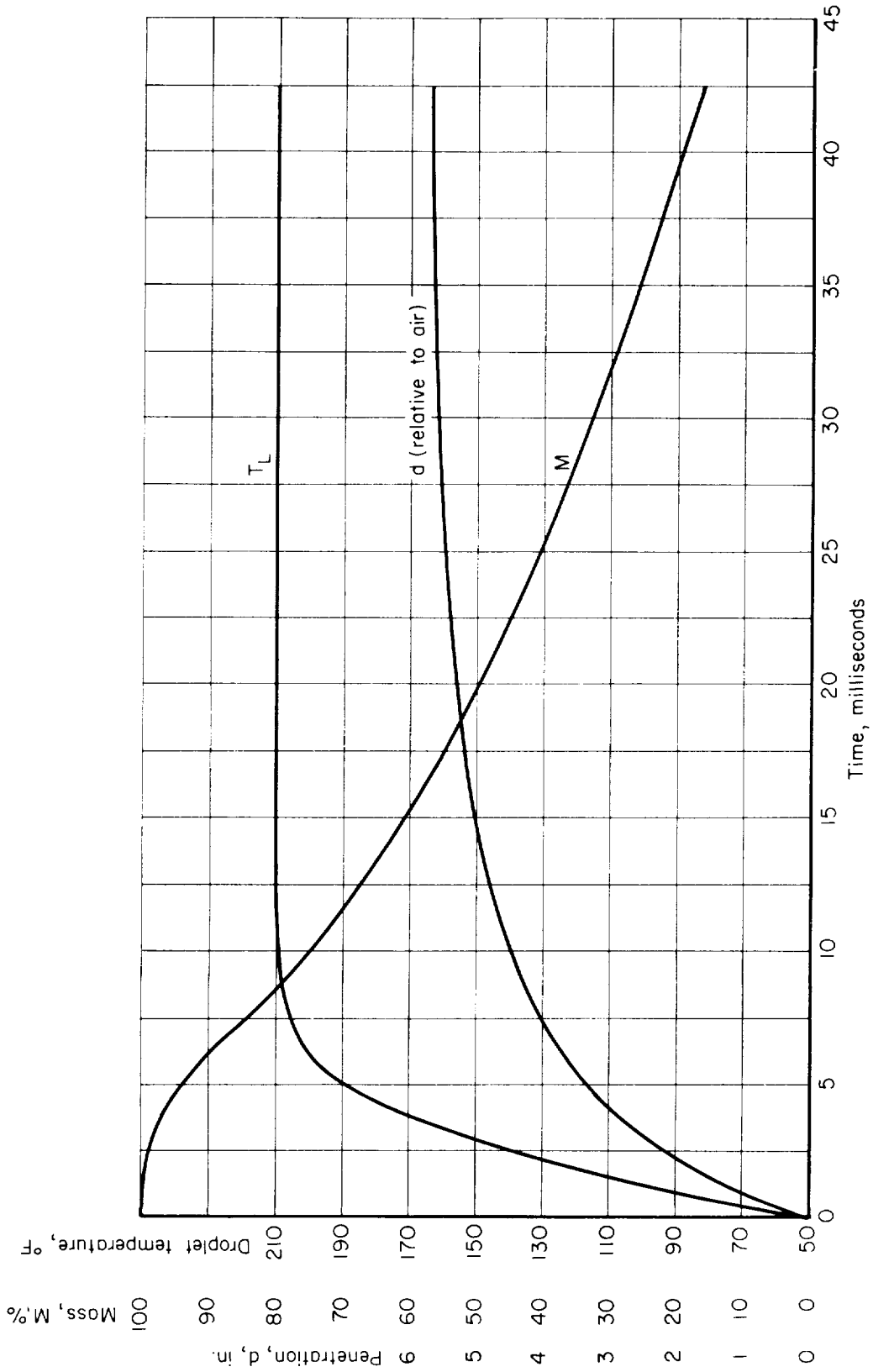
Figure 19.- Temperature-, mass-, and penetration-time histories of a
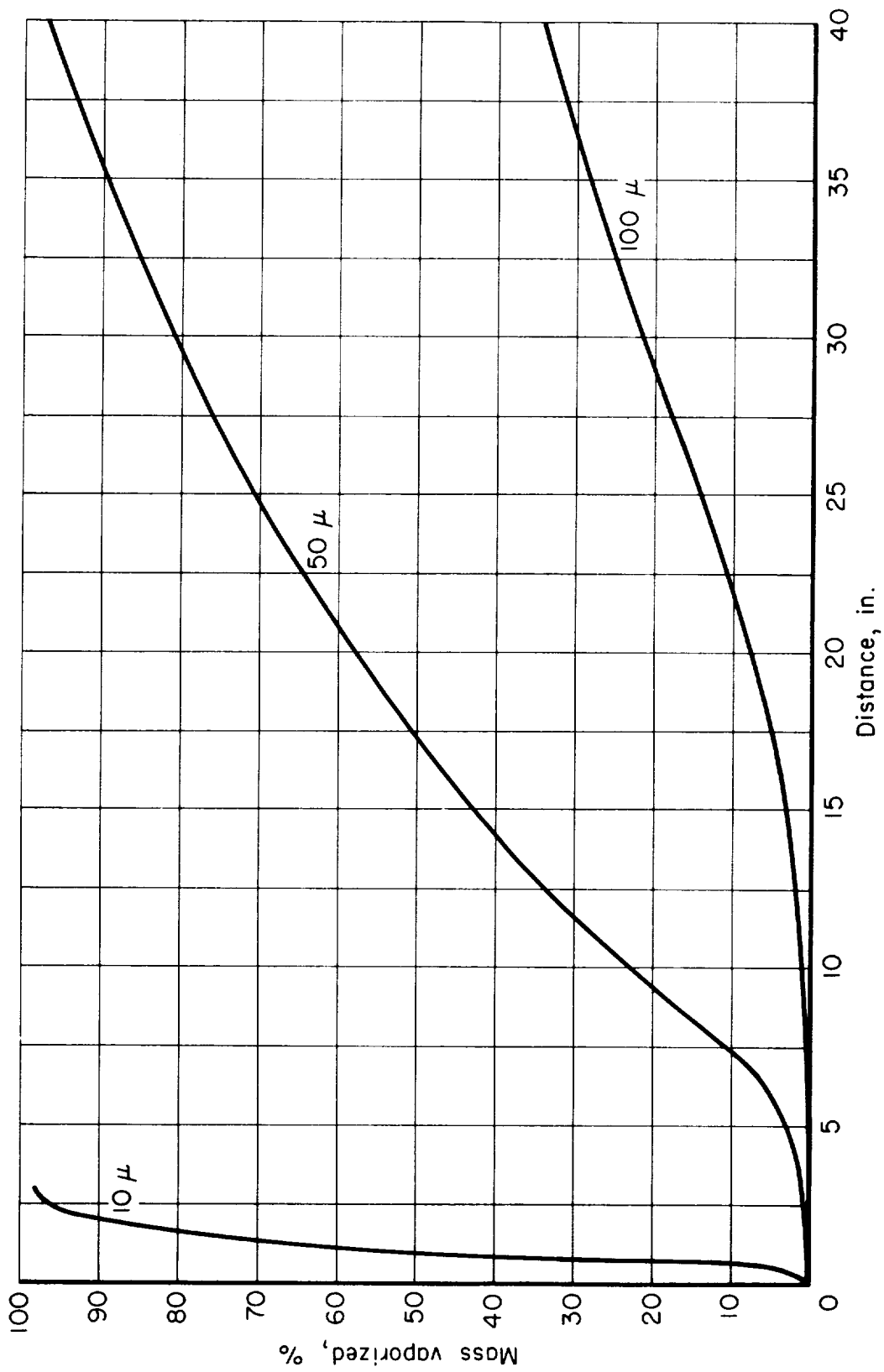50-micron n-octane droplet.

Figure 20.- Mass vaporized of each droplet versus distance traveled in combustion chamber.
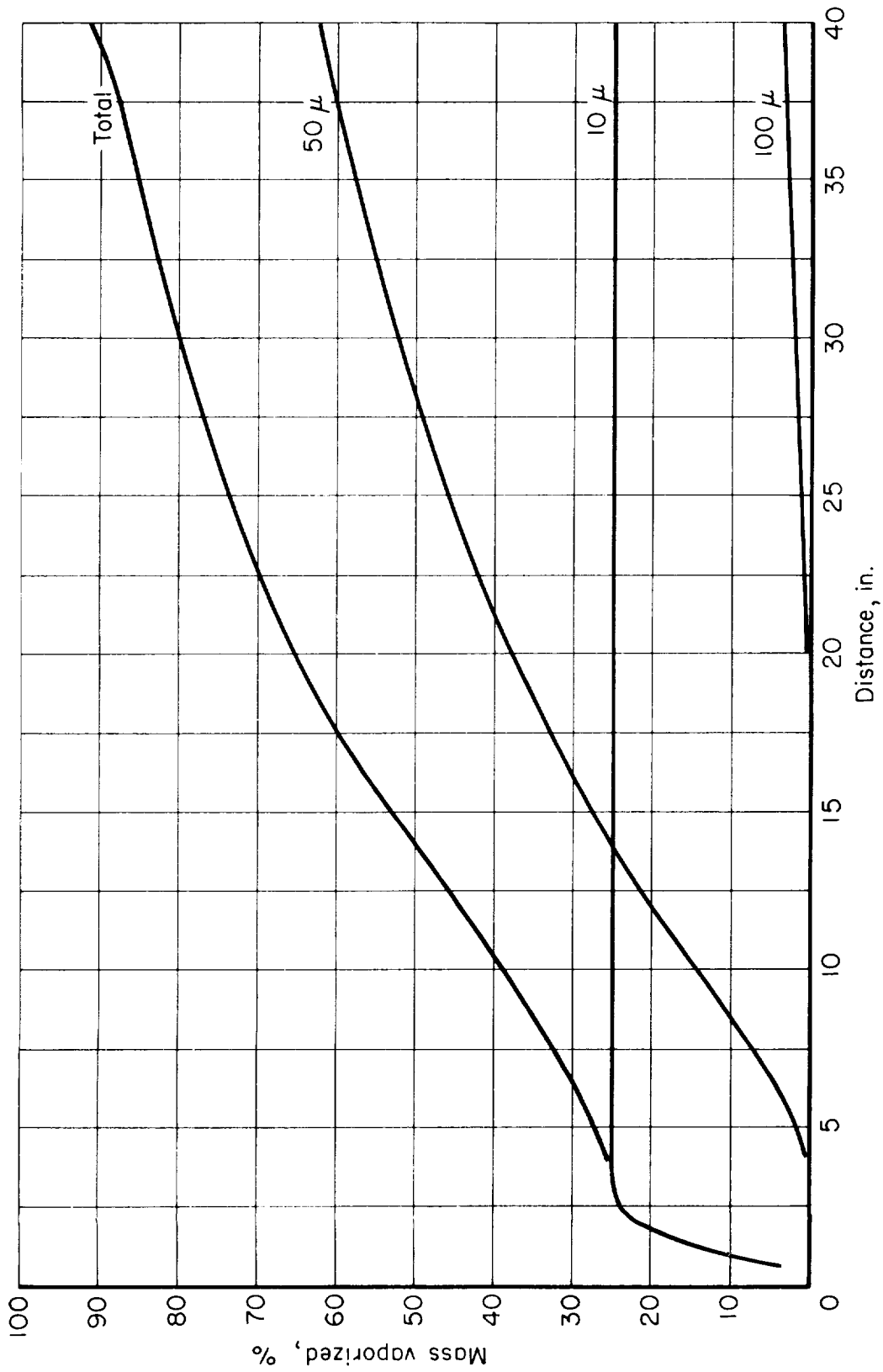
Figure 21.- Mass vaporized of each droplet size group and total mass vaporized (percentage of total fuel injected).
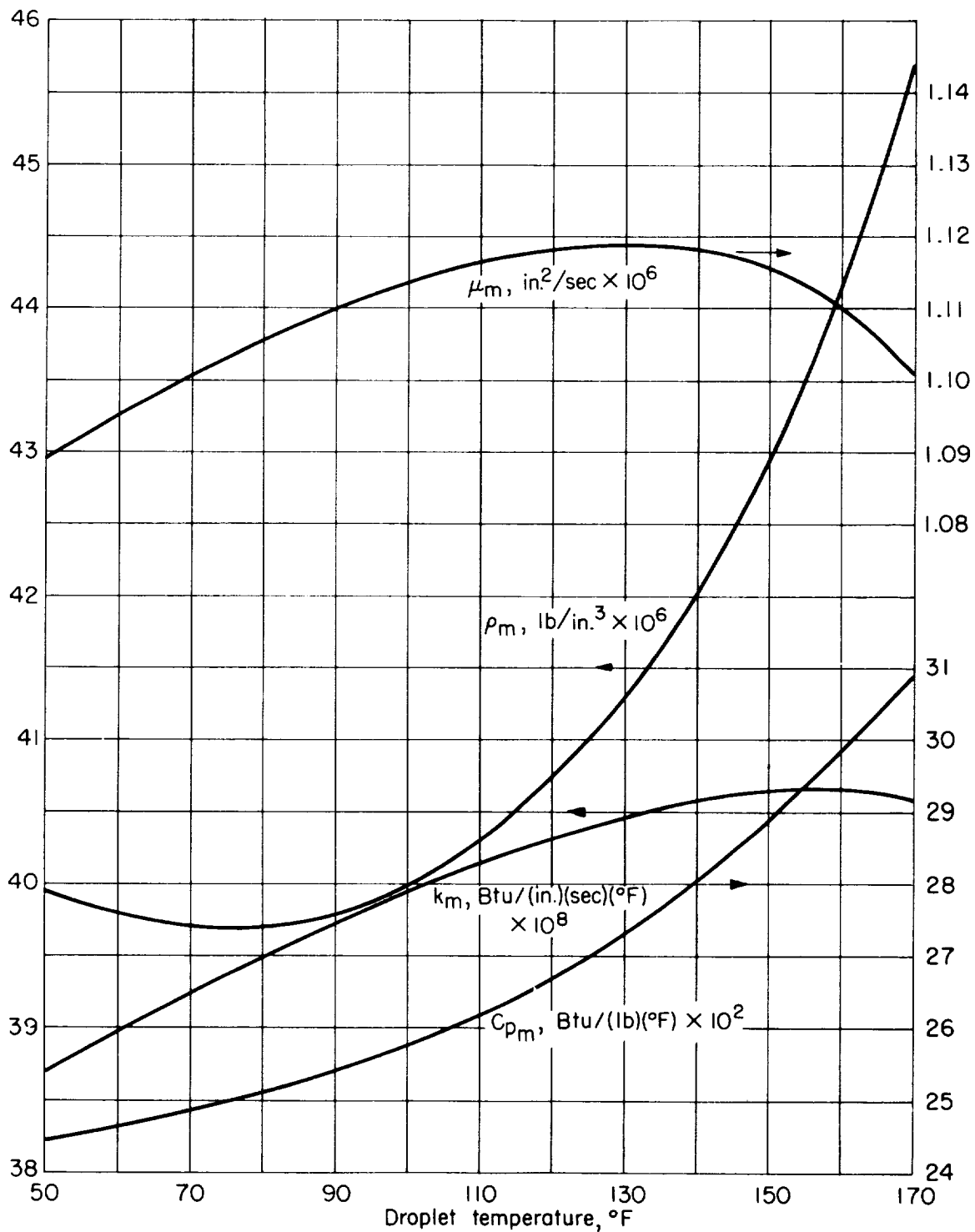
Figure 22.- Average properties of air-vapor mixture in film at
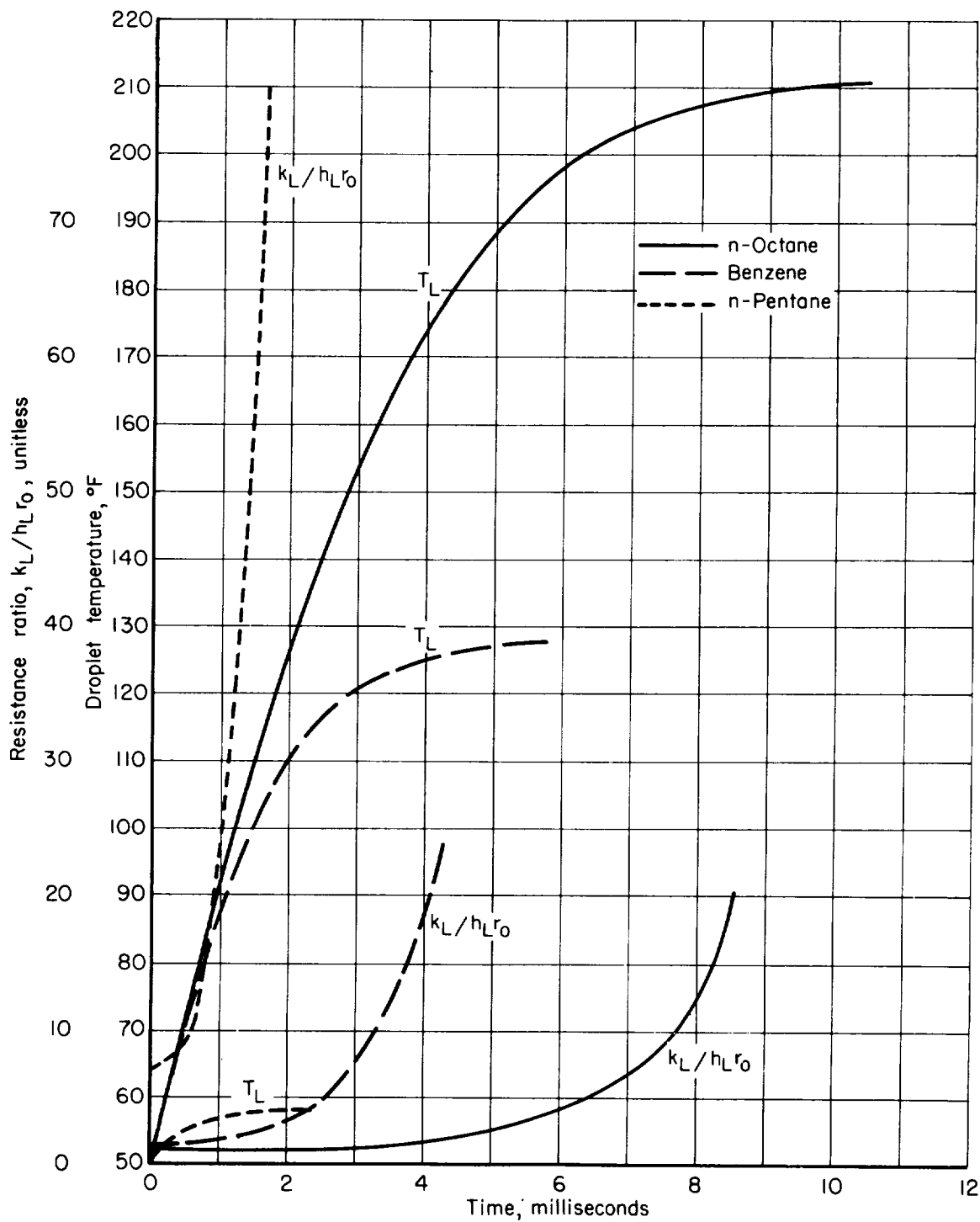different droplet temperatures. Air pressure, 1 atmosphere;
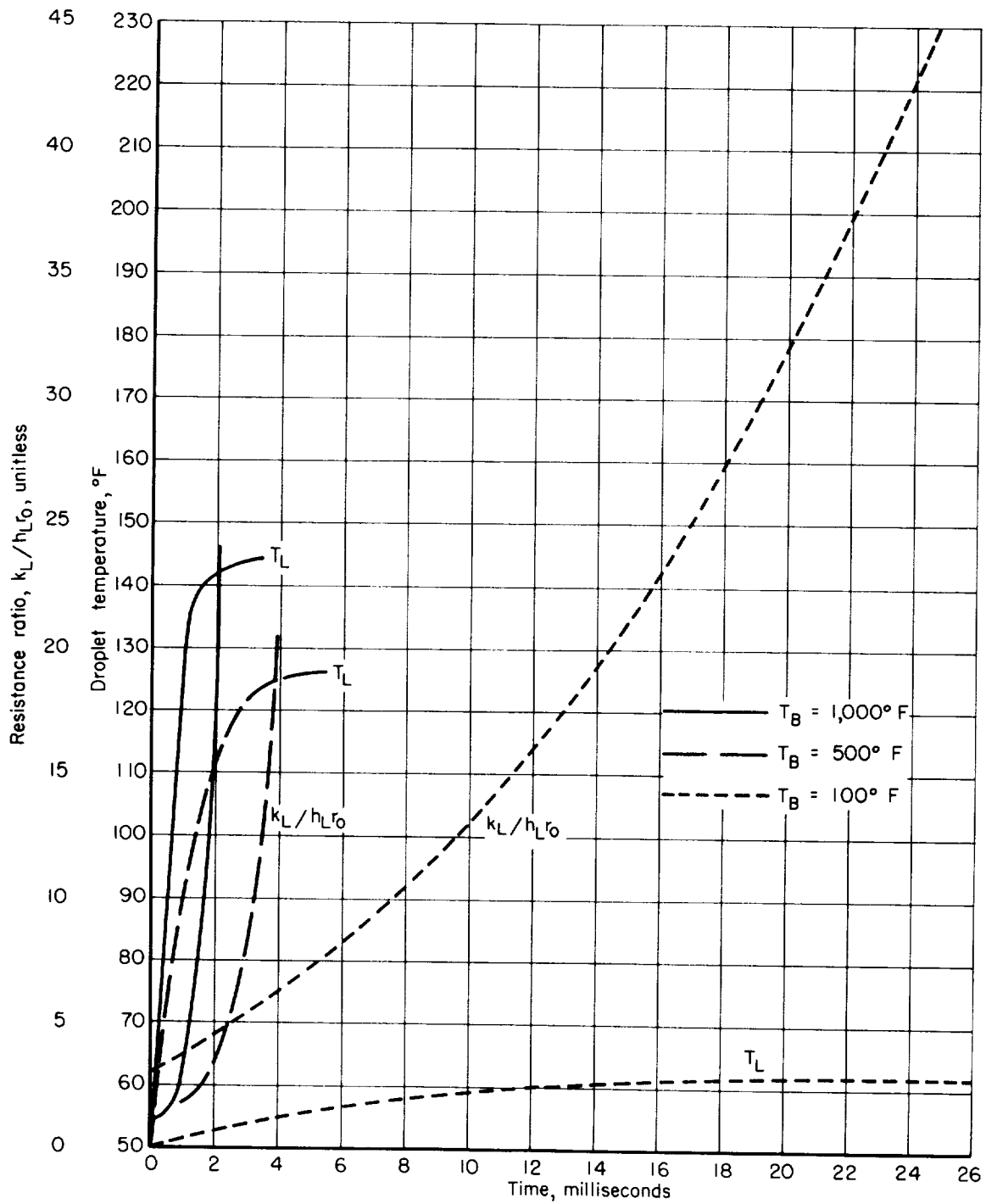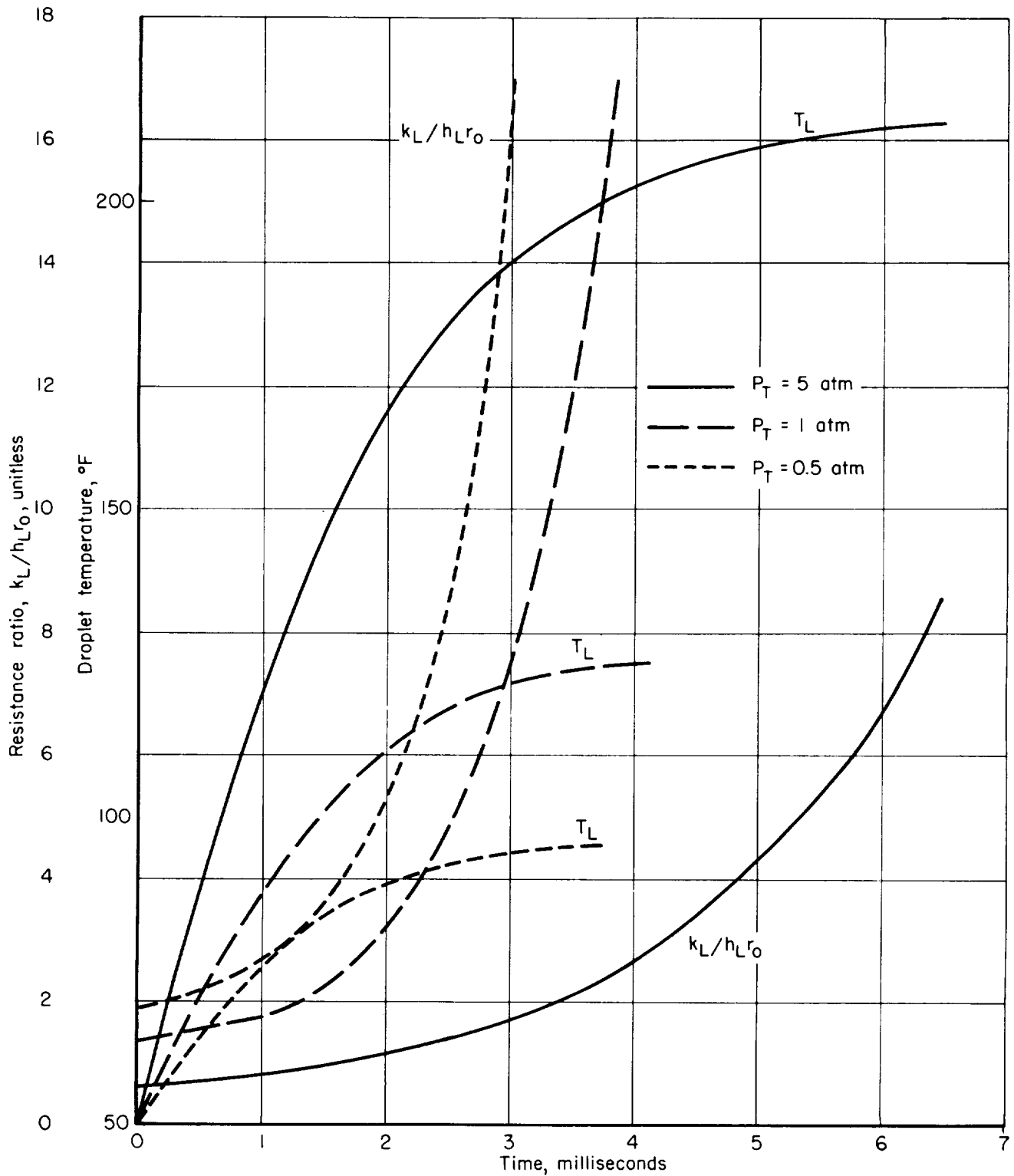air temperature, 200° F.

Figure 23.- Resistance ratio and droplet temperature for three fuels at 1-atmosphere air pressure and 500° F air temperature. $U_1 = 100$ fps; $r_{o1} = 50$ microns.

(a) At constant air pressure of 1 atmosphere.

Figure 24.- Resistance ratio and droplet temperature for benzene.
$U_1 = 100$ fps; $r_{ol} = 50$ microns.

(b) At constant air temperature of 500° F.

Figure 24.- Concluded.